Dark-matter results from 332 new live days of LUX data

Aaron Manalaysay
For the LUX Collaboration

Presented at:

Identification of Dark Matter
The University of Sheffield,
Sheffield, UK, 21 July, 2016

The LUX collaboration

Berkeley Lab / UC Berkeley

Bob Jacobsen	PI, Professor
Murdock Gilchriese	Senior Scientist
Kevin Lesko	Senior Scientist
Michael Witherell	Lab Director
Peter Sorensen	Scientist
Simon Fiorucci	Project Scientist
Attila Dobi	Postdoc
Daniel Hogan	Graduate Student
Kate Kamdin	Graduate Student
Kelsey Oliver-Mallory	Graduate Student

Brown University

Richard Gaitskell	PI, Professor
Samuel Chung	Graduate Student
Dongqing Huang	Graduate Student
Casey Rhyne	Graduate Student
Will Taylor	Graduate Student
James Verbus	Postdoc

University of Edinburgh, UK

Alex Murphy	PI, Professor
Paolo Beltrame	Research Fellow
Tom Davison	Graduate Student
Maria F. Marzioni	Graduate Student

Imperial College London, UK

Henrique Araujo	PI, Reader
Tim Sumner	Professor
Alastair Currie	Postdoc
Adam Bailey	Graduate Student
Khadeeja Yazdani	Graduate Student

Lawrence Livermore

Adam Bernstein	PI, Leader of Adv. Detectors Grp.
Kareem Kazkaz	Staff Physicist
Jingke Xu	Postdoc
Brian Lenardo	Graduate Student

LIP Coimbra, Portugal

Isabel Lopes	PI, Professor
Jose Pinto da	Assistant Professor
Vladimir Solovov	Senior Researcher
Francisco Neves	Auxiliary Researcher
Alexander Lindote	Postdoc
Claudio Silva	Postdoc
Paulo Bras	Graduate Student

SLAC Stanford (CWRU)

Dan Akerib	PI, Professor
Thomas Shutt	PI, Professor
Tomasz Biesiadzinski	Research Associate
Christina Ignarra	Research Associate
Wing To	Research Associate
Rosie Bramante	Graduate Student
Wei Ji	Graduate Student
T.J. Whitis	Graduate Student

SD Mines

Xinhua Bai	PI, Professor
Doug Tiedt	Graduate Student

SDSTA / Sanford Lab

David Taylor	Project Engineer
Markus Horn	Research Scientist
Dana Byram	Support Scientist

University at Albany

Matthew Szydagis	PI, Professor
Jeremy Mock	Postdoc
Sean Fallon	Graduate Student
Jack Genovesi	Graduate Student
Steven Young	Graduate Student

Texas A&M University

James White †	PI, Professor
Robert Webb	PI, Professor
Rachel Mannino	Graduate Student
Paul Terman	Graduate Student

UC Berkeley (Yale)

Daniel McKinsey	PI, Professor
Ethan Bernard	Project Scientist
Scott Hertel	Postdoc
Kevin O'Sullivan	Postdoc
Elizabeth Boulton	Graduate Student
Evan Pease	Graduate Student
Brian Tennyson	Graduate Student
Lucie Tvrznikova	Graduate Student
Nicole Larsen	Graduate Student

UC Davis

Mani Tripathi	PI, Professor
Britt Hollbrook	Senior Engineer
John Thomson	Development
Dave Hemer	Senior Machinist
Ray Gerhard	Electronics Engineer
Aaron Manalaysay	Project Scientist
Jacob Cutter	Graduate Student
James Morad	Graduate Student
Sergey Uvarov	Graduate Student

UC Santa Barbara

Harry Nelson	PI, Professor
Susanne Kyre	Engineer
Dean White	Engineer
Carmen Carmona	Postdoc
Scott Haselschwardt	Graduate Student
Curt Nehrkorn	Graduate Student
Melih Solmaz	Graduate Student

University College London, UK

Chamkaur Ghag	PI, Lecturer
James Dobson	Postdoc
Sally Shaw	Graduate Student

University of Maryland

Carter Hall	PI, Professor
Jon Balajthy	Graduate Student
Richard Knoche	Graduate Student

University of Rochester

Frank Wolfs	PI, Professor
Wojtek Skutski	Senior Scientist
Eryk Druszkiewicz	Graduate Student
Dev Ashish Khaitan	Graduate Student
Diktat Koyuncu	Graduate Student
M. Moongweluwan	Graduate Student
Jun Yin	Graduate Student

University of South Dakota

Dongming Mei	PI, Professor
Chao Zhang	Postdoc

University of Wisconsin

Kimberly Palladino	PI, Asst Professor
Shaun Alsum	Graduate Student

Overview

- LUX refresher
- Original LUX results (2014) and re-analysis (2015)
- Details of internal electric fields
- Grid conditioning
- 332 day run
- Data salting
- WIMP-search data

L U X

Large Underground Xenon experiment

A direct-detection search, looking primarily (but not only) for WIMP dark matter

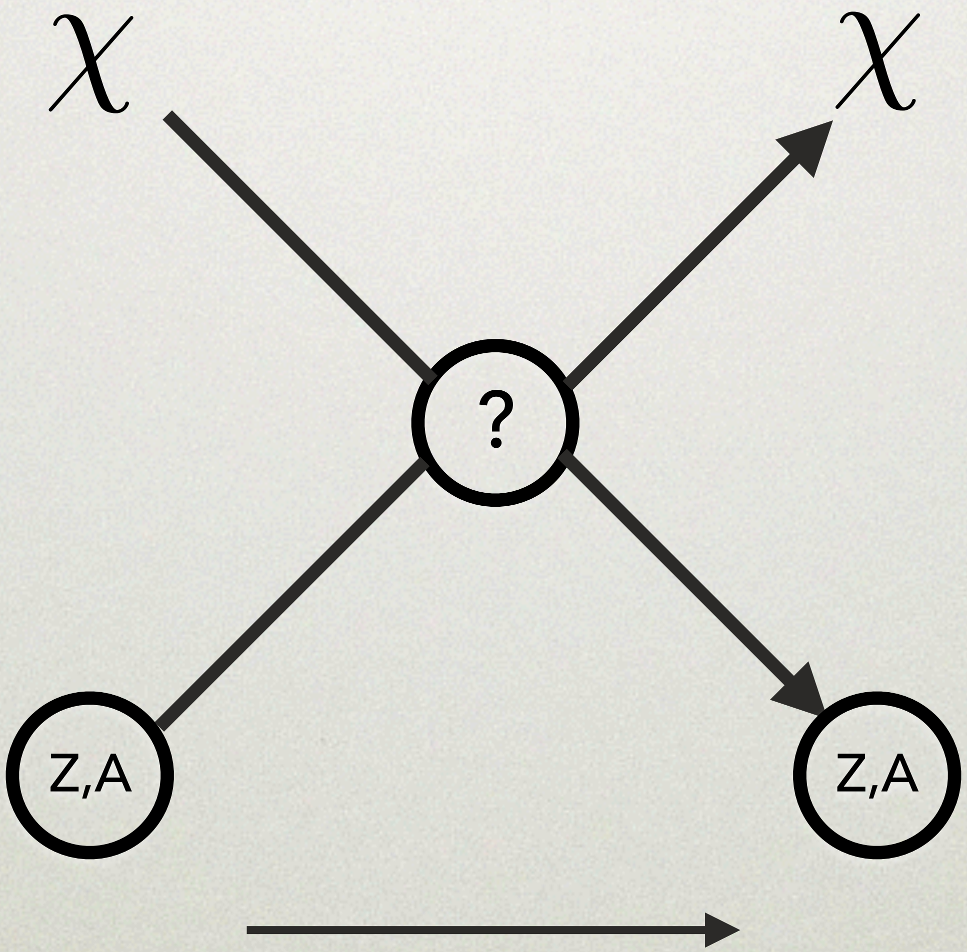

WHY USE LIQUID XENON TO LOOK FOR WIMPS?

Why use liquid xenon?

Large signal

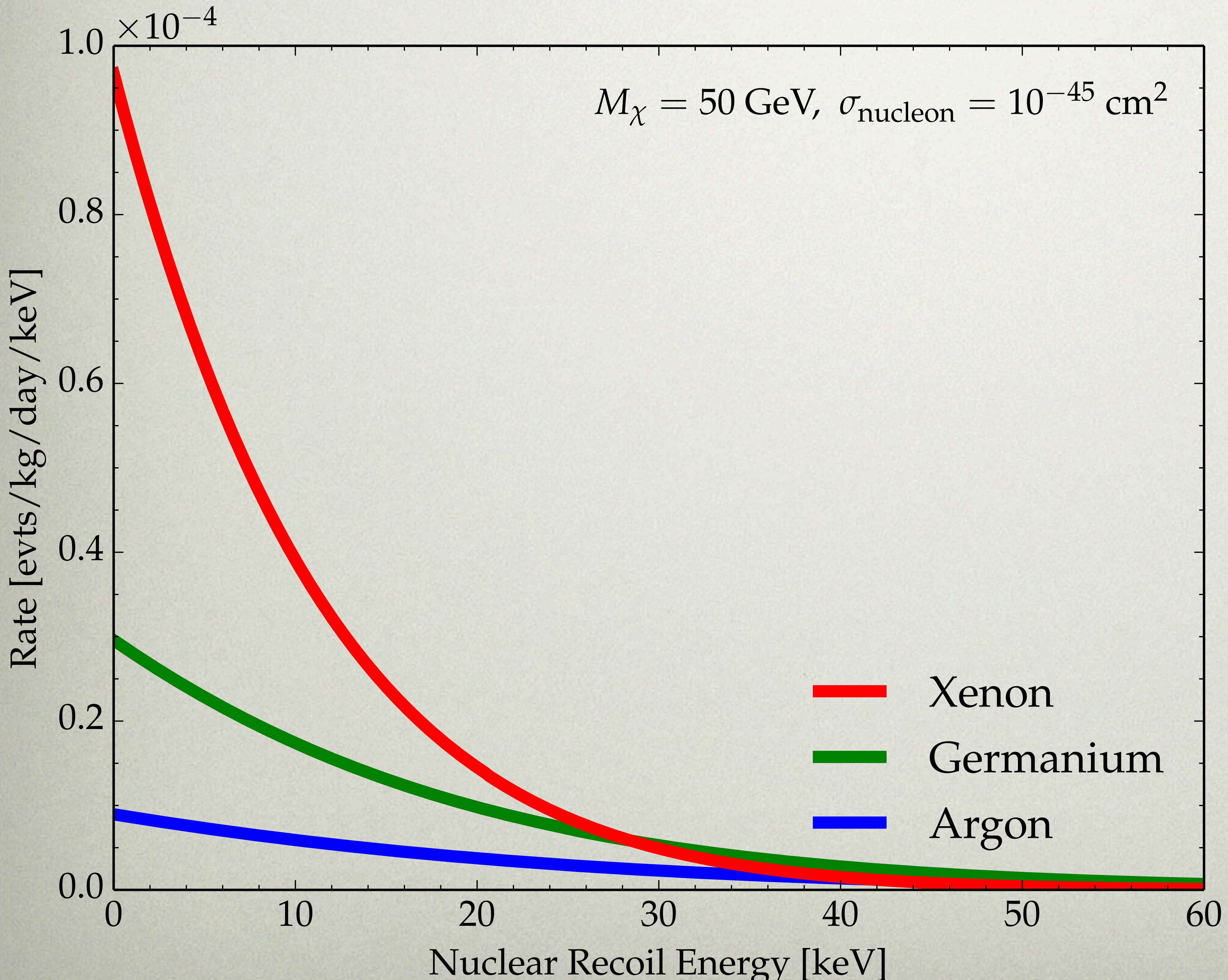

- Scalar WIMP-nucleus interactions lead to an A^2 enhancement in the differential rate relative to other commonly used detection media.
- Natural xenon contains ~50% odd isotopes, giving high sensitivity to spin-dependent interactions.

Why use liquid xenon?

Low background

Event rate (DRU)*

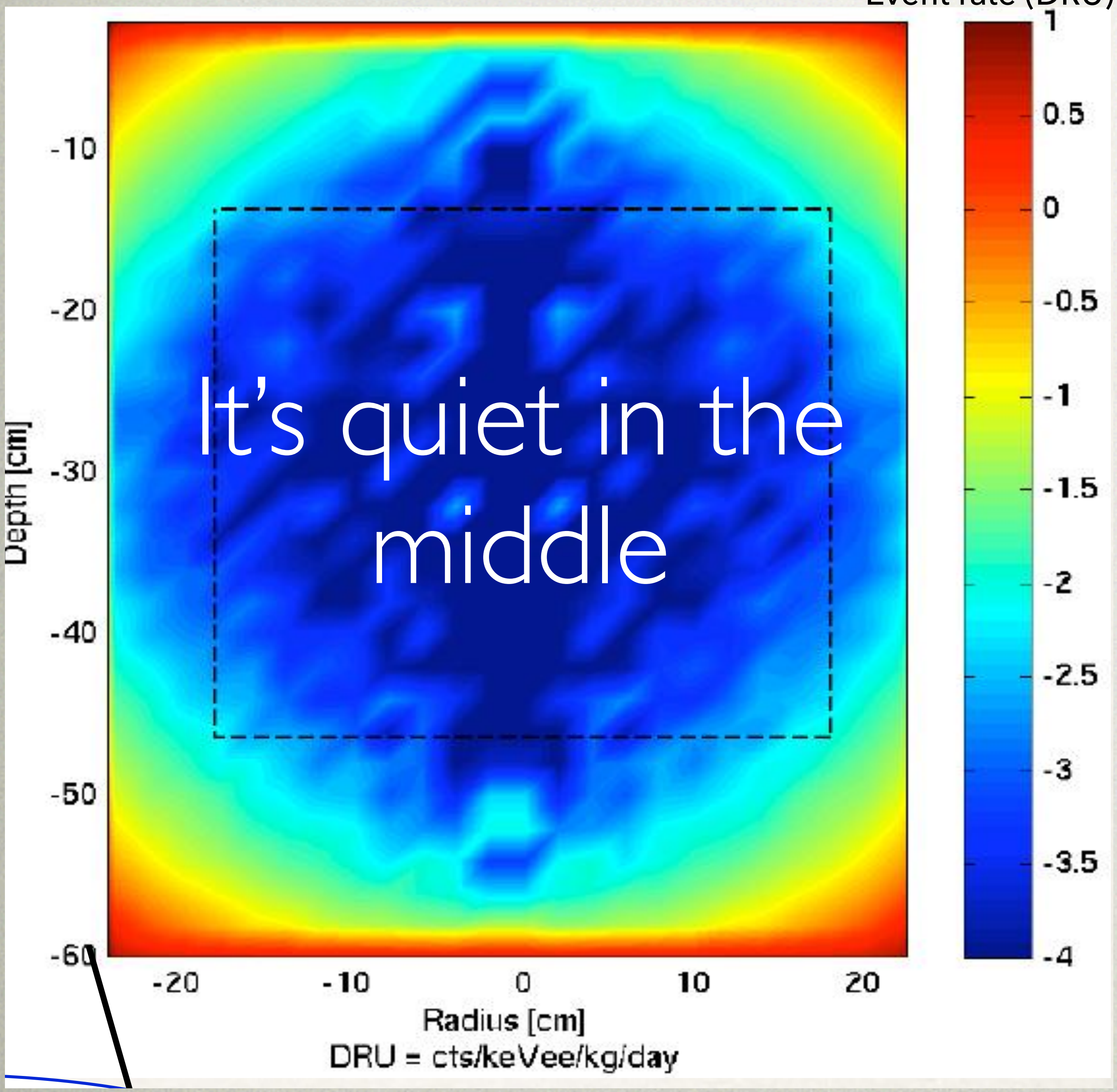

* "DRU" = evt/kg/day/keV

- Liquid detectors are scalable up to large size.
- Dual-phase time projection chambers feature 3-D localization of events.
- The combination of these two features permits an ultra-low-background inner region to be defined. **We are sensitive to signals that would cause as little as a few events per century in a kilogram of xenon.**

Detection technique

- LUX is a dual-phase time projection chamber (like most other liquid-noble DM experiments); essentially a cylinder of LXe.
- Primary scintillation light ("S1") is emitted from the interaction vertex, and recorded by an array of PMTs on top and bottom.
- Electrons emitted from the interaction are drifted by an applied field to the surface and into the gas, where they emit proportional scintillation light ("S2"), also recorded by the PMTs.
- This design permits:
  - **3-D localization of each vertex.**
  - **Identification of multiple scatters (via S2 count).**
  - **ER/NR discrimination (via S2/S1)**
  - **Sensitivity to single ionization electrons.**

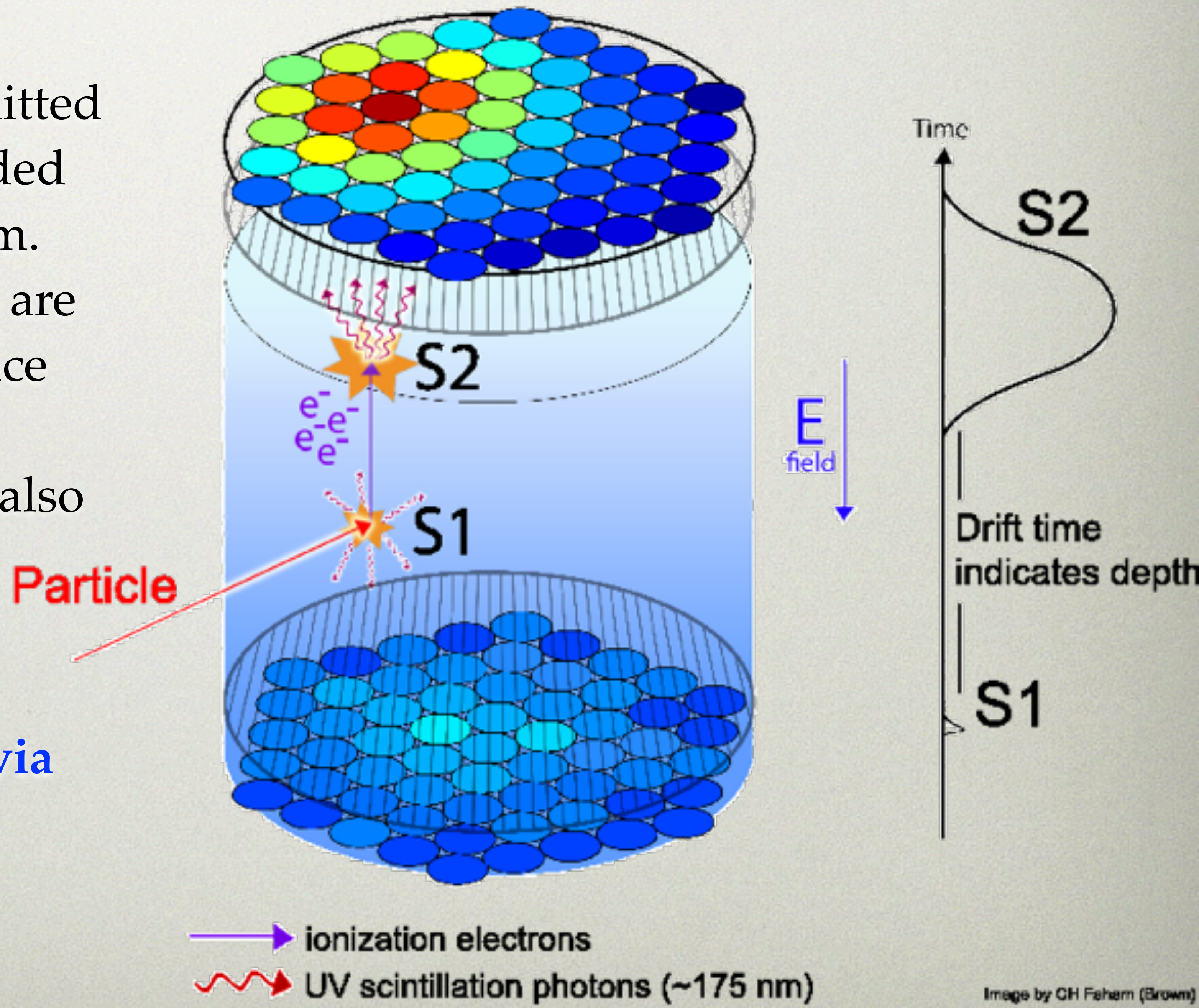

LUX DETECTOR

- 48cm diameter by 48 cm height dodecagonal "cylinder".
- 250.9 kg LXe in active region
- 61 PMTs on top, 61 on bottom, specially produced for low radiogenic BGs and VUV sensitivity.
- Xenon was pre-purified via chromatographic separation, reducing residual krypton.
- Liquid is continuously recirculated (¼ tonne per day) to maintain chemical purity.
- Ultra-low BG titanium cryostat.

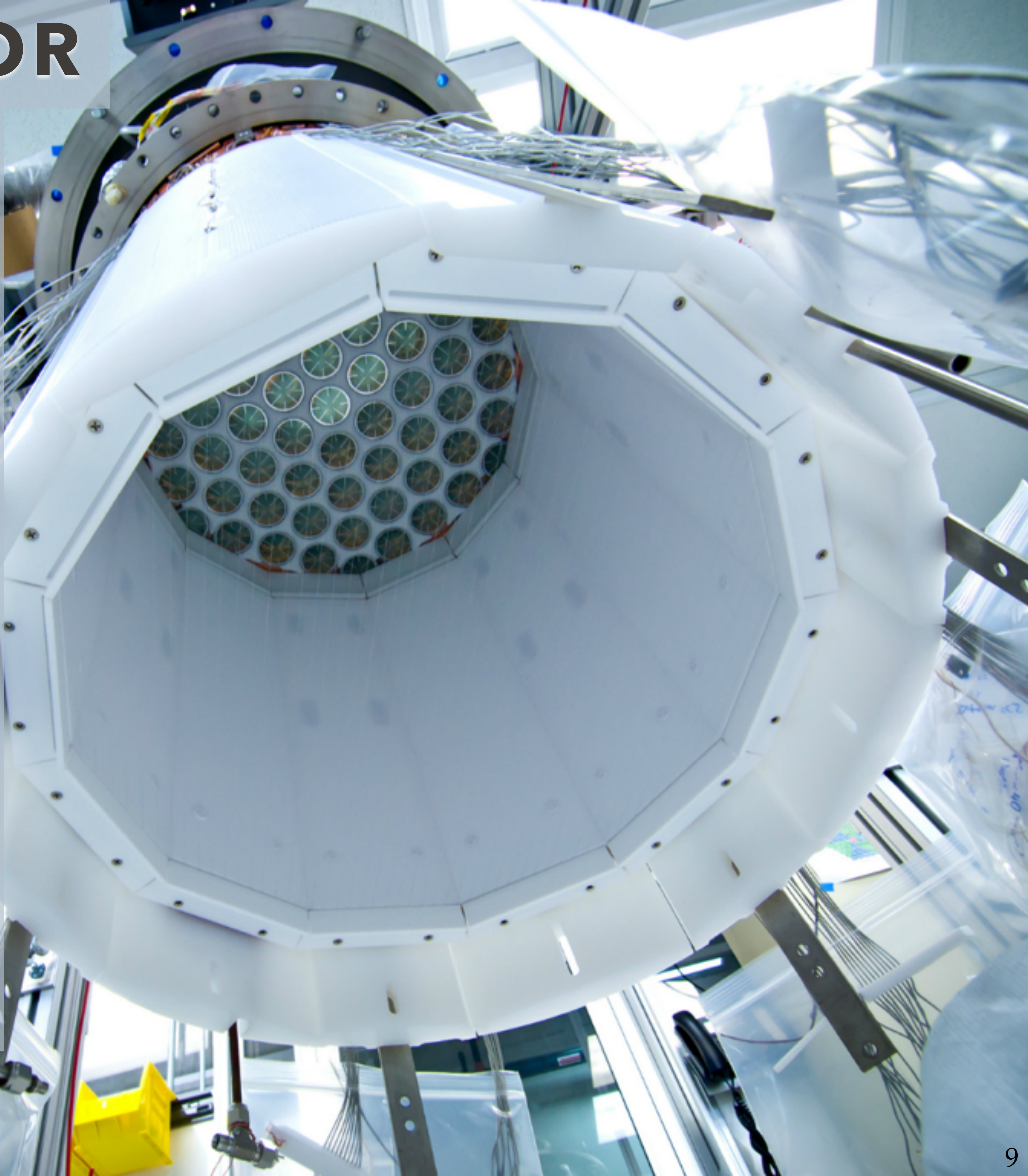

Sanford Underground Research Facility

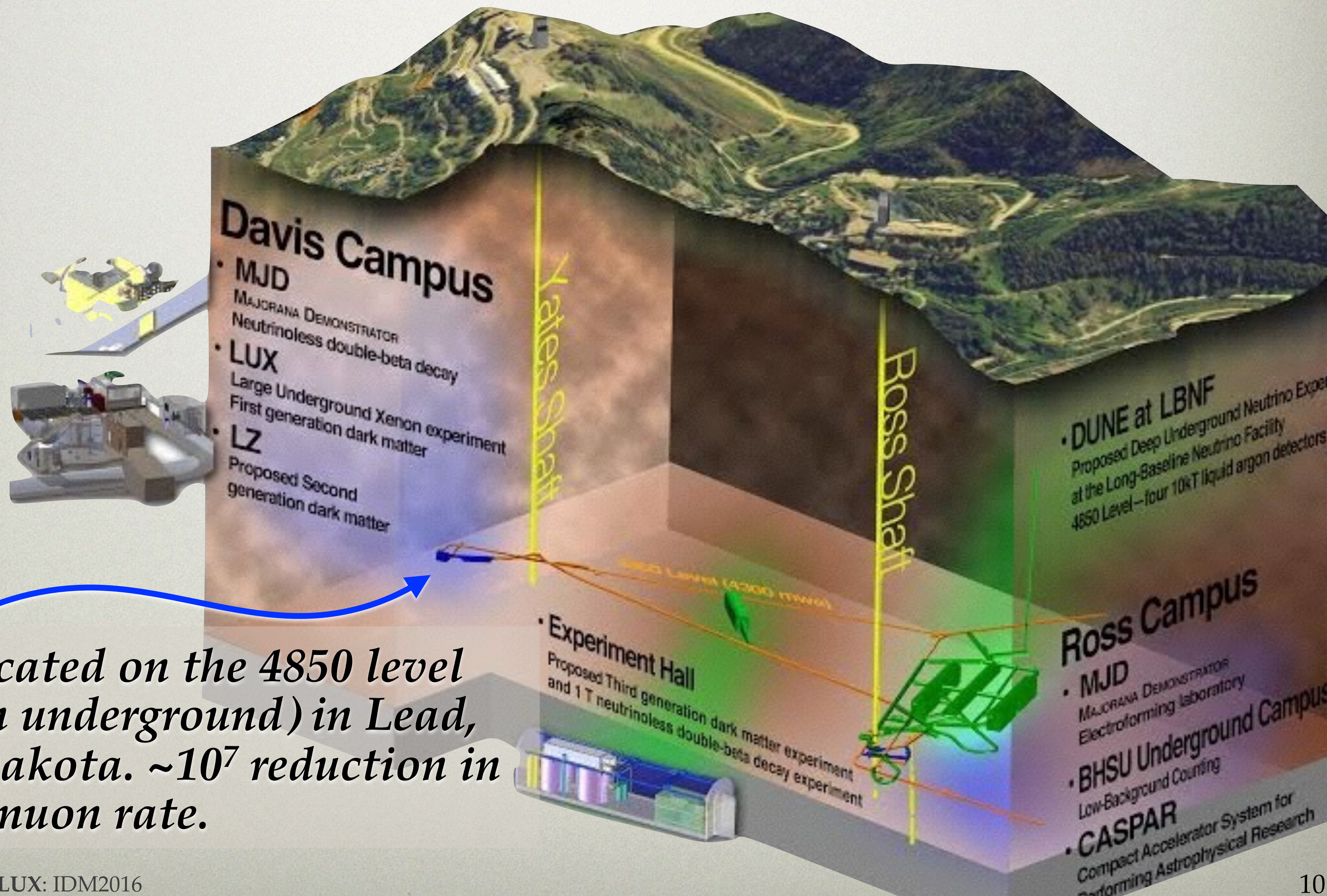

***LUX*, located on the 4850 level (~1.5 km underground) in Lead, South Dakota. ~10^7 reduction in cosmic muon rate.**

Calibrations

LUX has taken calibrations very seriously. We make heavy use of:

- **^{83m}Kr**: 1.8hr half life, monoenergetic, injected ~weekly. Spatially uniform!
- **CH_3T** (tritiated methane): Removed on a ~8 hr timescale by our purification system. Injected 2-3 times per year. Spatially uniform! Used to define our ER band.
- **Deuterium-Deuterium** neutron generator: 2.45MeV monoenergetic, collimated neutron beam, incident at any desired height. Used to define our NR band.

See talks by Sally Shaw and Rick Gaitskell

LUX timeline

2008: LUX funded (DOE+NSF)

2012 (Jul): Underground lab complete, LUX moves UG

2013 (Apr): Commissioning complete

2014 (Mar): First results (3 months) reported

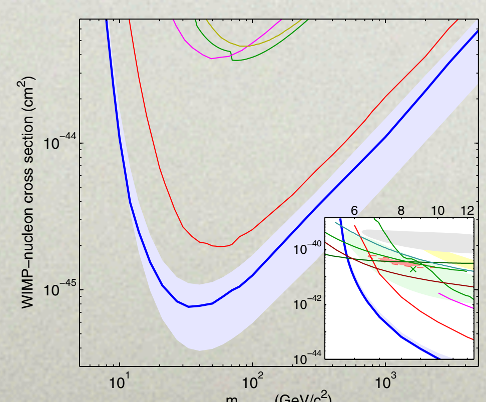

2014 (Sep): 332-day run started!

2015 (Dec.) 3-month run reanalysis posted. Published 2016 (Apr).

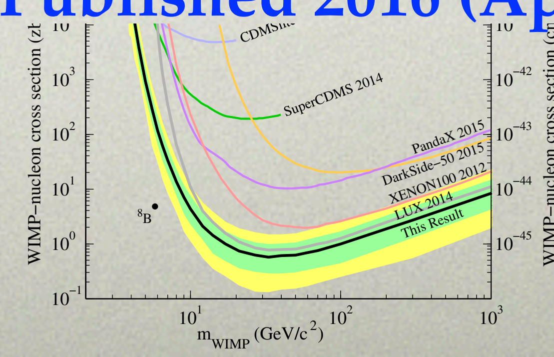

2016 (May): Run finished

2016 (July): 332 days DM results presented

LUX2014/2015 — 95 live days

- Back-to-back Phys.Rev.Letters on spin independent and dependent WIMP-nucleon couplings from the LUX2014 data (Presented in 2015).

Also see talks by M.F. Marzioni and N. Larsen

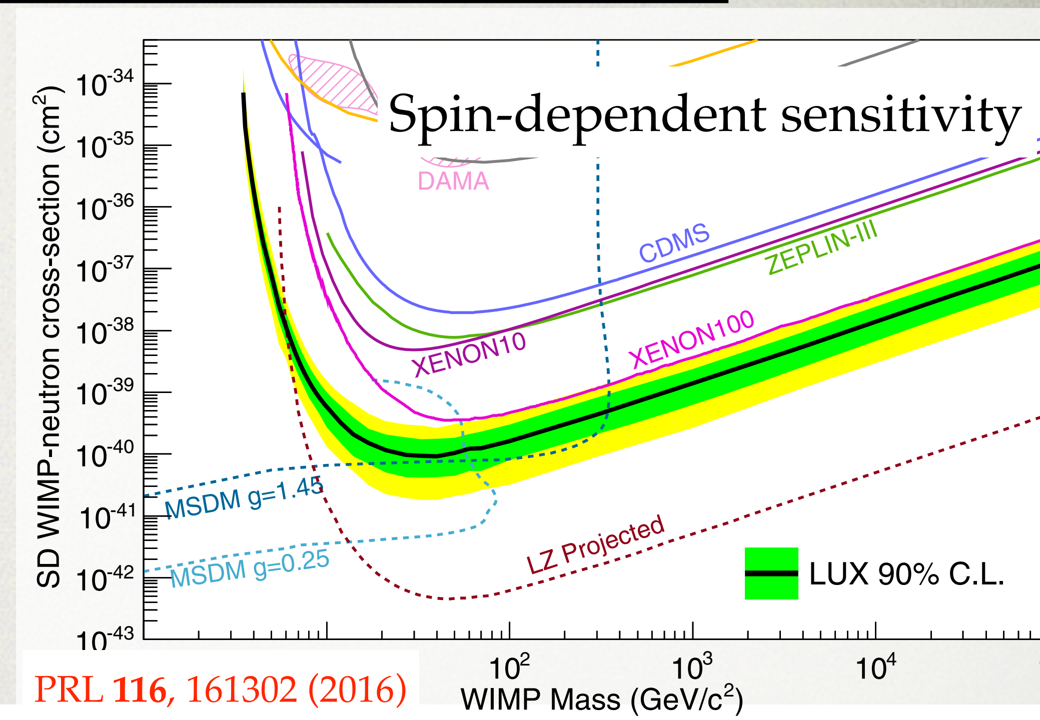

PRL **116**, 161302 (2016)

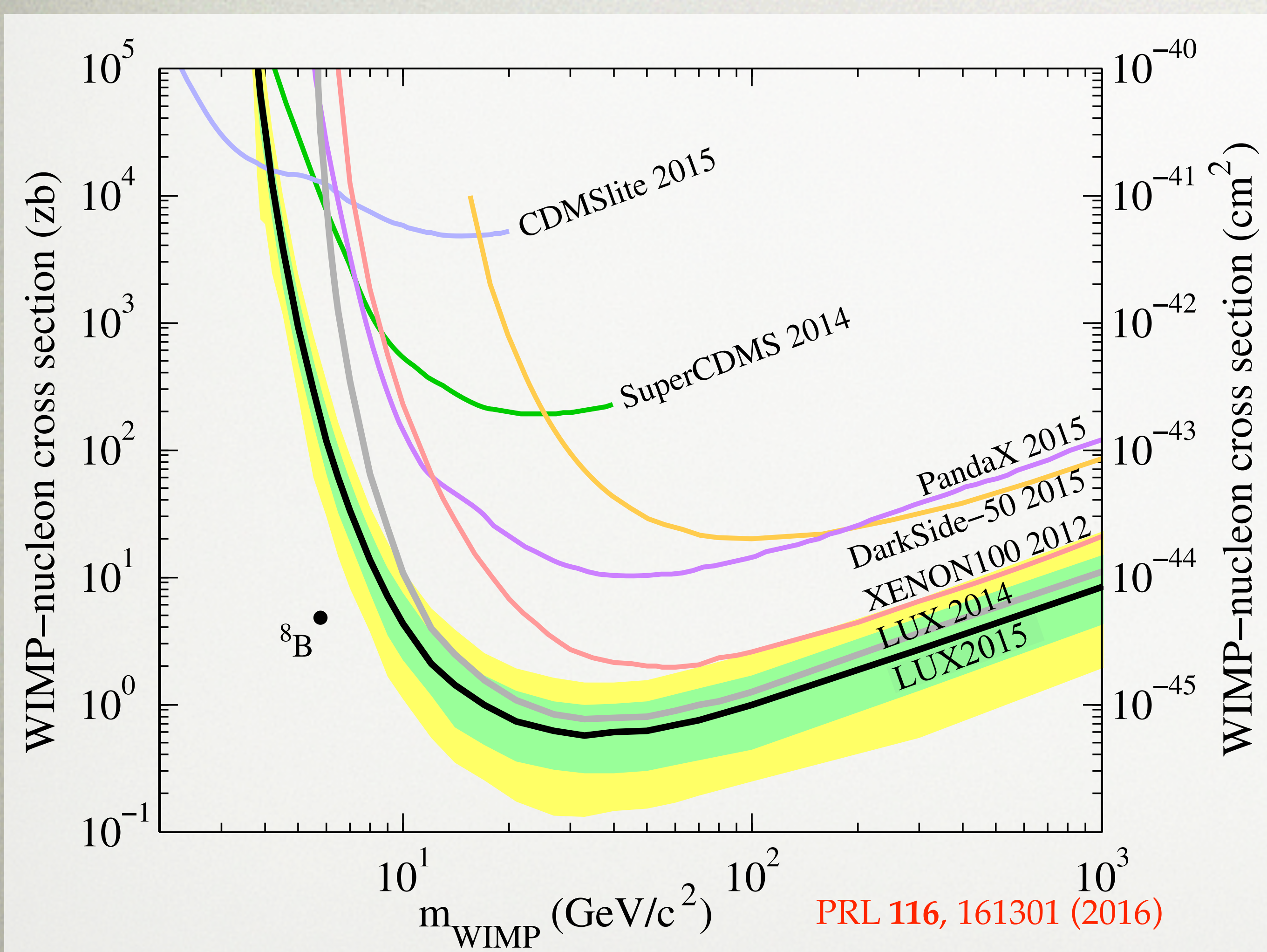

PRL **116**, 161301 (2016)

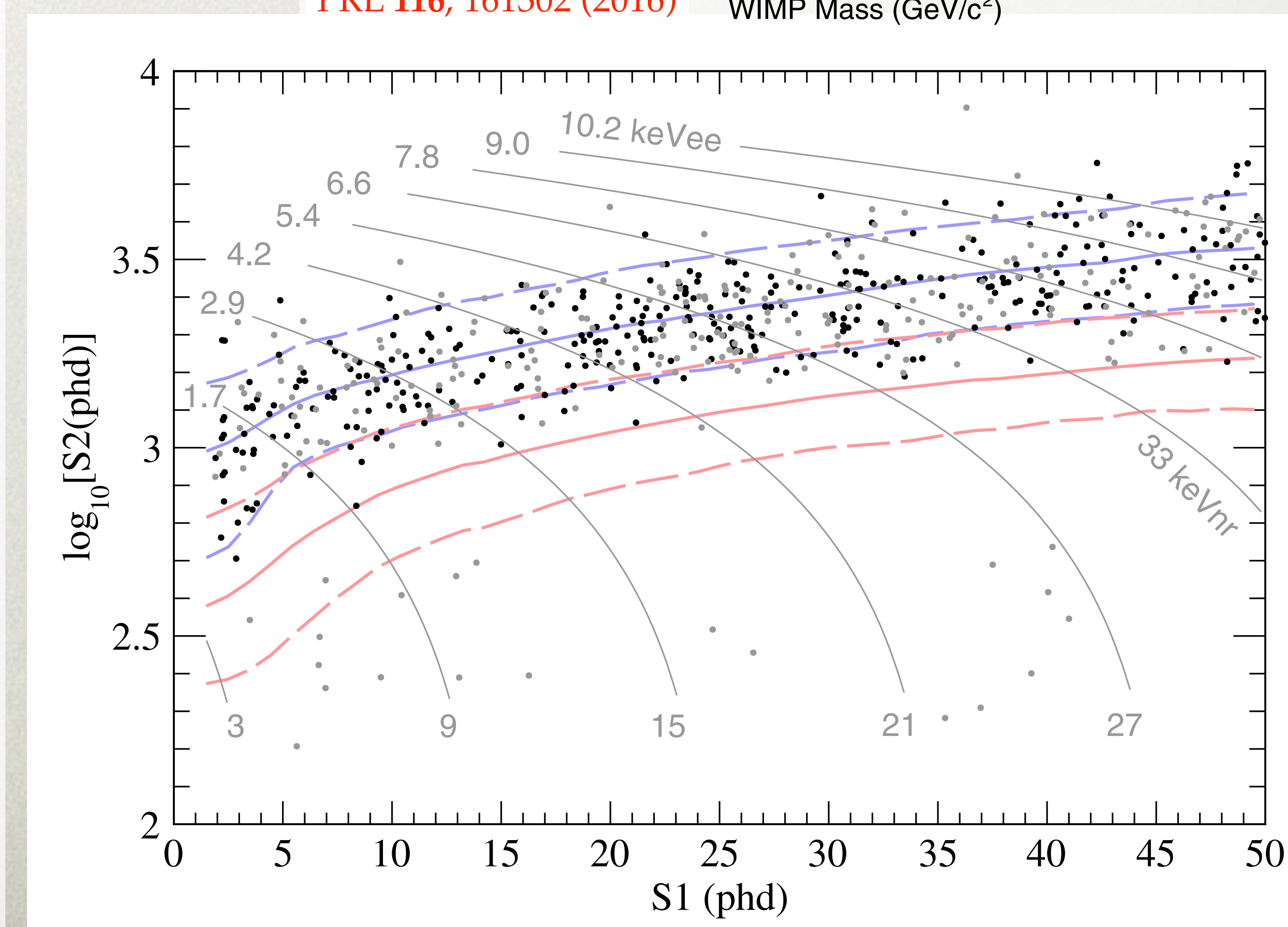

Electric-field uniformity

- Field-shaping rings help to ensure a uniform field magnitude throughout the ~90 liters, though a residual radial component does creep into the active region.
- Electrons therefore exit the liquid surface (where they are detected) at a radius smaller than that of the interaction vertex.
- The shape of the detector wall, as measured, is therefore not a vertical line.
- Measured coordinates ("S2 space") are squeezed relative to physical coordinates ("real space"), though they represent the same actual volume. **Fiducial volume is not decreased.**

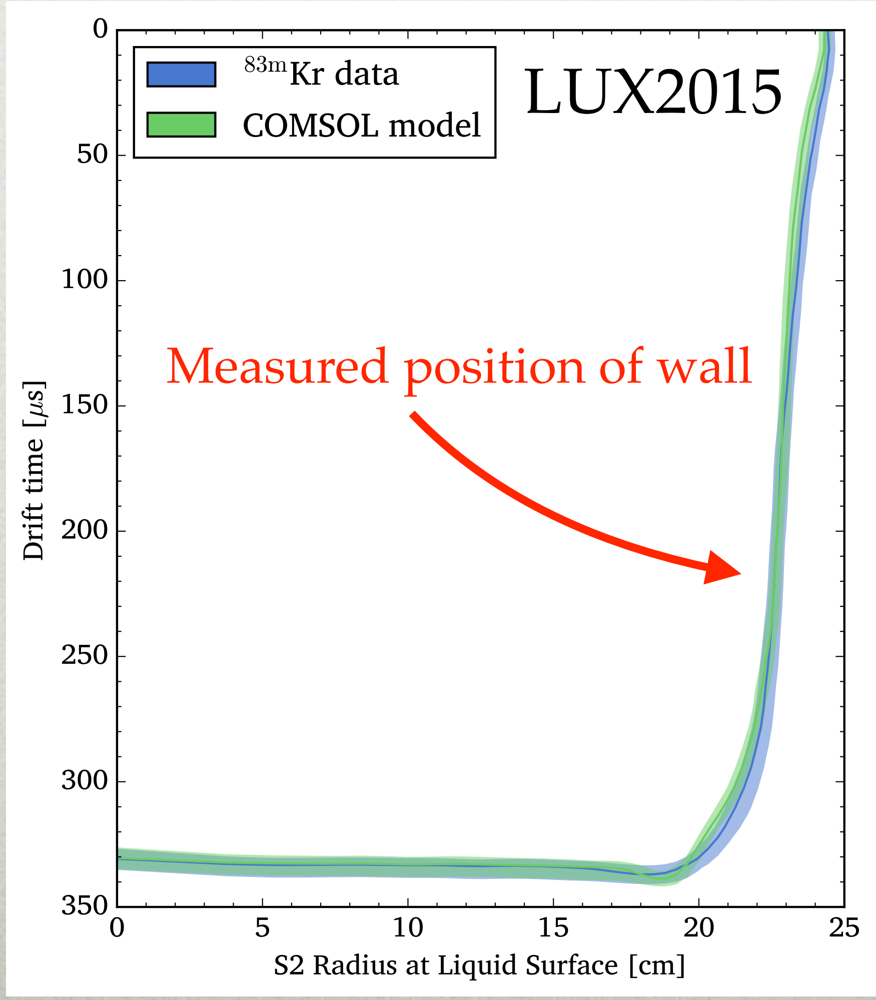

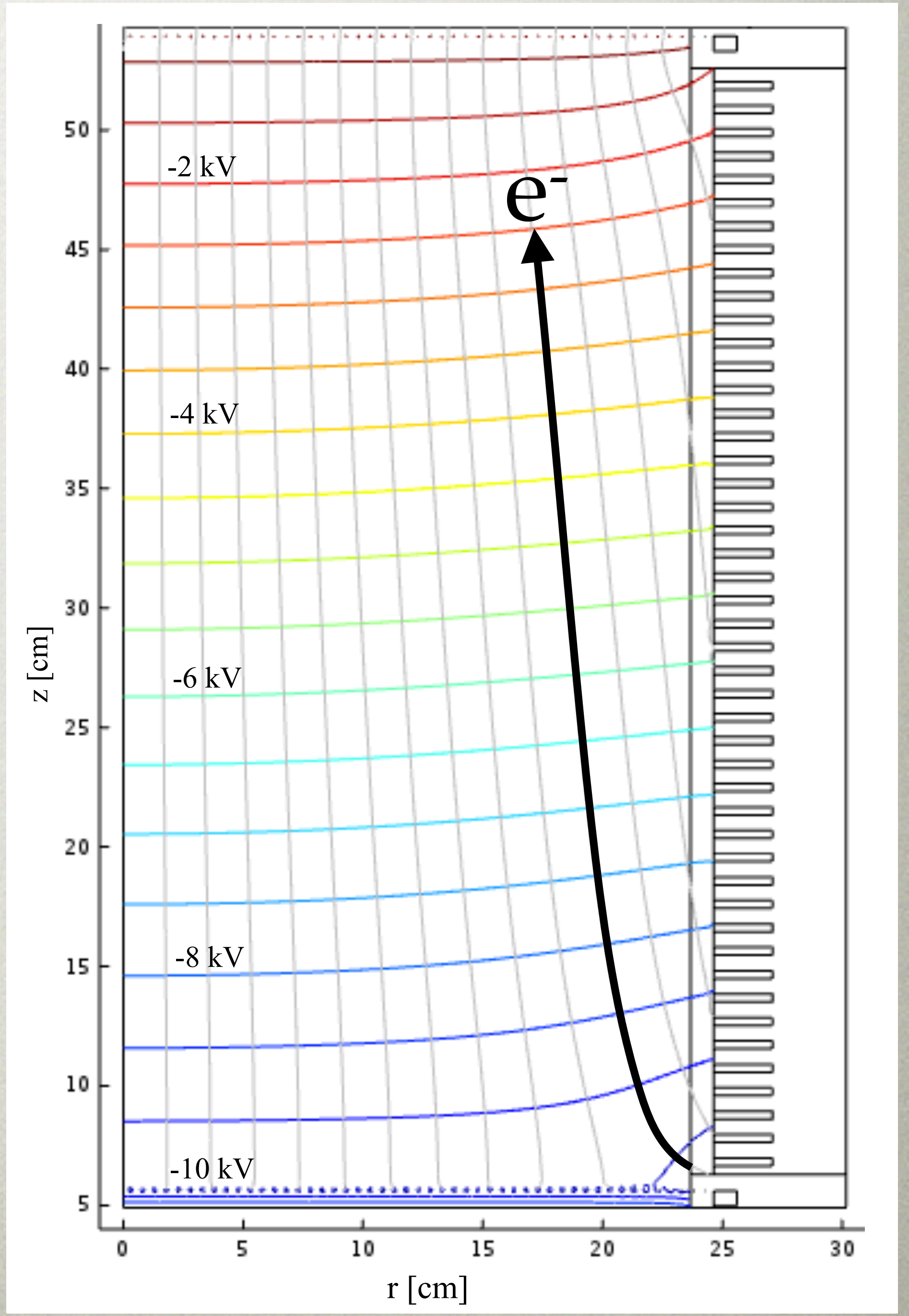

Grid conditioning

The LUX2015 results featured:

- 50% electron extraction efficiency

In order to improve these values, after LUX2014 (and following calibrations), the LUX electrodes were "conditioned". The voltage is raised for an extended period of time until significant current is drawn, in the middle of the threshold for sparking.

The result of the conditioning is:

- 75% electron extraction efficiency.

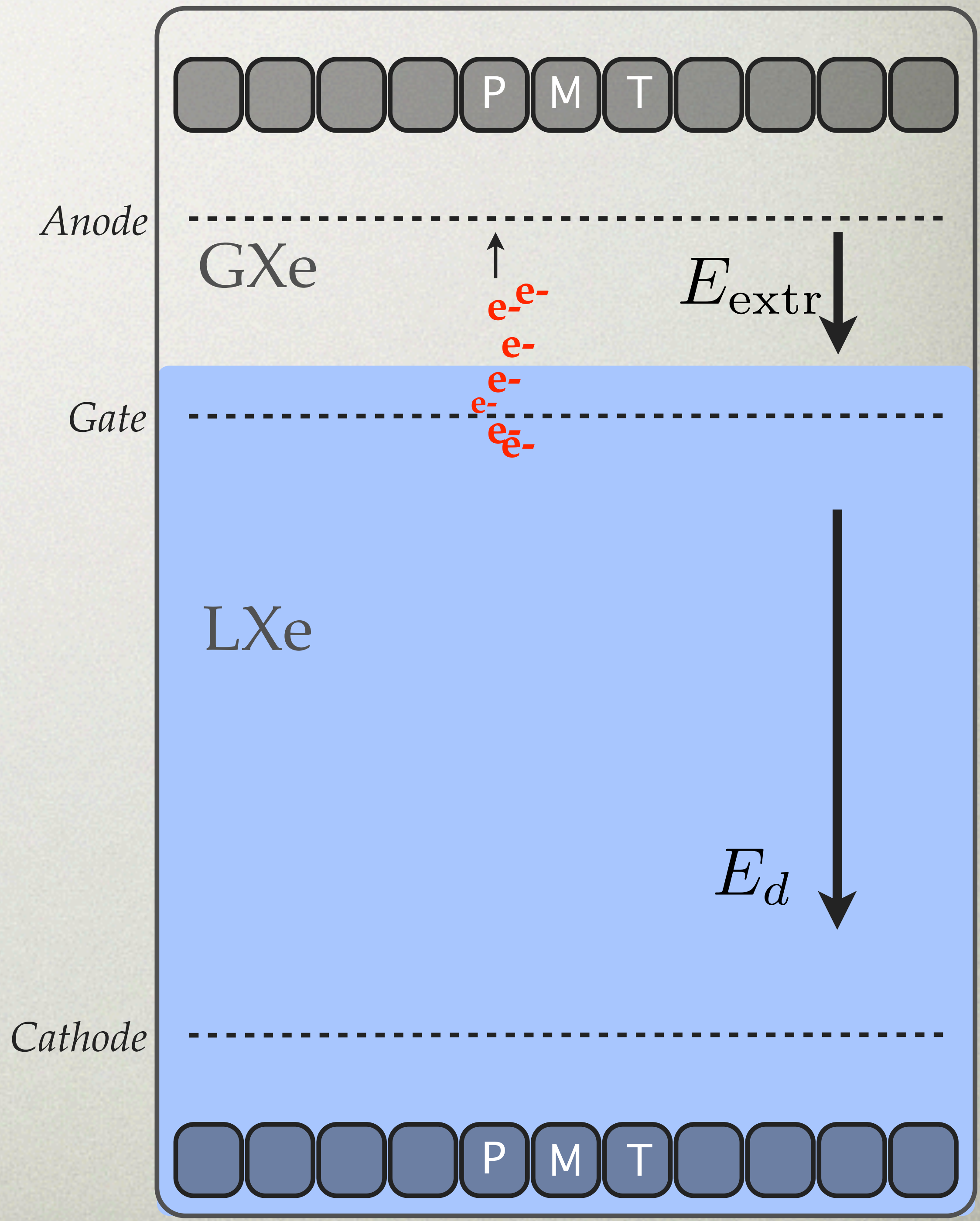

Grid-conditioning side effects

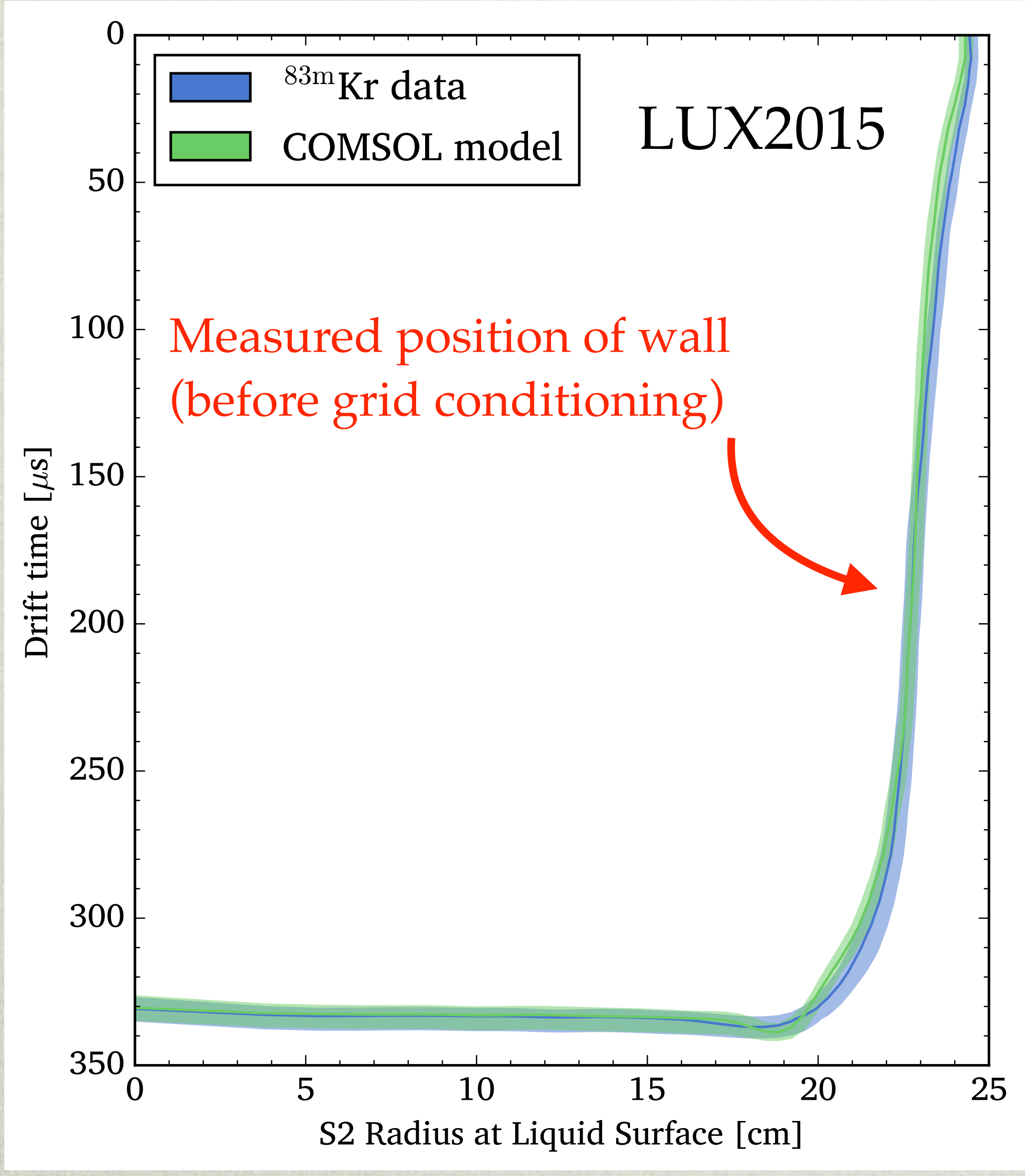

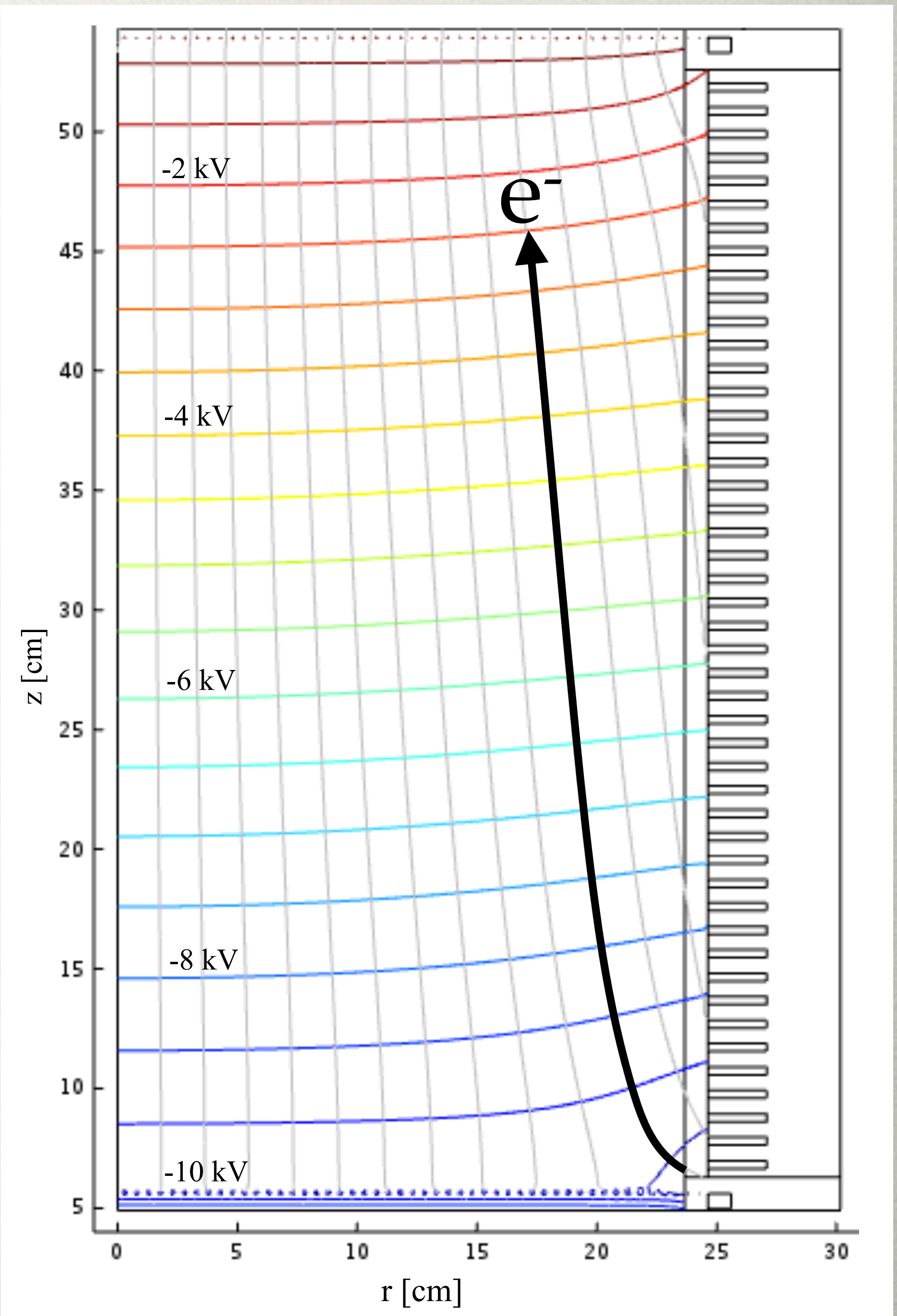

Grid-conditioning side effects

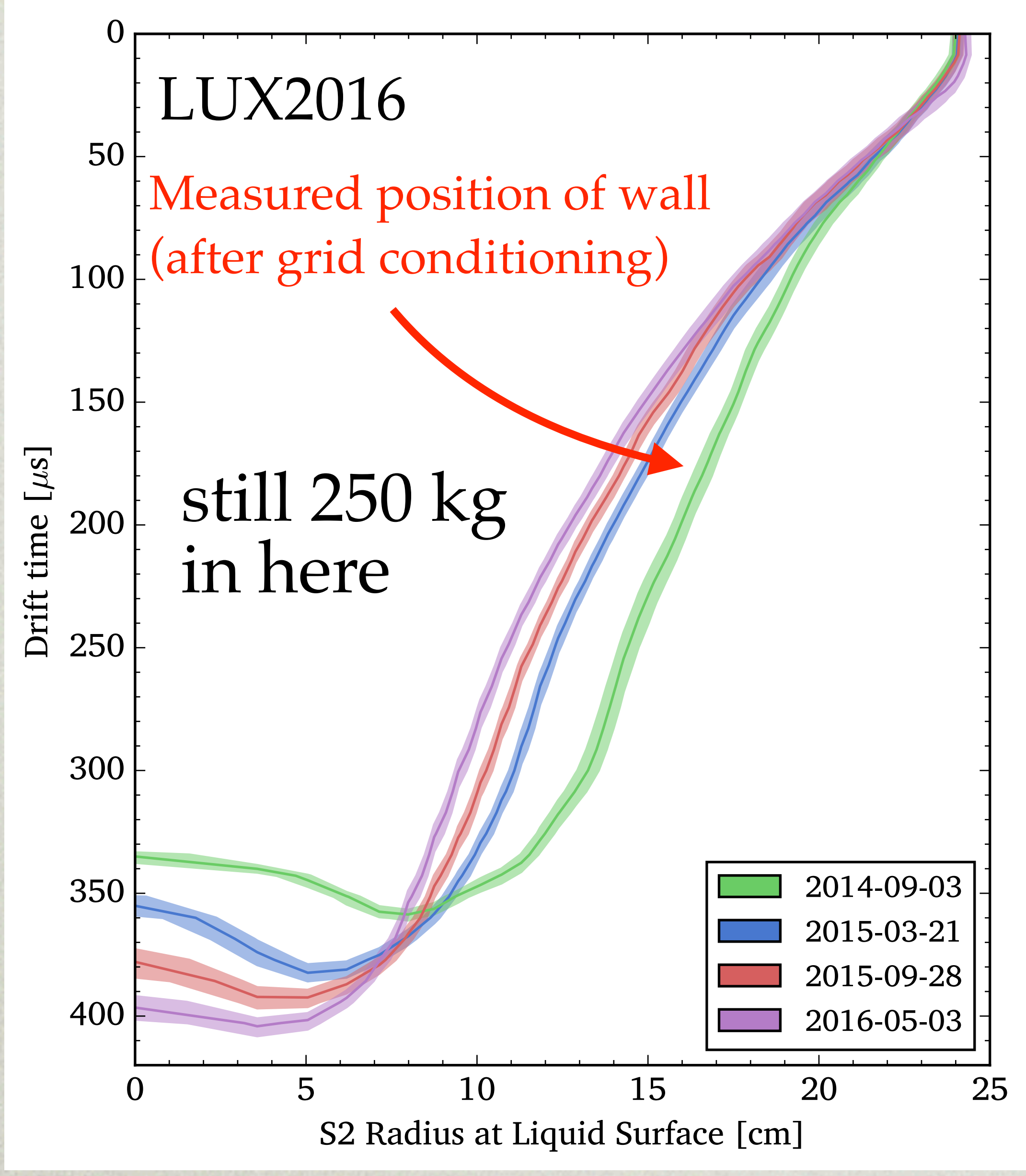

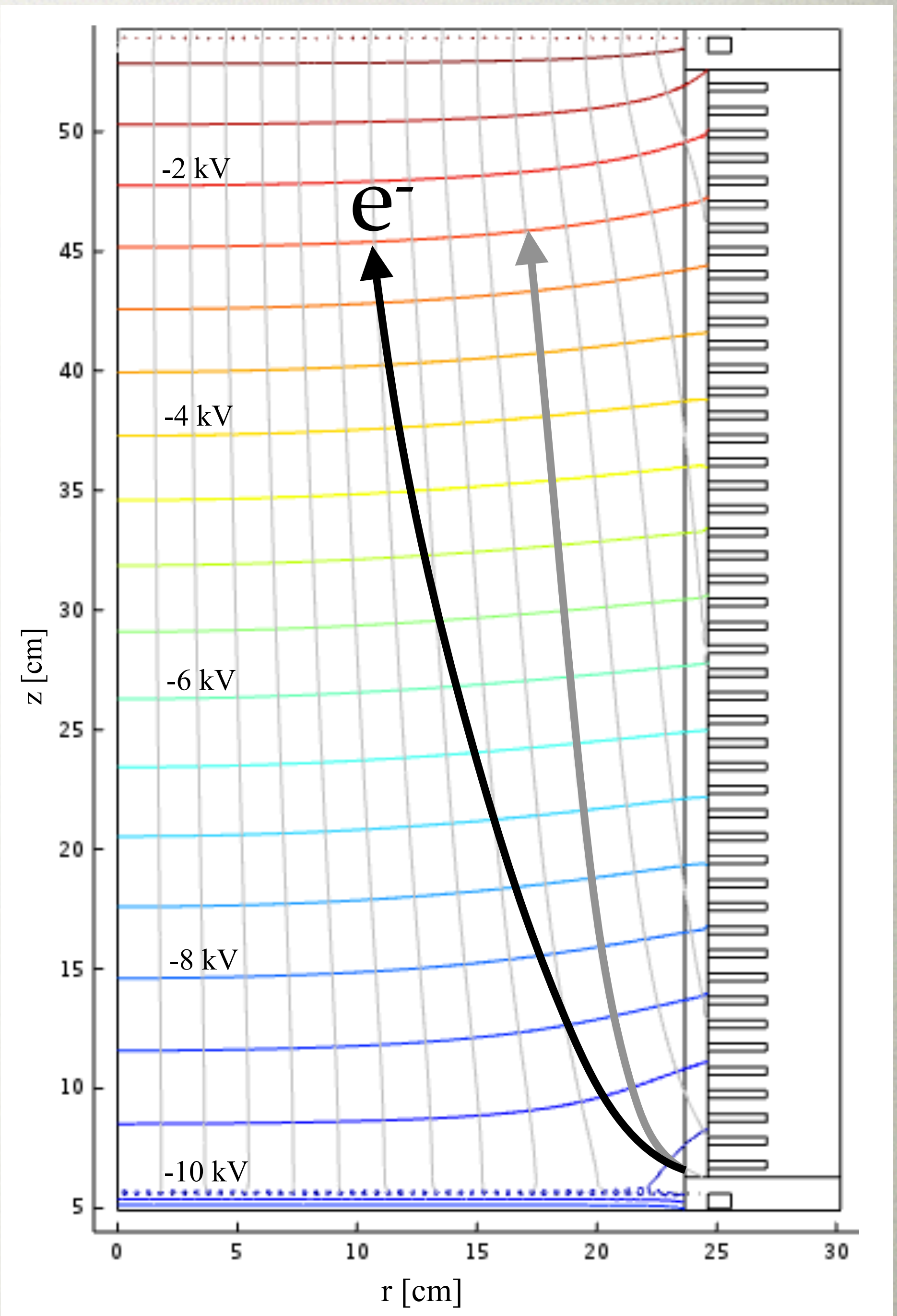

- After grid conditioning, the radial field component increased significantly.

Grid-conditioning side effects

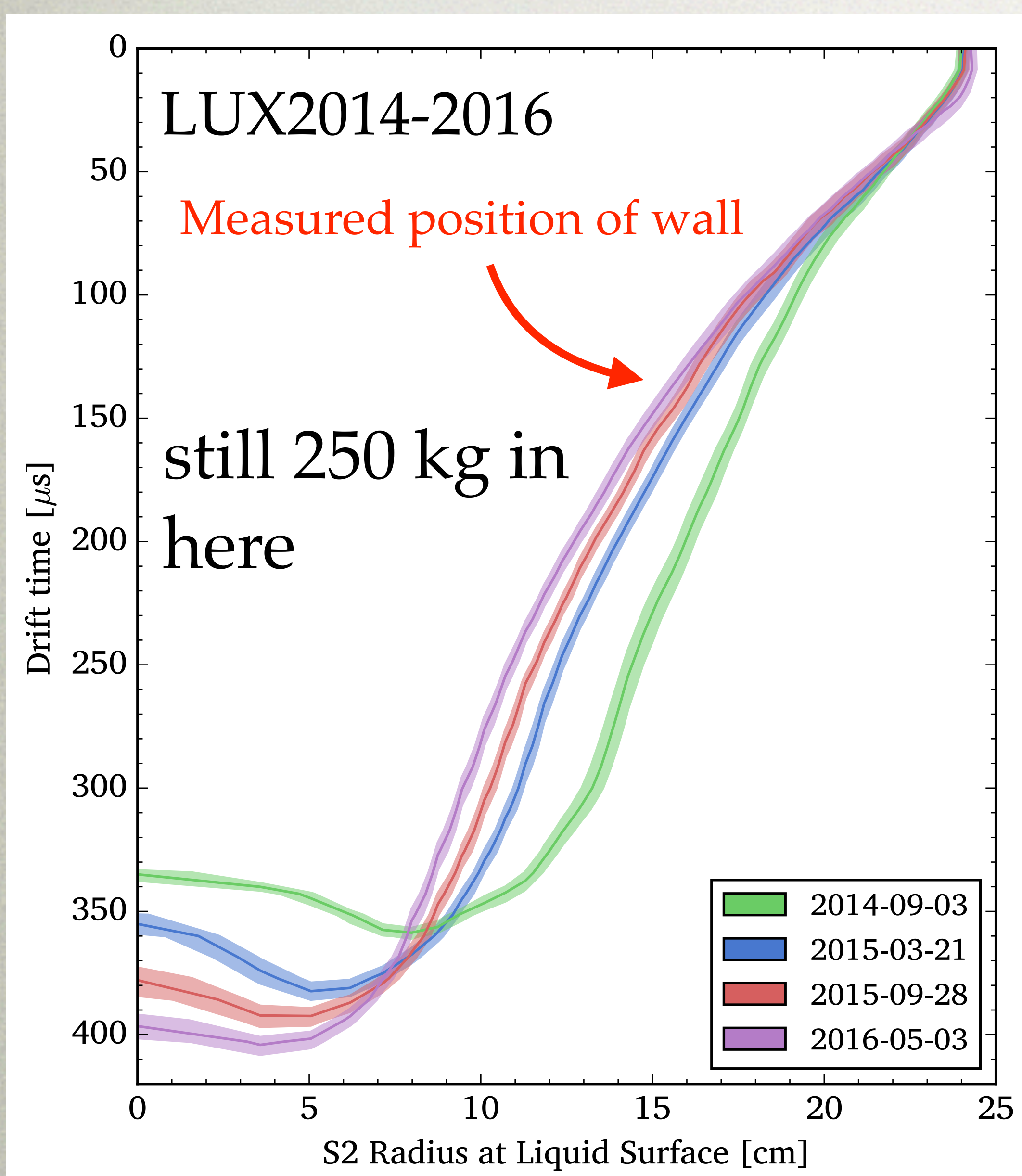

- After grid conditioning, the radial field component increased significantly.
- The physical position of the wall of course has not changed (i.e. our active volume is unchanged), but the **measured** wall radius depends on the depth of the event.
- The measured wall radius is not axially symmetric.
- The measured wall radius varies slowly in time.

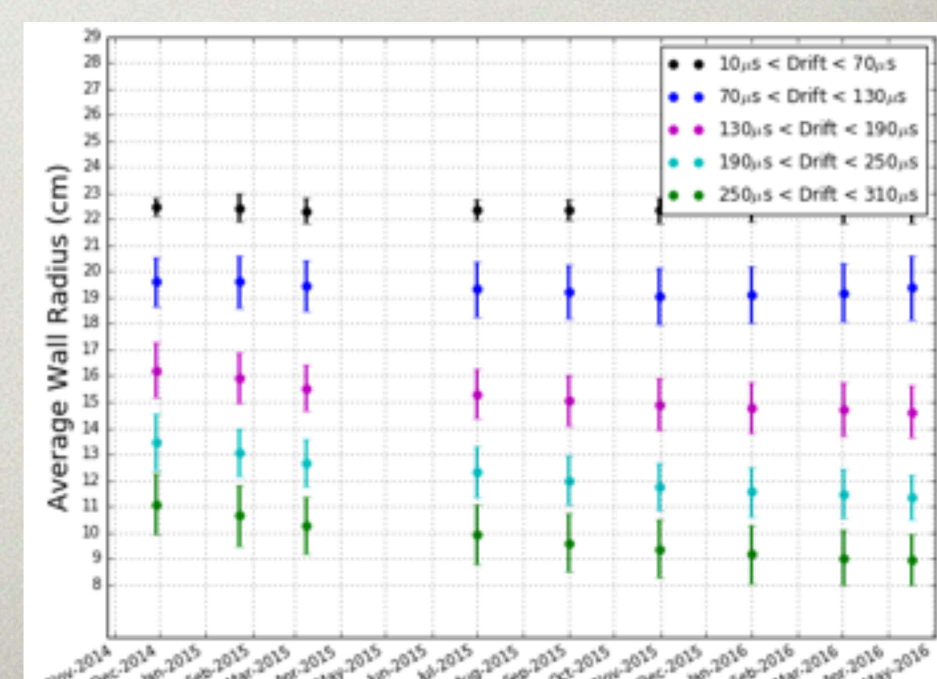

Modeling the E-field

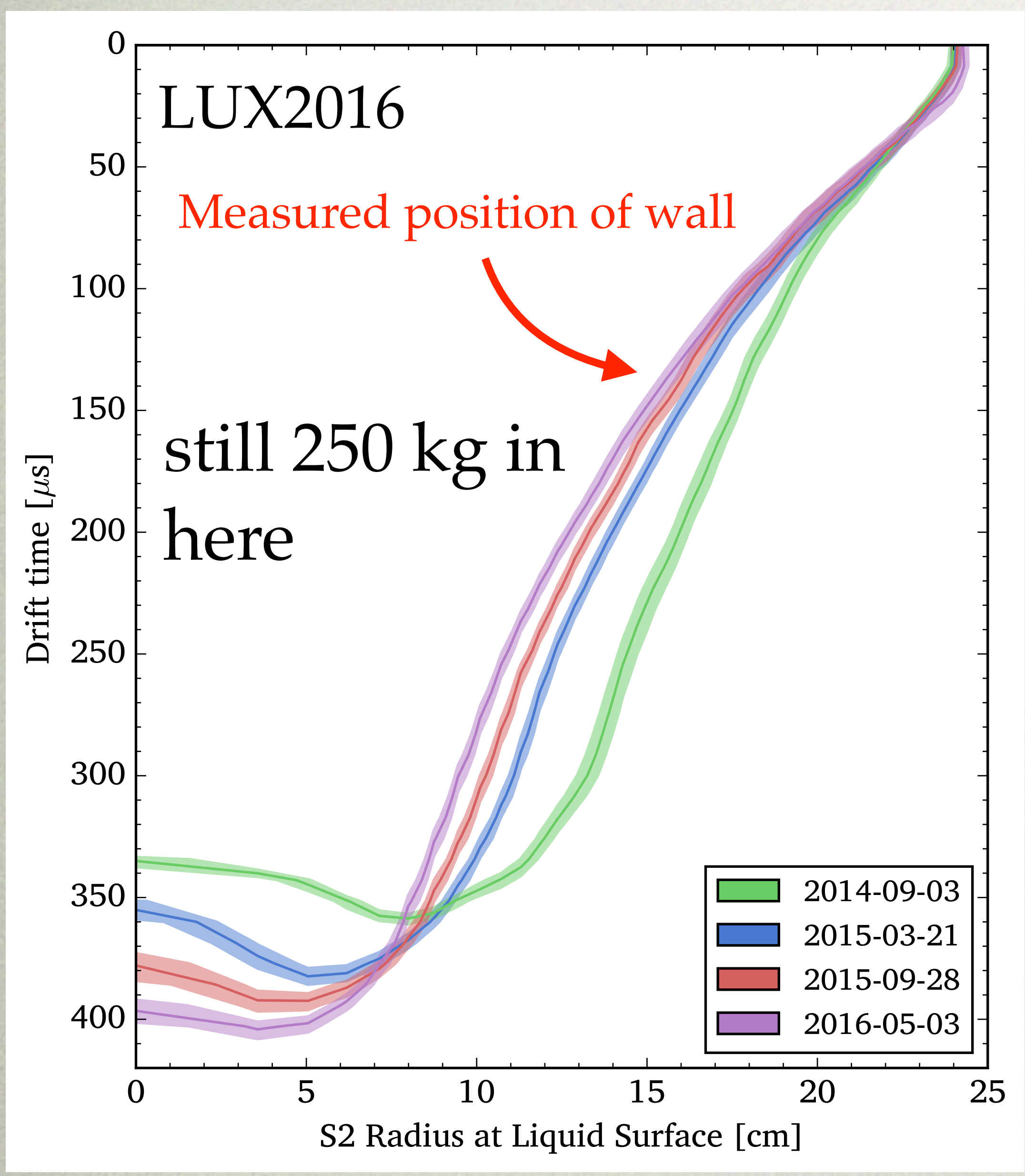

- The effect is consistent with a buildup of negative charge on the PTFE walls of the TPC.

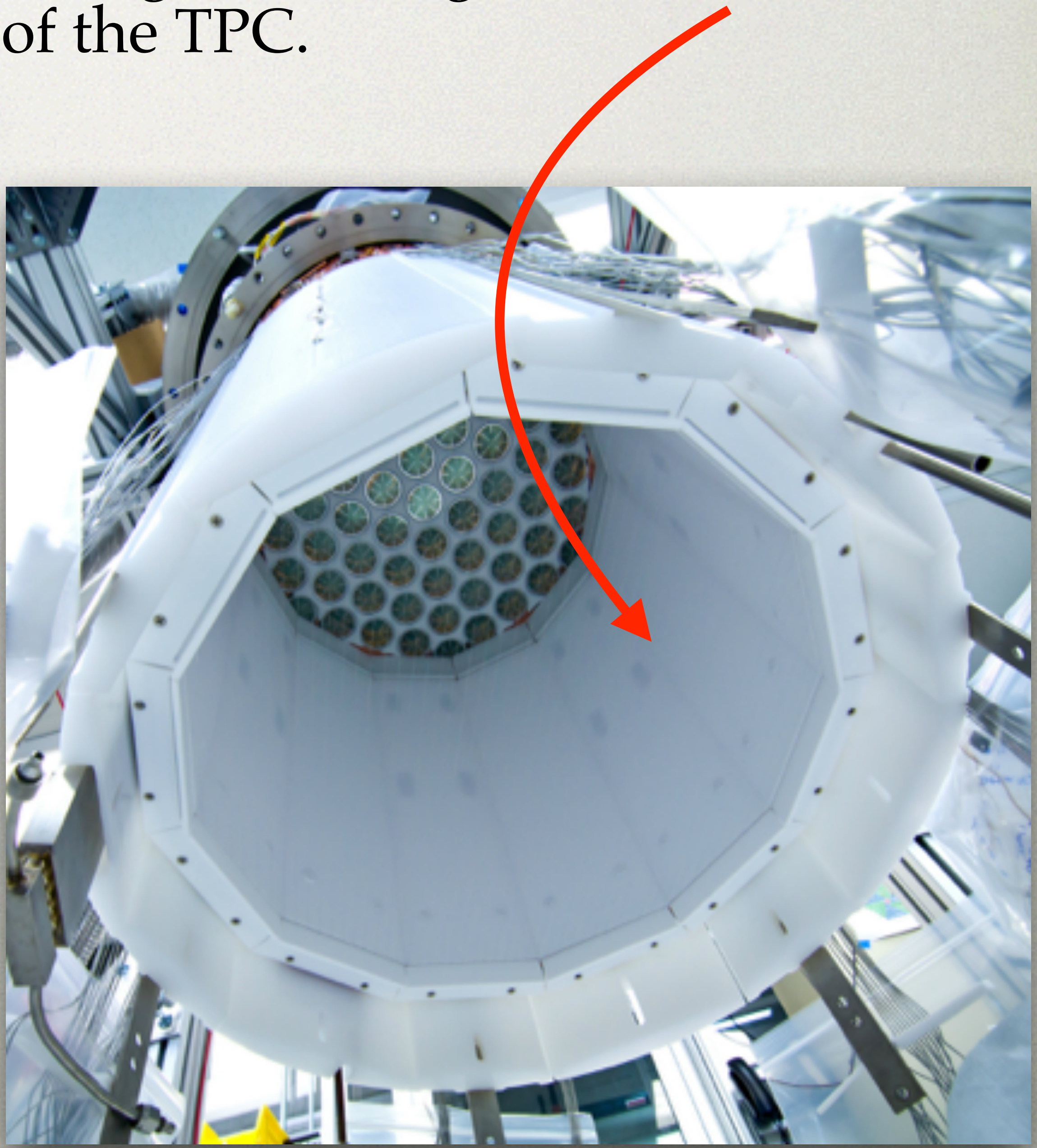

- We have built a fully 3D electrostatic field model which traces the evolution of this effect in time.
- Calibration data allows for robust calculation of fiducial volume.

Modeling the E-field

- Fully 3-D model is constructed in the COMSOL Multiphysics® FEM simulation software.
- Charges are added (non-uniformly) to the walls and the 3-D field is calculated.
- The 3D field map is combined with the known field dependence on the electron drift speed to obtain a mapping between "real space" and "S2 space" coordinates.
- Results are compared to the observed distribution of ^{83m}Kr decays, and the charge densities are iterated until a best-fit is obtained.

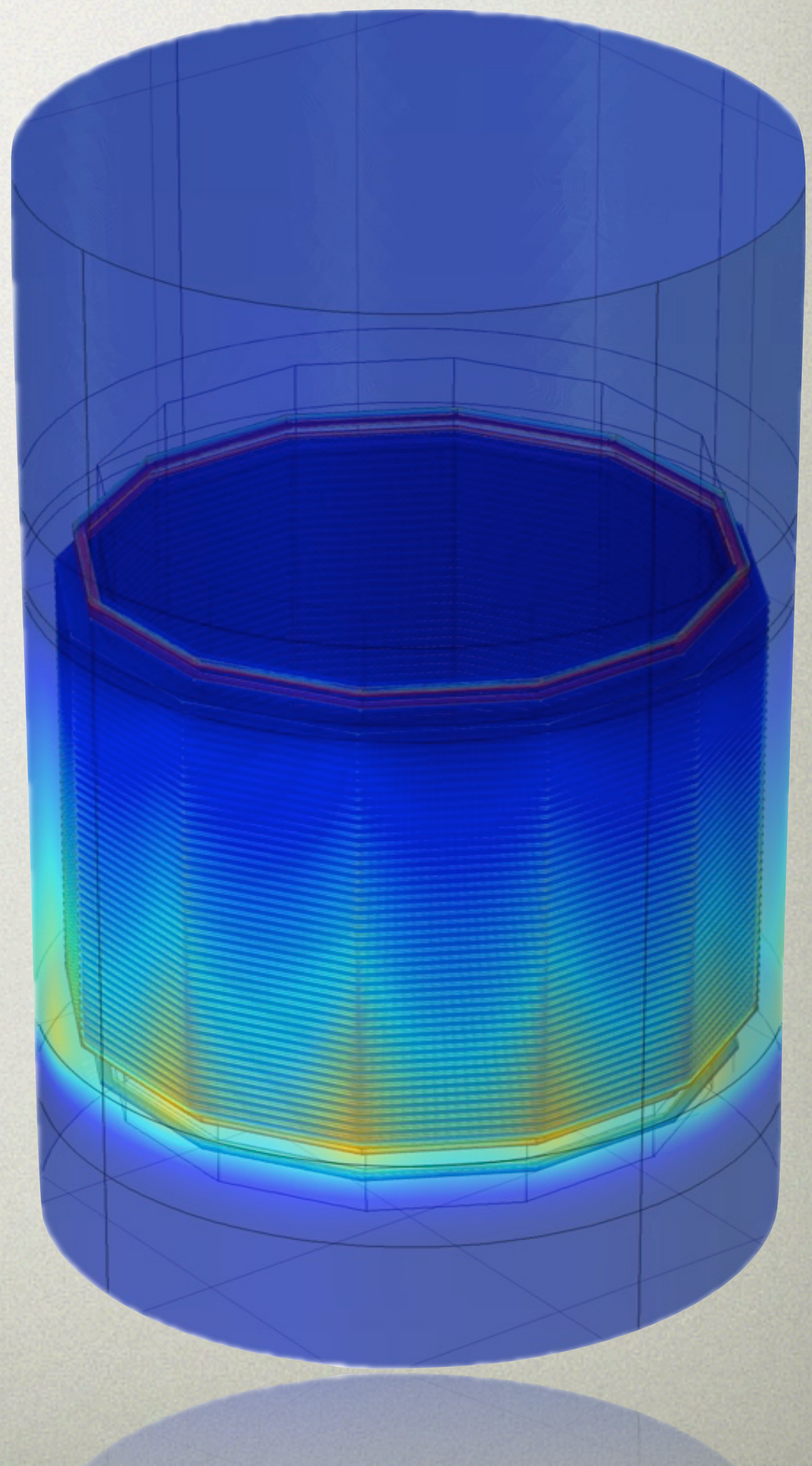

Modeling the E-field

- Fully 3-D model is constructed in the COMSOL Multiphysics® FEM simulation software.
- Charges are added (non-uniformly) to the walls and the 3-D field is calculated.
- The 3D field map is combined with the known field dependence on the electron drift speed to obtain a mapping between "real space" and "S2 space" coordinates.
- Results are compared to the observed distribution of ^{83m}Kr decays, and the charge densities are iterated until a best-fit is obtained.
- 10x variation in field magnitude

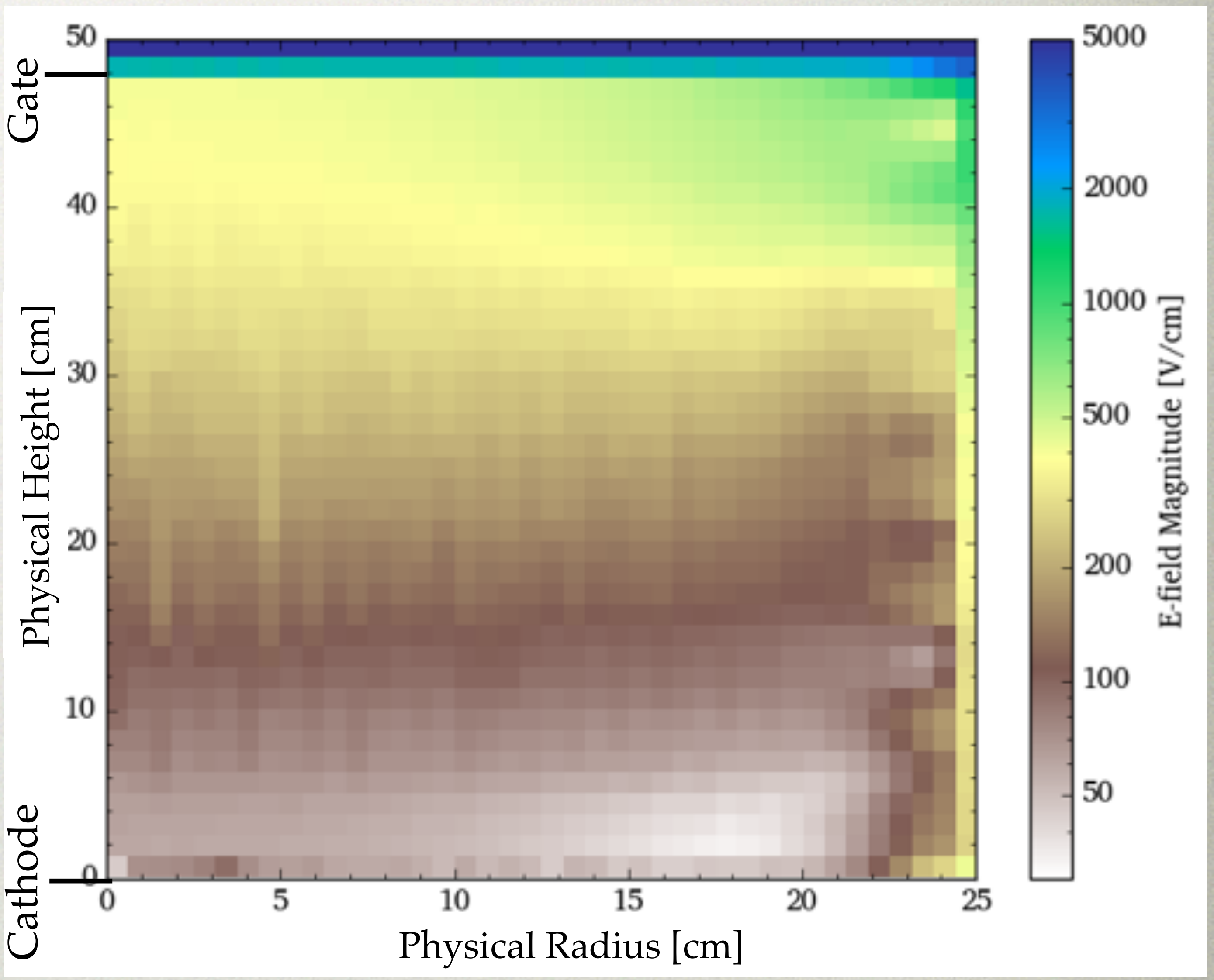

Variation in time of wall charge

- Average wall charge is observed to increase in magnitude over time.
- Wall charge is concentrated in the upper portion of the PTFE walls.

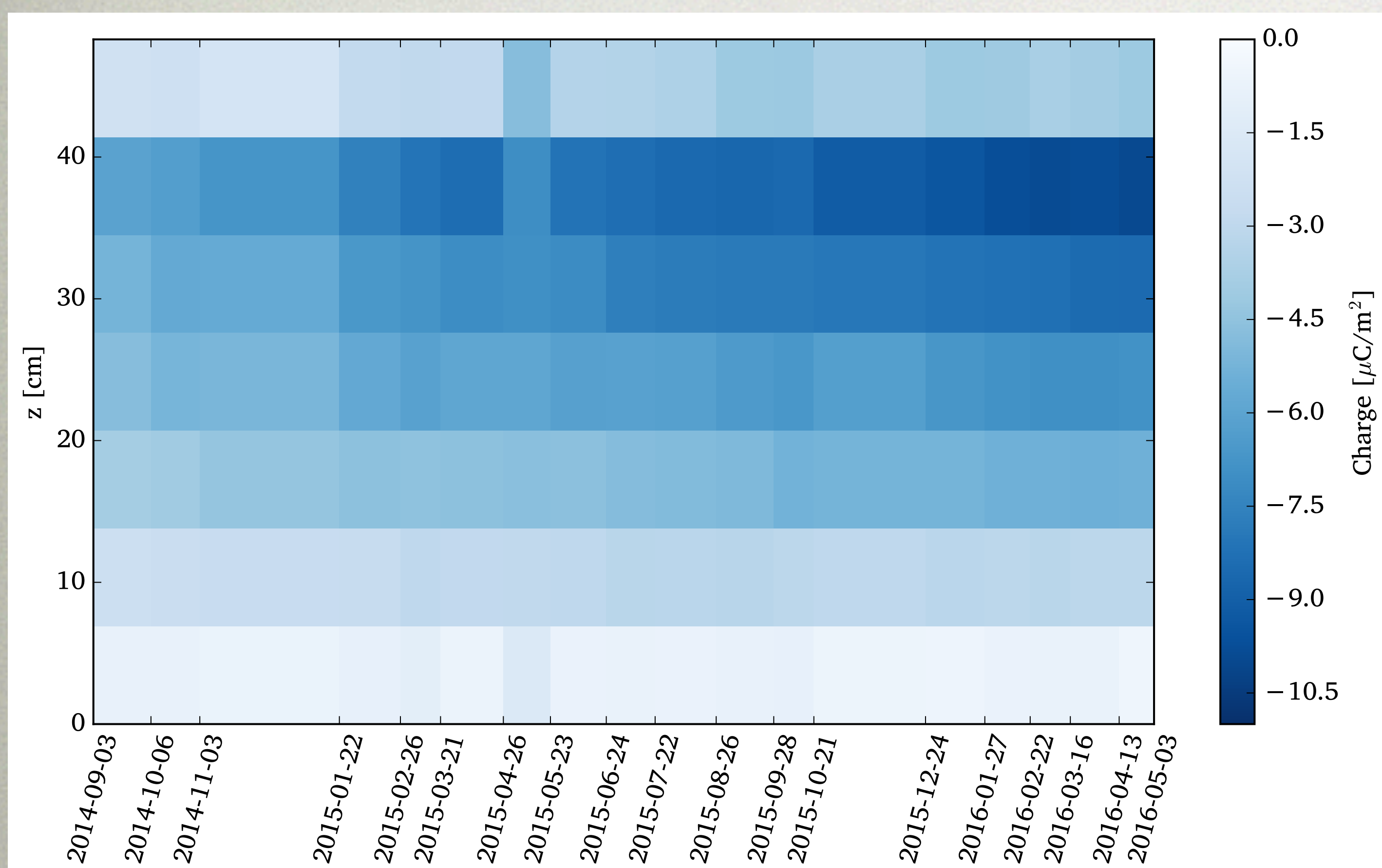

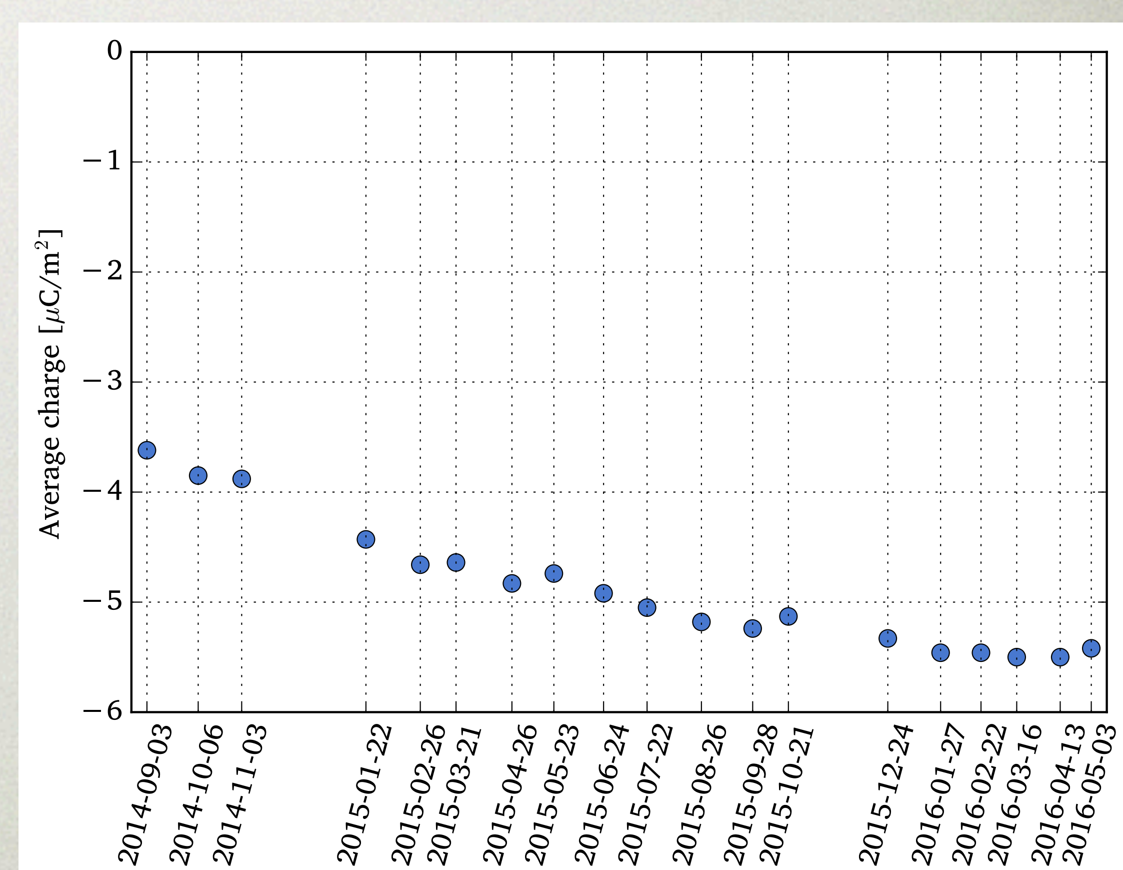

Determination of fiducial volume

^{83m}Kr calibration

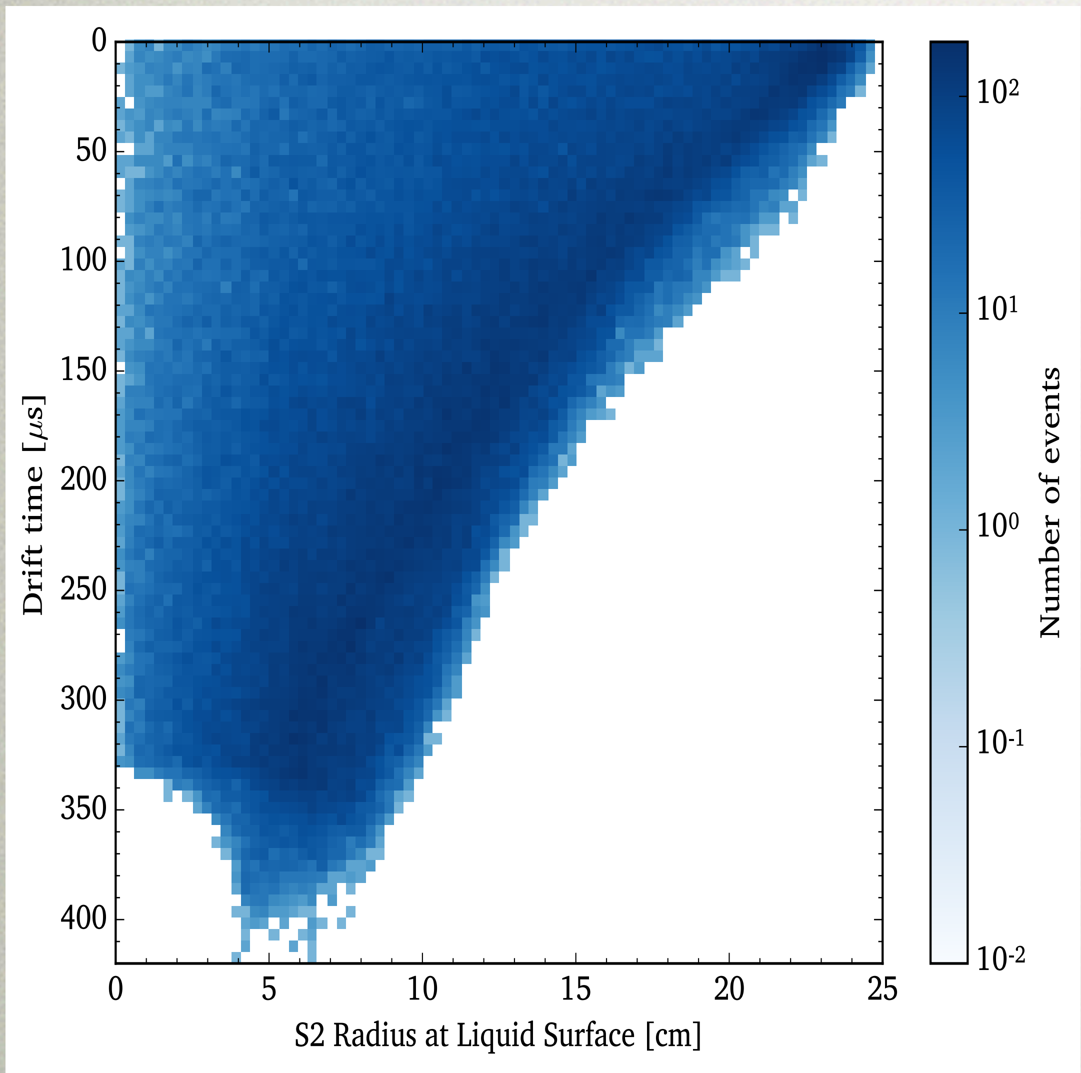

How does one determine fiducial mass in such a situation?

- Calibrations with ^{83m}Kr are performed every week.
- The injected Kr mixes uniformly in the active volume within ~10 min timescale.
- The mass surviving any fiducial cut can be found by:

$$\text{Fiducial Mass} = 251\,\text{kg} \times \frac{\text{Num. evts. passing fiducial cut}}{\text{Num. evts. total}}$$

- CH_3T calibrations (smaller S2) are used to determine systematic uncertainty.

Position corrections

- Size of the S1 depends on the location of the event (due to geometrical light collection), and S2 (due to electronegative impurities)
- Normally, one develops a geometrical correction factor by flat fielding a mono-energetic source.
- However, a spatially varying E-field ALSO affects S1 and S2 sizes, but differently for every particle type and energy.

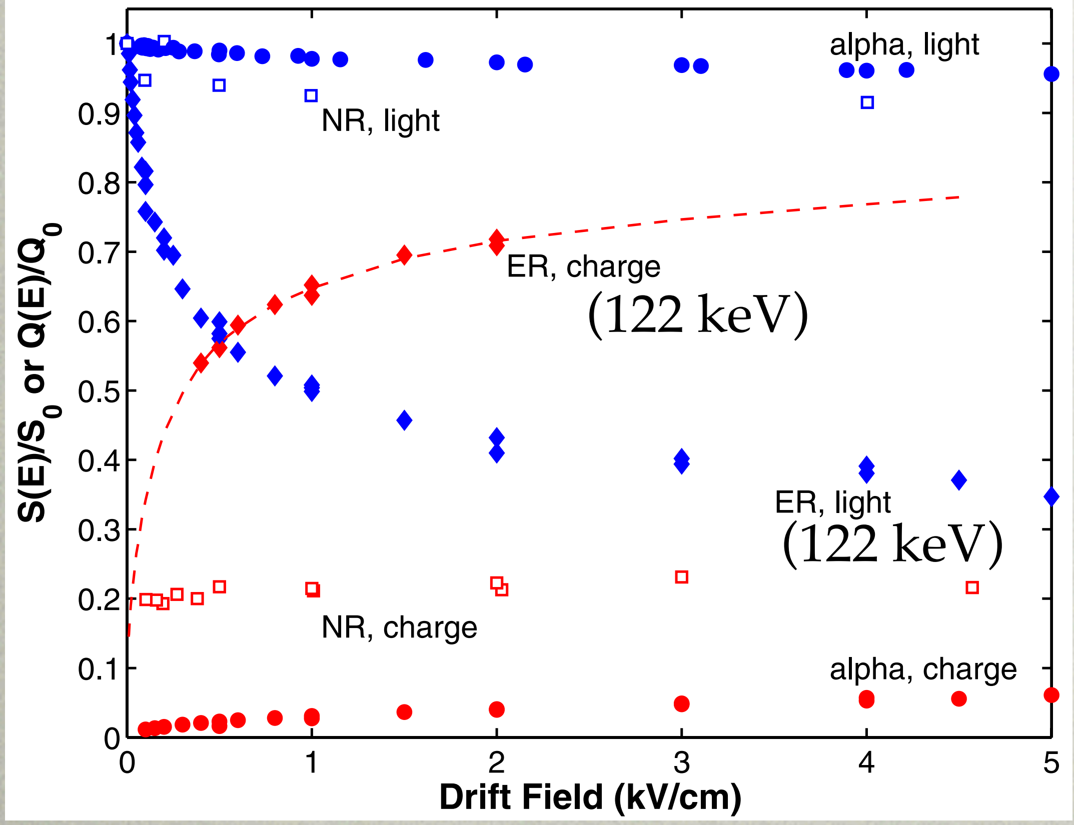

E. Aprile *et al*. PRL **97** (2006) 081302, astro-ph/0601552

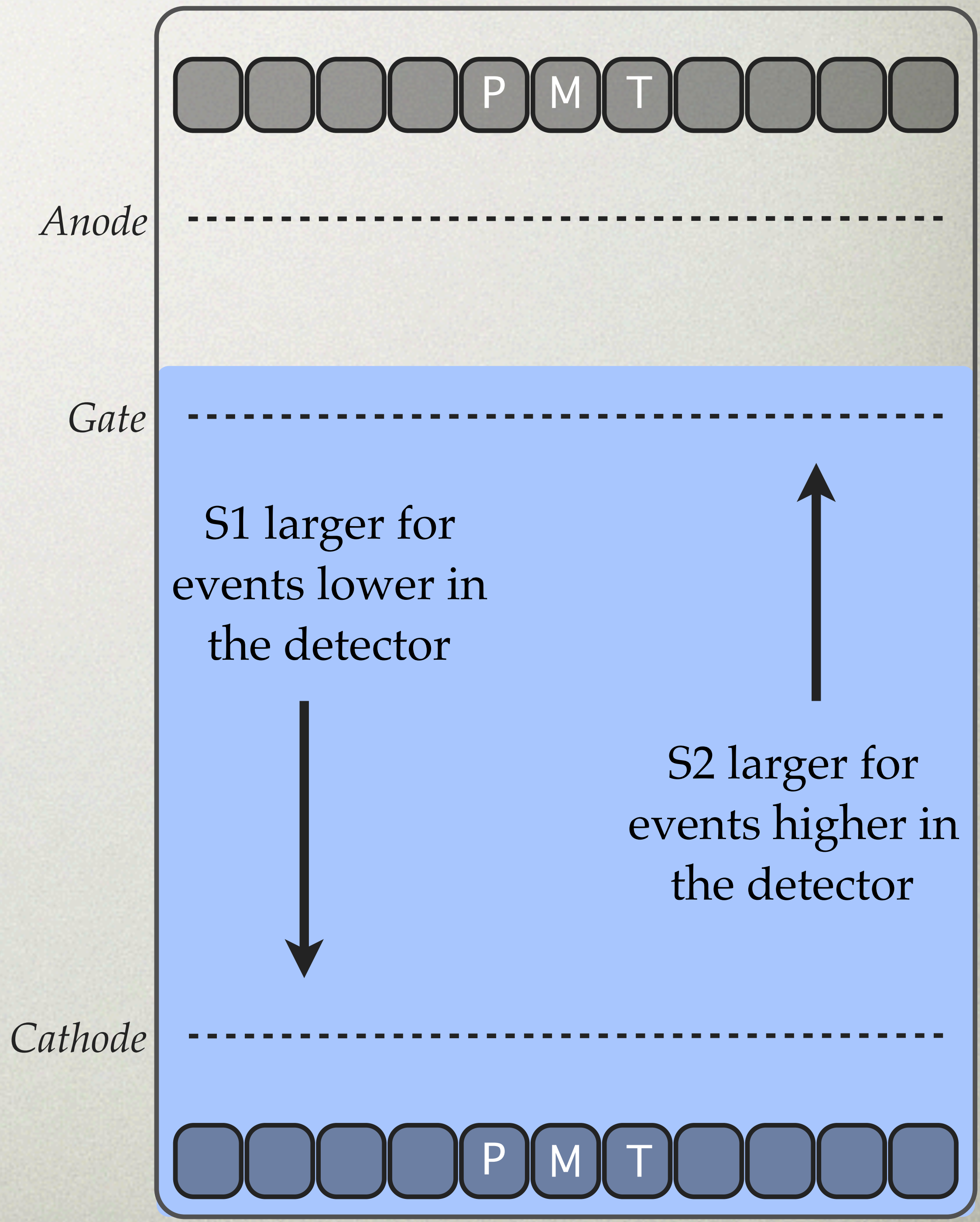

Position corrections

- Our strategy is:
  - Disentangle position effects from field effects.
  - Apply a correction to account for position effects only.
- ^{83m}Kr has two decays close in time. The ratio of the first-to-second S1 pulse area depends on field alone. This allows us to measure the component of variation due to applied field alone.

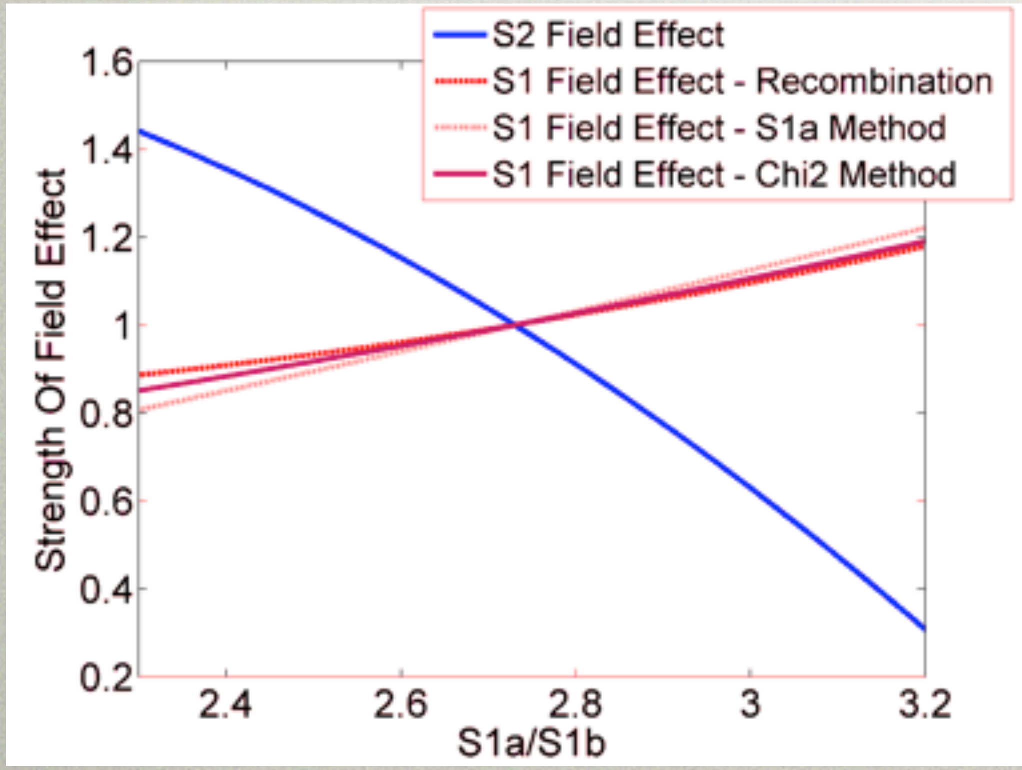

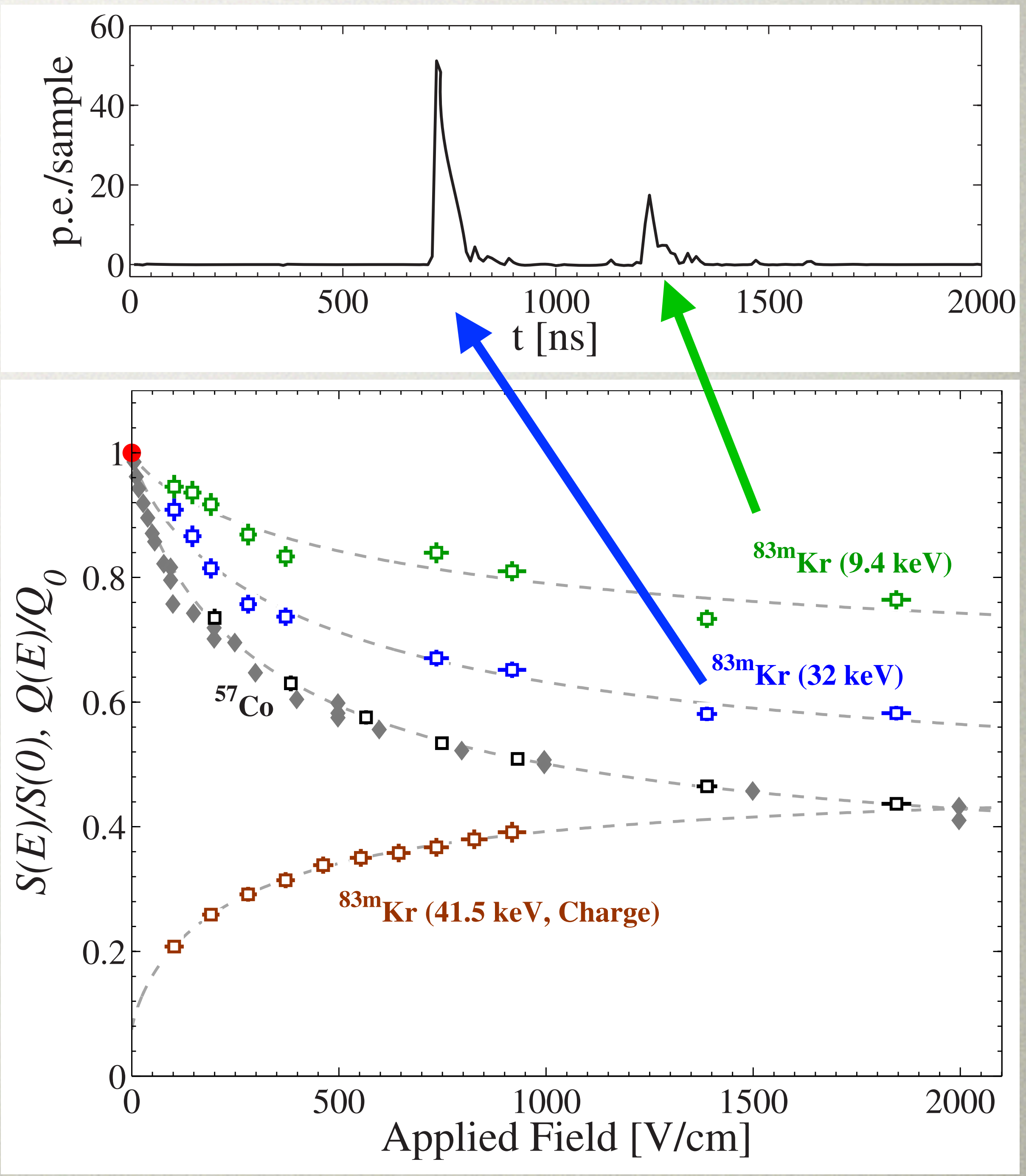

A.Manalaysay *et al.*, Rev.Sci.Instrum. **81** (2010) 073303, 0908.0616

Dealing with a varying/changing field

How to deal with a field that is varying in space and varying in time?

—> Break the Run up into *M* time bins
—> Break the detector volume up into *N* voxels
In each of the *M*x*N* segments, treat that segment as having a uniform detector model for ER and NR response (i.e. constant applied field and other detector parameters).

Too few segments —> Field variation not adequately accounted for.
Too many segments —> Calibration data too sparse; computational resources become strained.

4x4 segments adequately captures the field variation.
—>We effectively have 16 independent detectors

Data parameter space

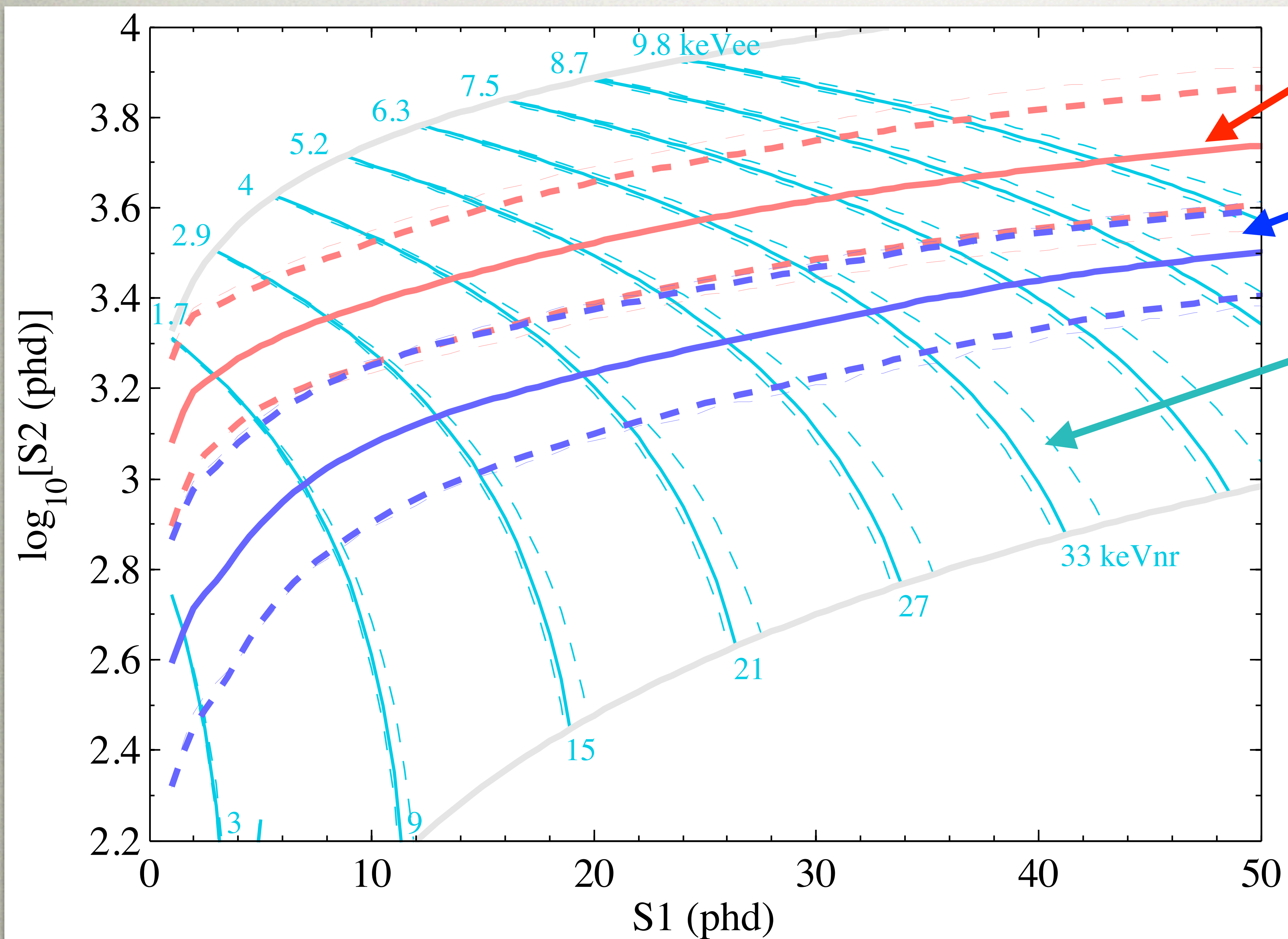

- Likelihood analysis performed in observed quantities (data not converted to energy: model converted to S1, S2)
- Dashed curves are 10-90%-iles.

Framework for modeling ER and NR response

http://nest.physics.ucdavis.edu

- We use the Noble Element Simulation Technique (NEST) as a framework for modeling the S1 and S2 response of LXe due to a variety of particles, energies, and applied fields. **Developed and based on world's data.**
- The NEST model is "tuned" to each of the 16 detectors by varying the applied field until we see a match between model and calibration data.

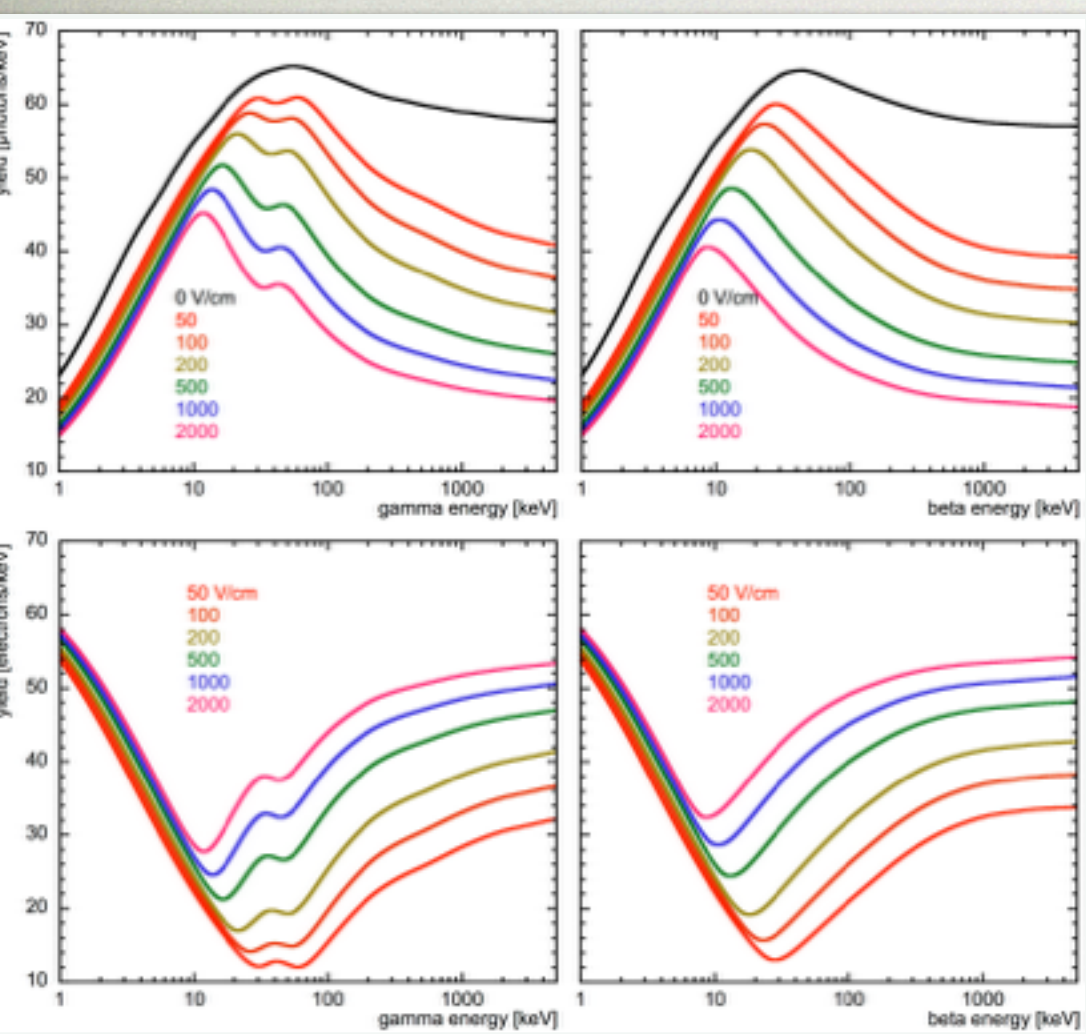

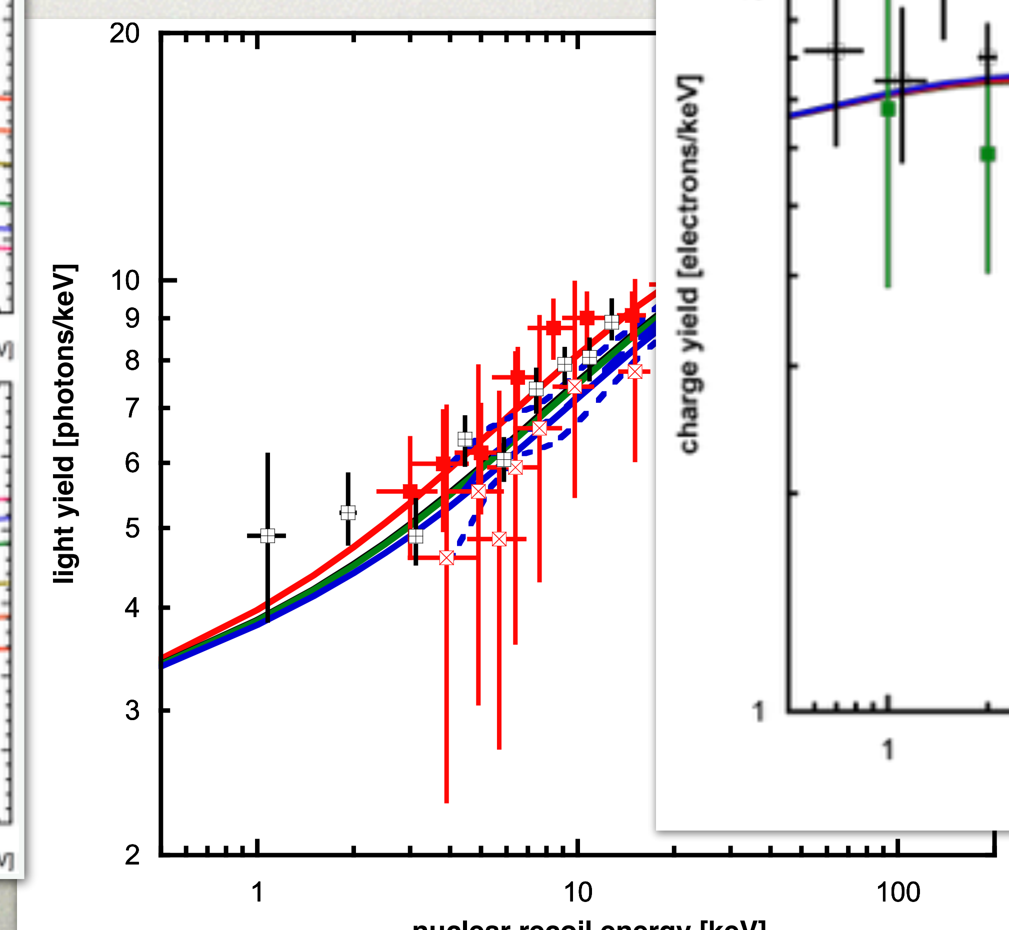

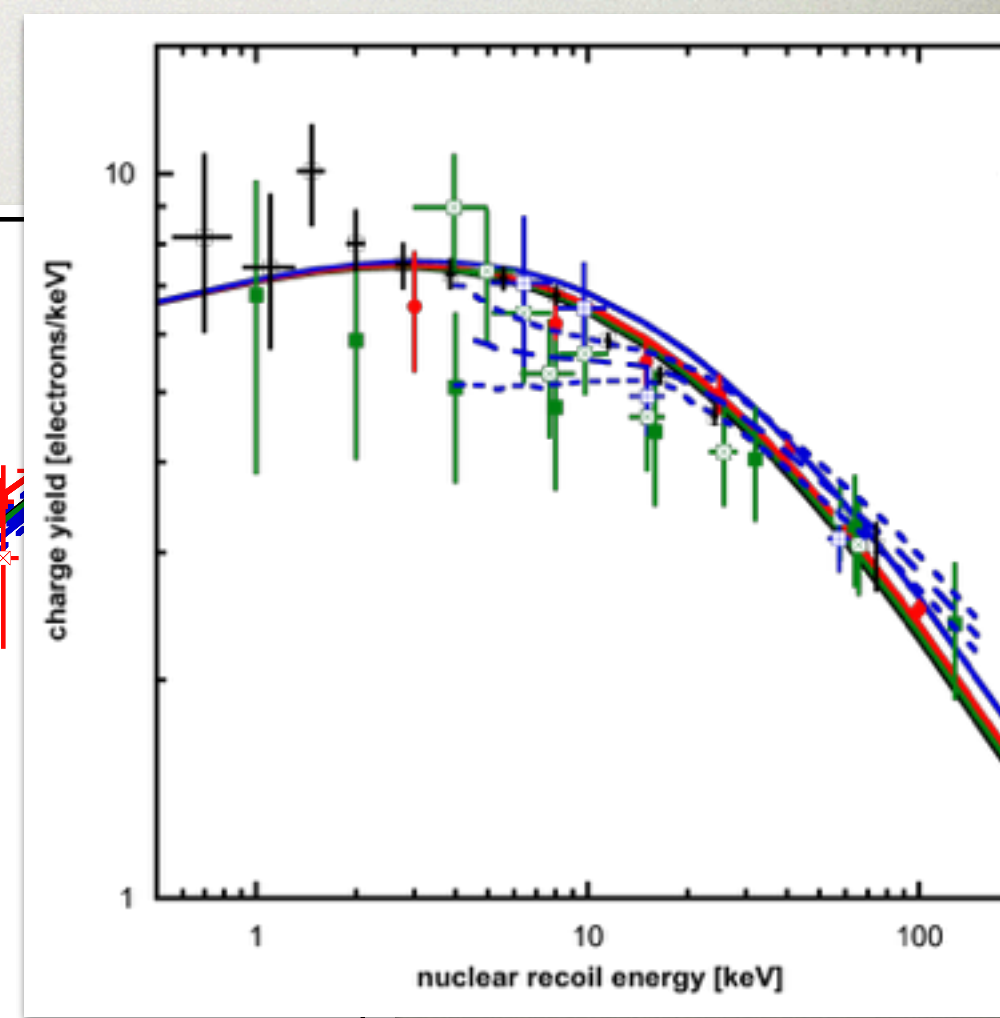

Periodic calibrations

Sep.2014 → May 2016

Top ↑ Bottom

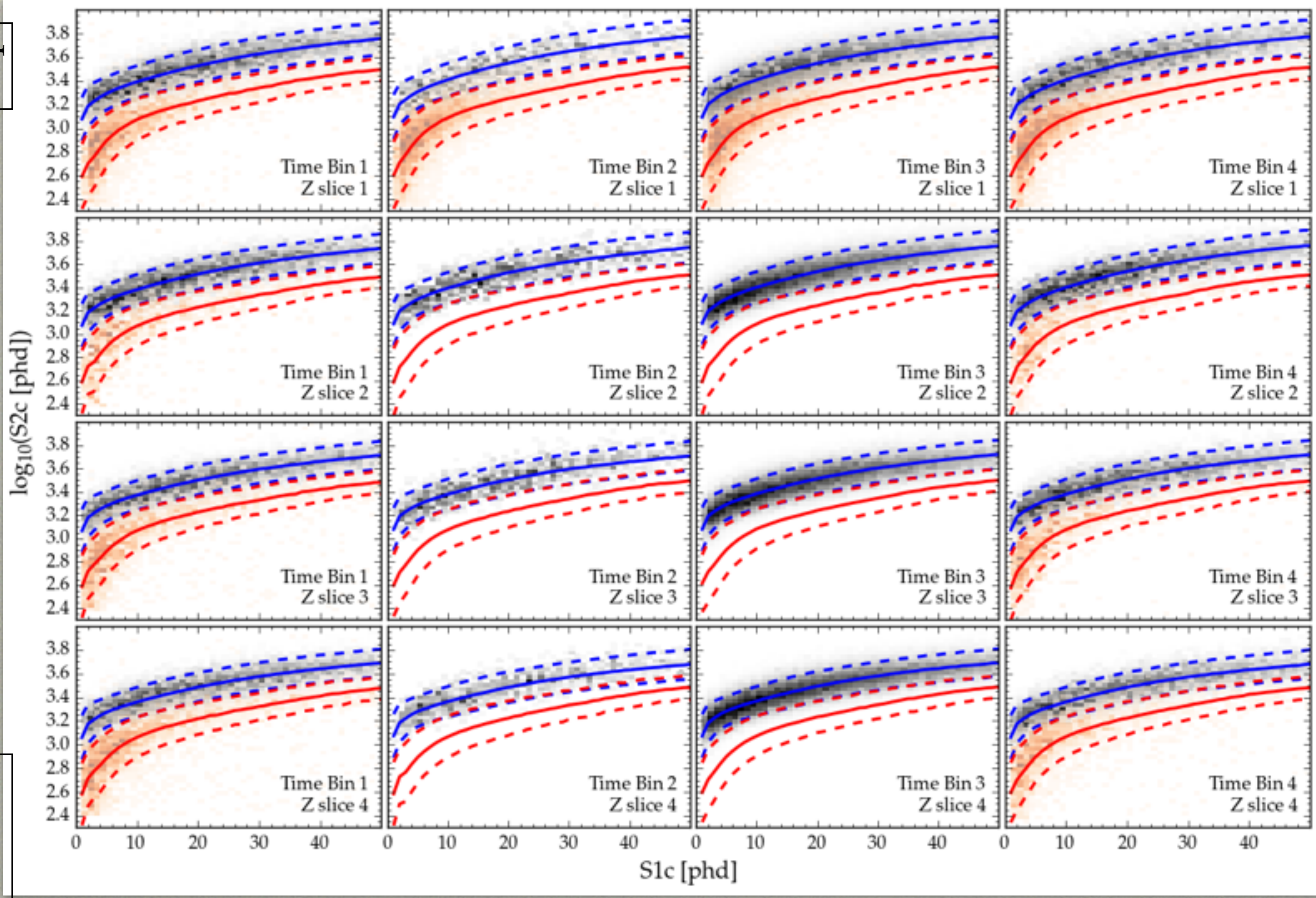

Gray density: CH_3T calibration (ER)

Orange density: DD calibration (NR)

Solid lines: NEST model, band mean.

Dashed lines: NEST model, 10-90 percentile.

Periodic calibrations

Sep.2014 → May 2016

Top ↑ Bottom

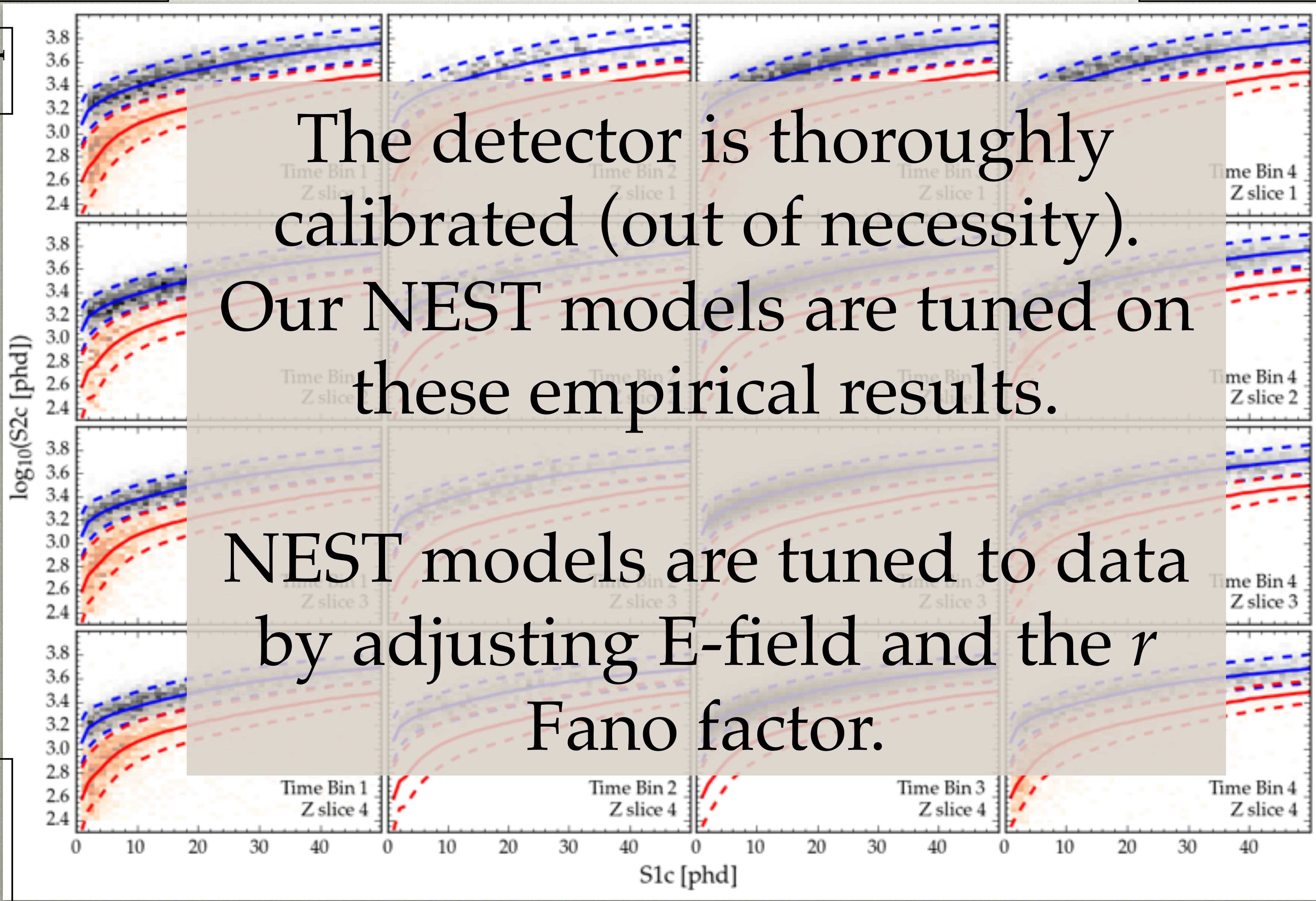

The detector is thoroughly calibrated (out of necessity). Our NEST models are tuned on these empirical results.

NEST models are tuned to data by adjusting E-field and the *r* Fano factor.

Gray density: CH_3T calibration (ER)

Orange density: DD calibration (NR)

Solid lines: NEST model, band mean.

Dashed lines: NEST model, 10-90 percentile.

Radiogenic backgrounds

- Backgrounds from radioisotopes in detector materials have not changed since the previous LUX results.

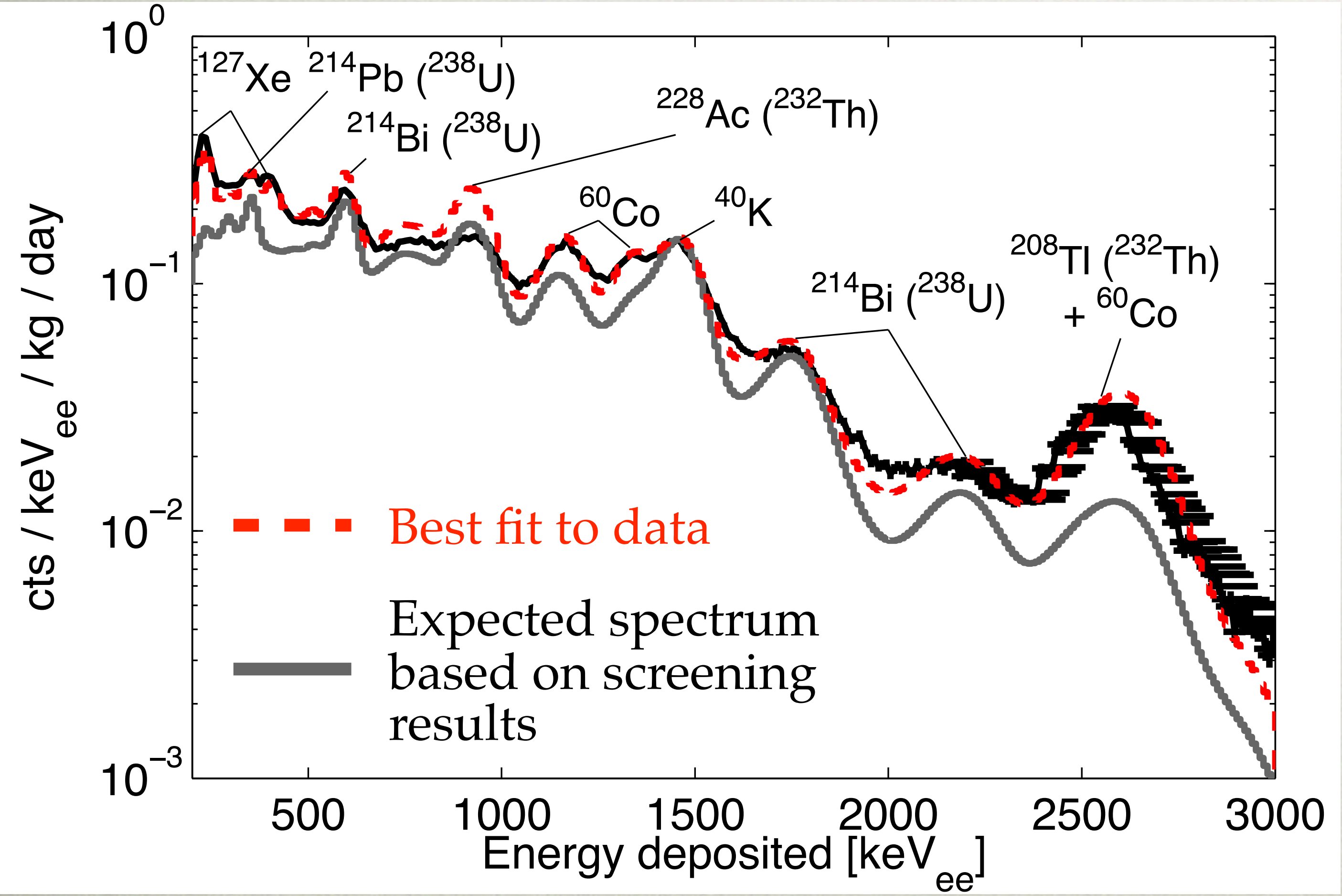

D.S. Akerib *et al.*, Astropart.Phys. **62** (2015) 33, 1403.1299

- In the first LUX results, there was a residual amount of ^{127}Xe among our stock of Xe, and was included as a background component.
- Here, the ^{127}Xe has decayed away and we neglect its contribution (>20 half lives at the beginning of this data set).

Wall-surface backgrounds

- Radon plate-out on PTFE surfaces survives as ^{210}Pb and its daughters (mainly ^{210}Bi and ^{210}Po).
- Betas and ^{206}Pb recoils into the LXe travel negligible distance, but they can be reconstructed some distance from the wall as a result of position resolution (especially for small S2 sizes).
- These sources can be used to define the radius of the wall in measured coordinates, for any combination of drift-time and ϕ

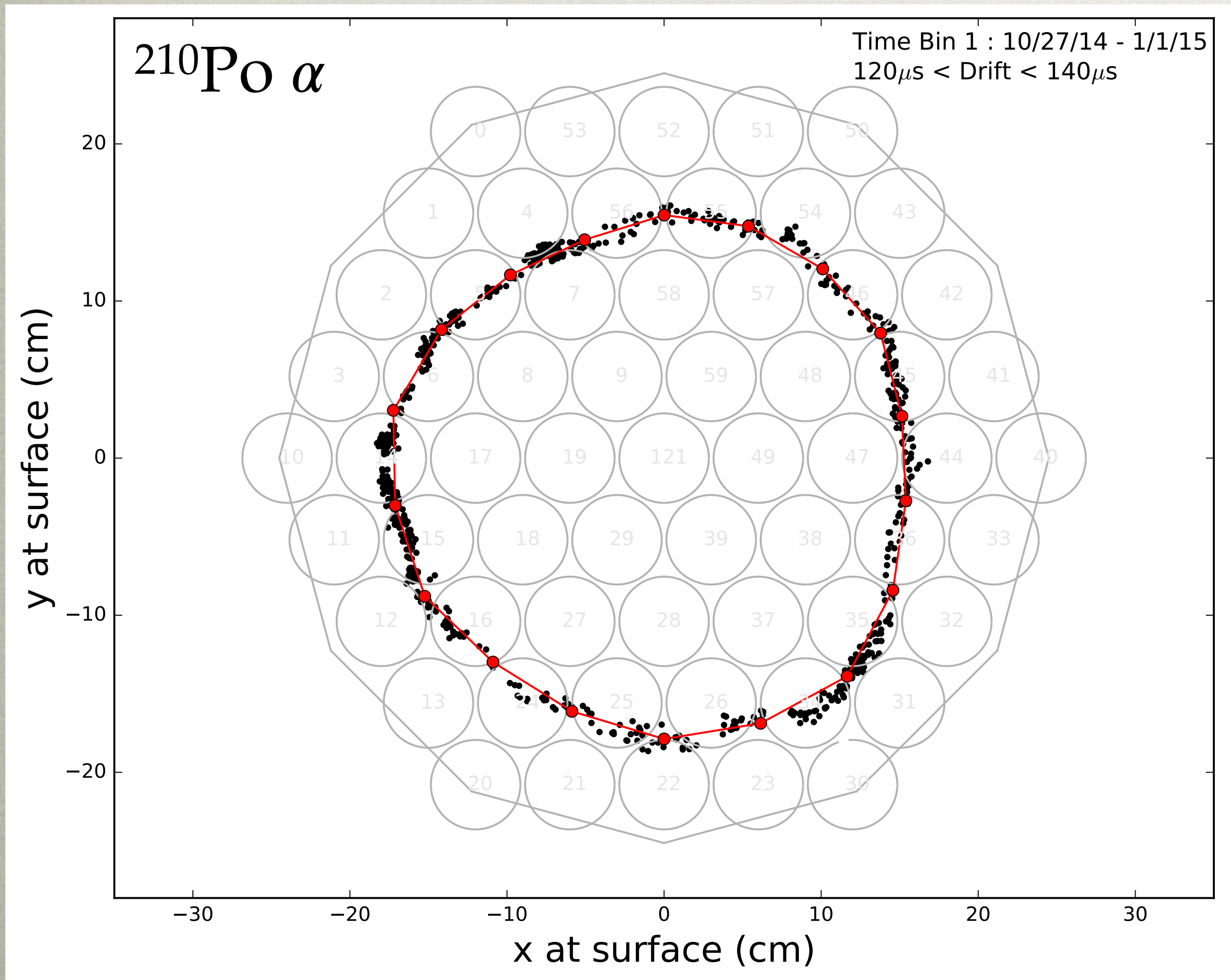

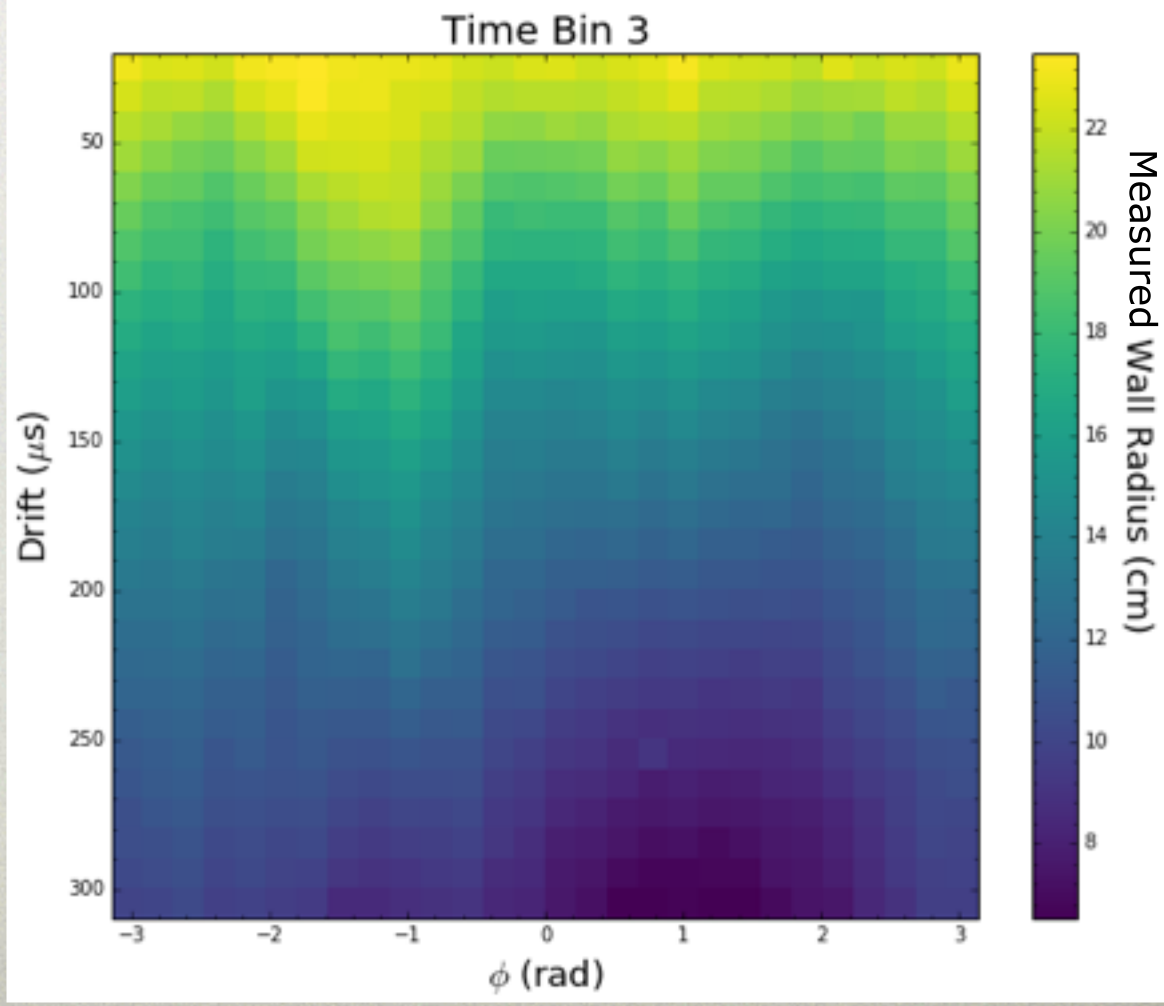

Wall-surface backgrounds

- Radon plate-out on PTFE surfaces survives as ^{210}Pb and its daughters (mainly ^{210}Bi and ^{210}Po).
- Betas and ^{206}Pb recoils into the LXe travel negligible distance, but they can be reconstructed some distance from the wall as a result of position resolution (especially for small S2 sizes).
- We define our fiducial volume as 3cm inwards from the measured wall.

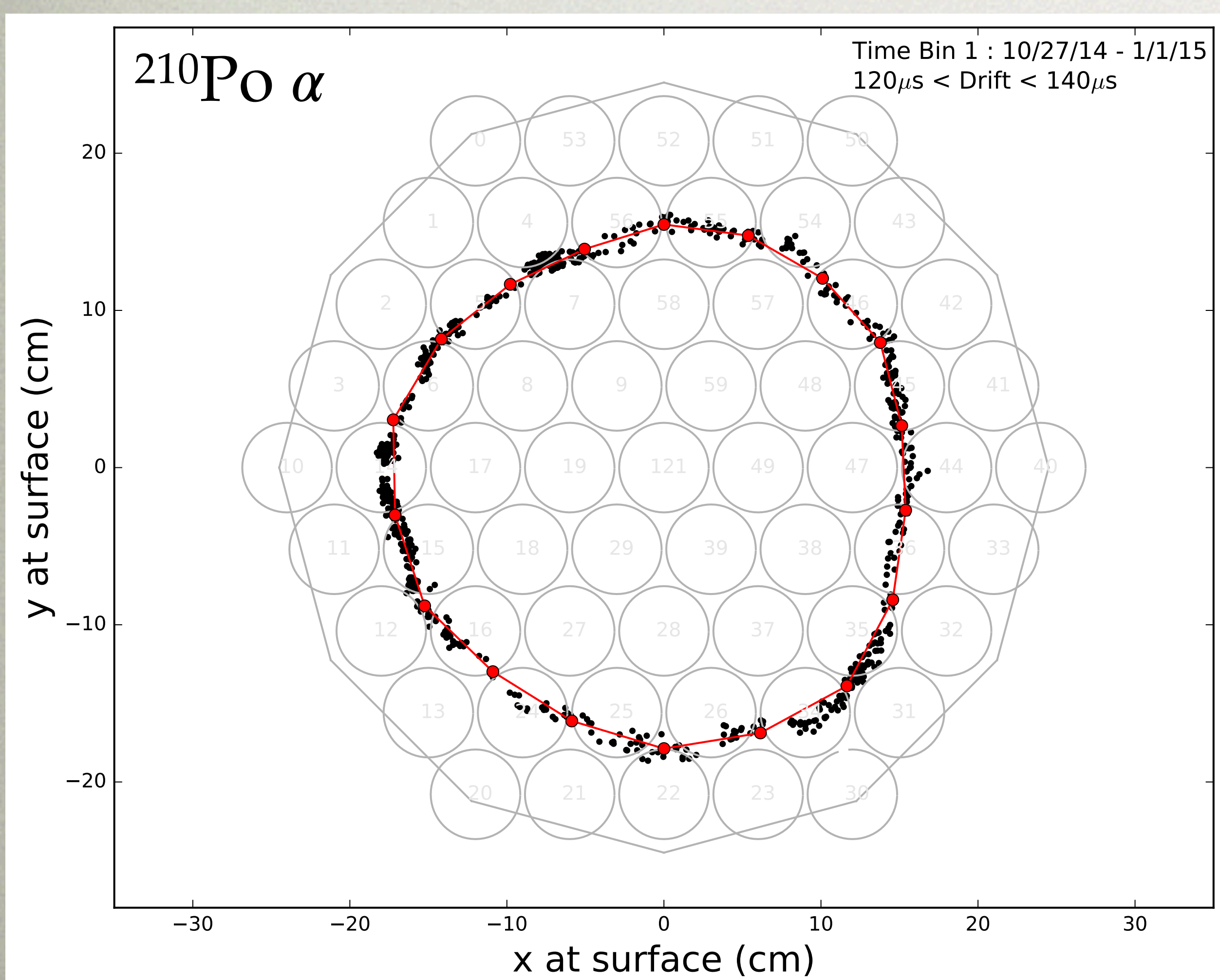

Fiducial boundary

Increasing S2

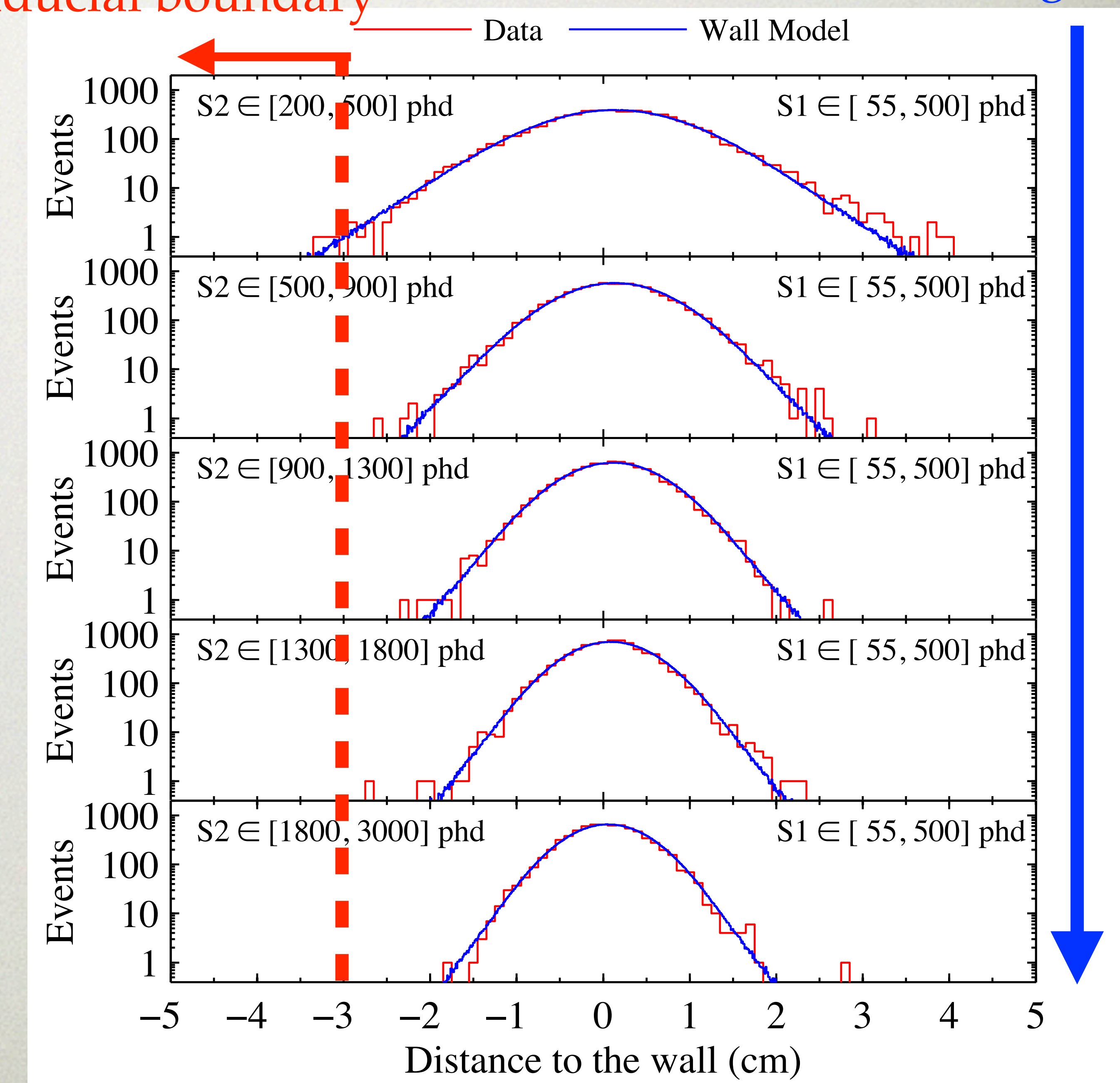

Into detector ⟷ Out of detector

Fiducial definition

- We define our fiducial boundary as 3cm inwards from the observed wall in S2 space (done in 3D).

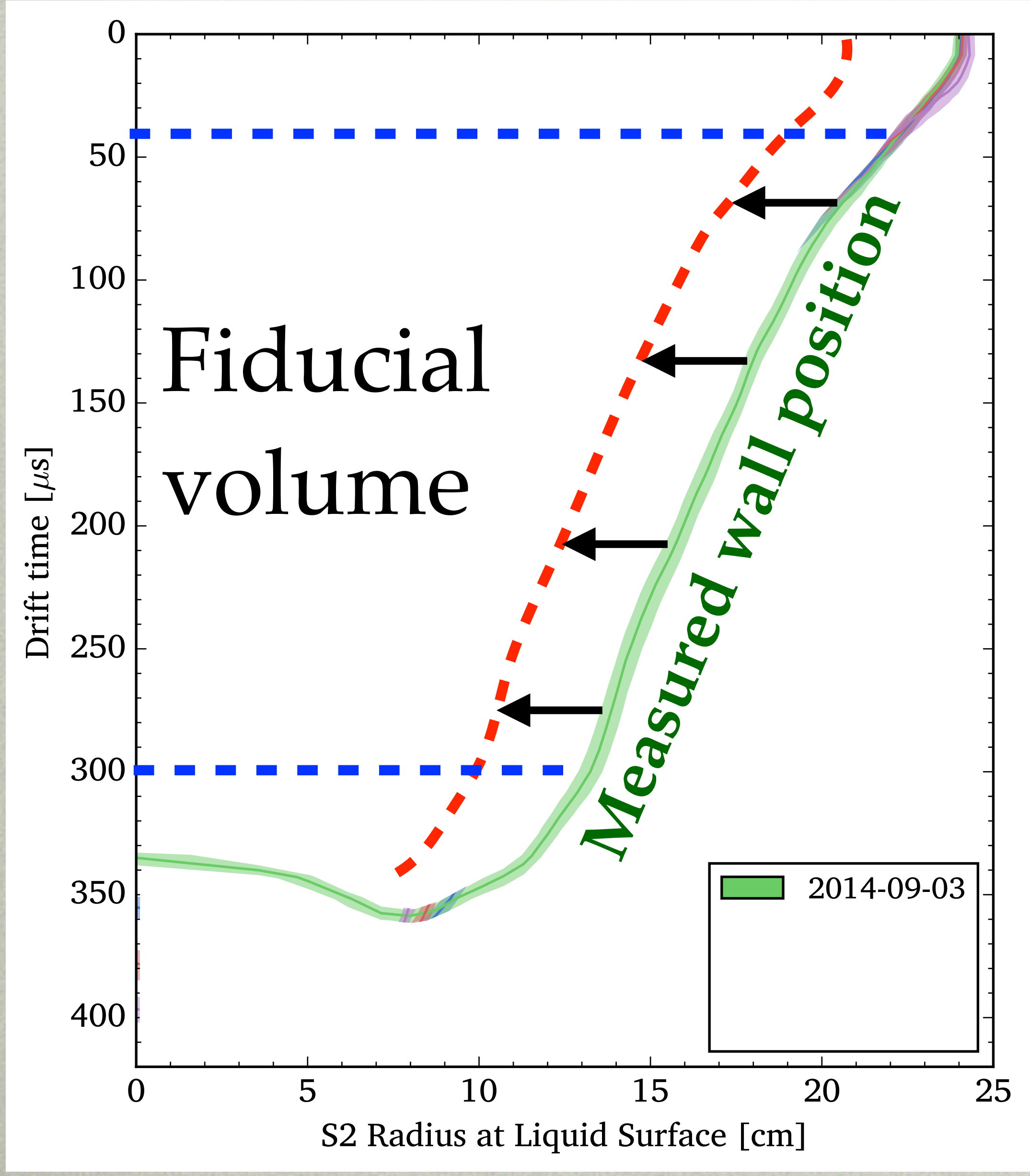

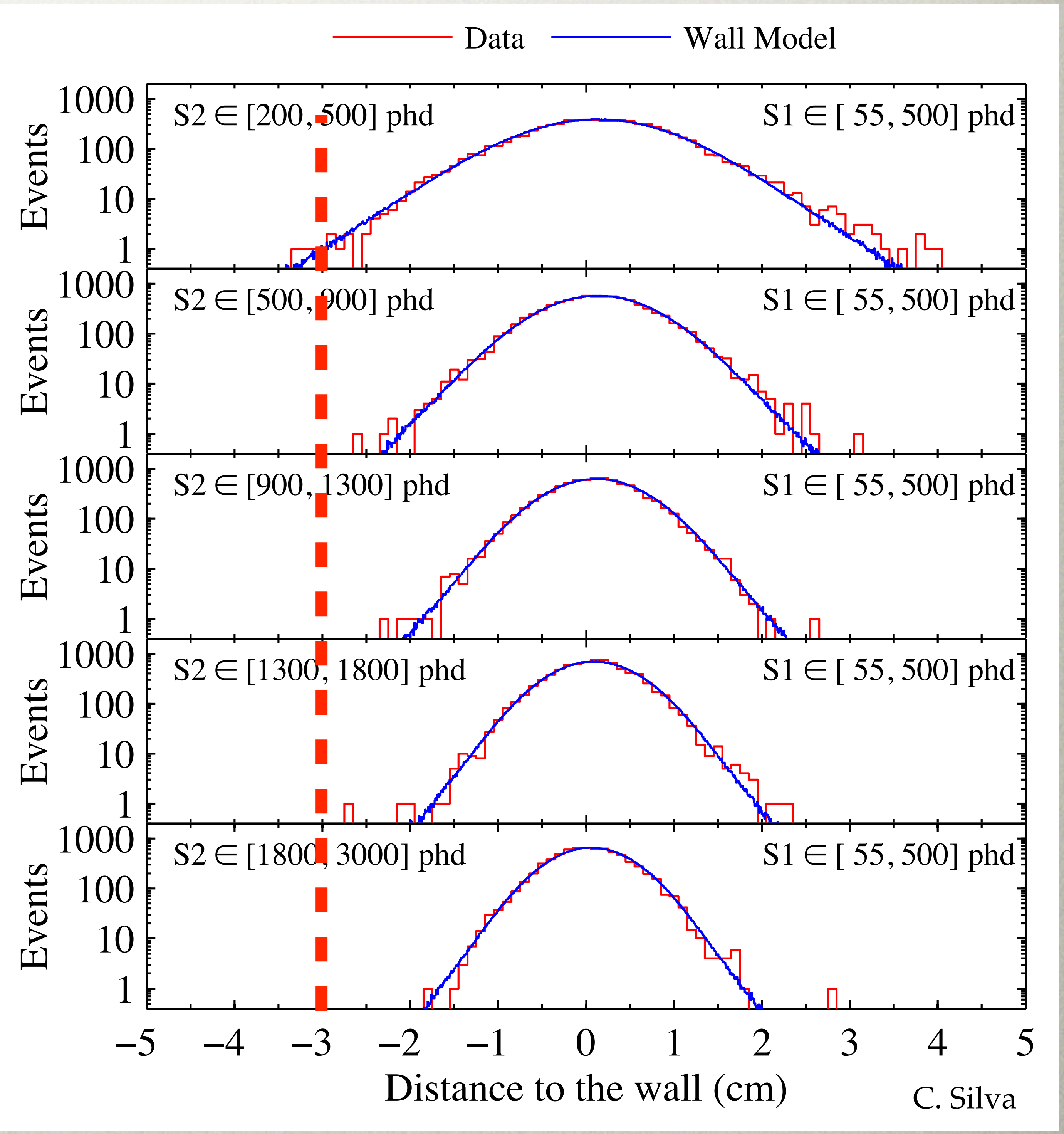

Into detector ⟷ Out of detector

Background estimates

Background source	Expected number below NR median
External gamma rays	1.51 ± 0.19
Internal betas	1.2 ± 0.06
Rn plate out (wall background)	8.7 ± 3.5
Accidental S1-S2 coincidences	0.34 ± 0.10
Solar ^{8}B neutrinos (CNNS)	0.15 ± 0.02
Neutrons	0.3 ± 0.03

← Figure of merit only (we do a likelihood analysis)

} Bulk volume, but leakage at all energies (external gamma rays, internal betas)

} Low-energy, but confined to the edge of our fid. volume[*] (Rn plate out)

} In the bulk volume, low-energy, in the NR band (accidental S1-S2 coincidences, solar ^{8}B neutrinos, neutrons)

[*] Our likelihood analysis includes position information, so these events have low $\mathscr{L}$(signal)

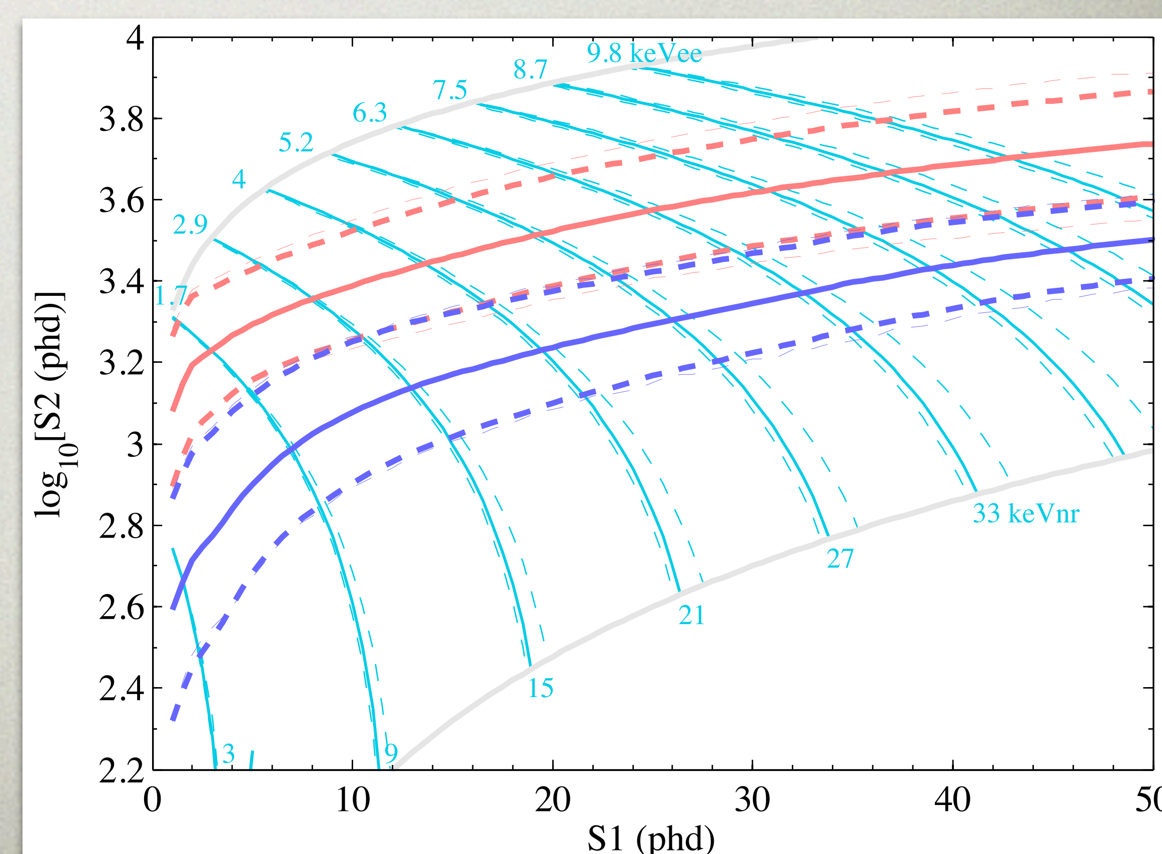

Profile Likelihood Analysis

- Data are compared to models in an un-binned, 2-sided profile-likelihood-ratio (PLR) test.
- 5 un-binned PLR dimensions:
  - Spatial: r, ϕ, drift-time (raw-measured coordinates)
  - Energy: S1 and $\log_{10}$(S2)
- 1 binned PLR dimension:
  - Event date
- The data in the upper-half of the ER band were compared to the model (plot at right) to assess goodness of fit.

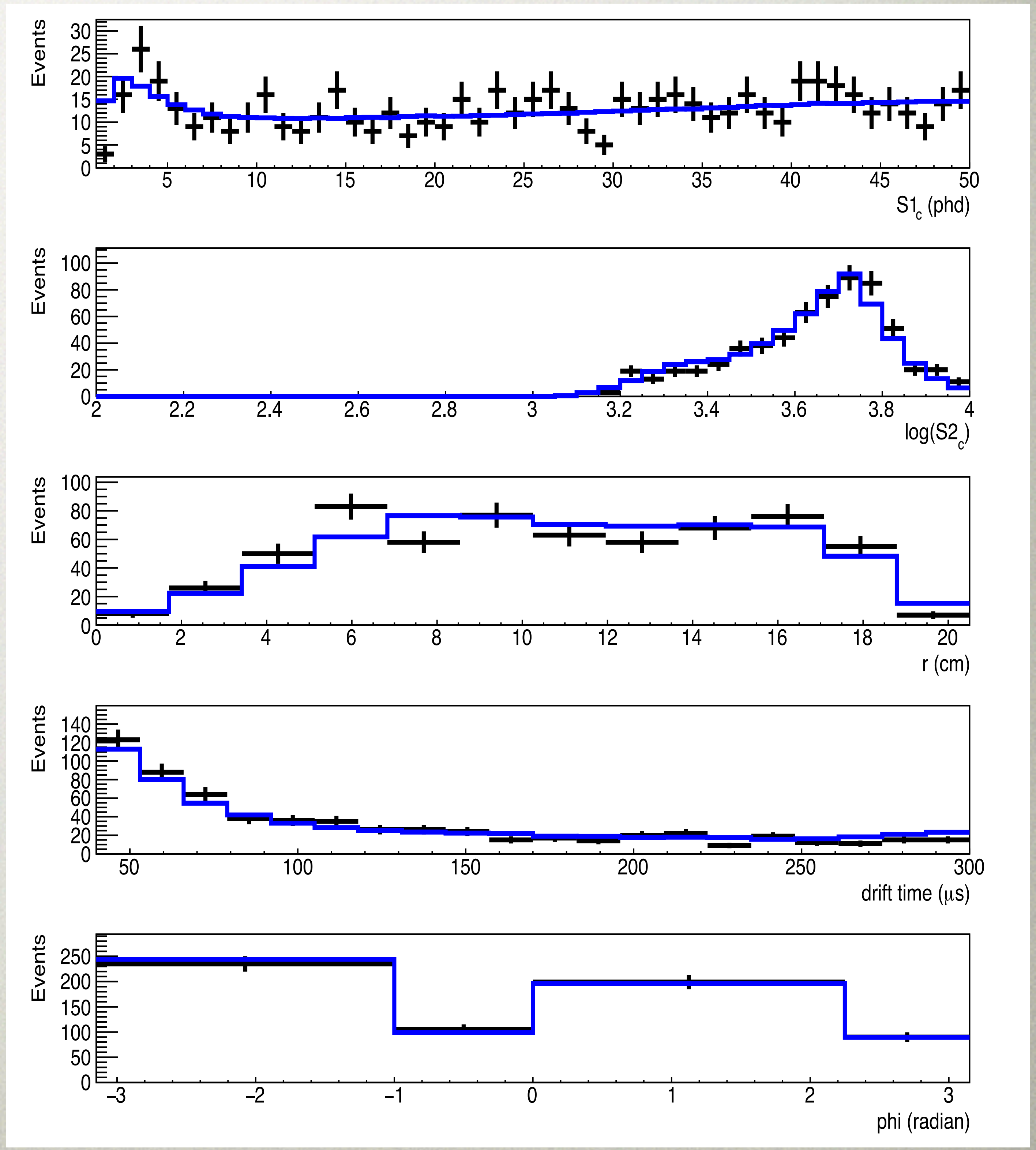

Cut efficiencies

- Cuts on the S2 topology are applied, targeting:
  - S2 waveform ("Gas-event" and "Merged S2")
  - S2 PMT hit pattern "S2 hit-pattern cut"
- Flat signal acceptance at high S2, falling to 60% acceptance at S2 threshold.

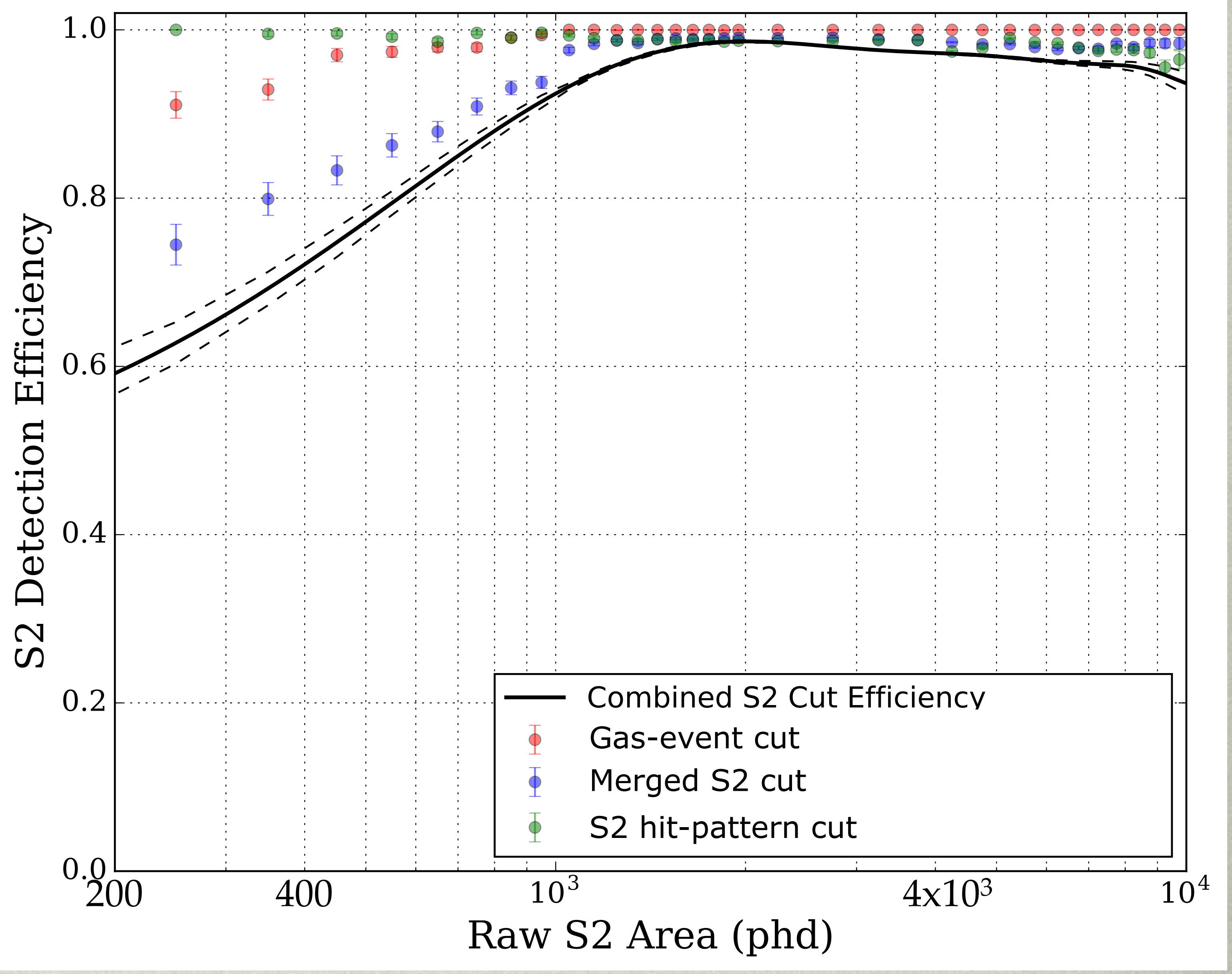

Details of the WIMP search

- 11 September 2014 — 3 May 2016
- Live time (332.0 days)
  - Time-bin 1 `(2014.09.09–2014.12.31)`: 46.8 live-d (31.8 d not salted)
  - Time-bin 2 `(2015.01.01–2015.03.31)`: 46.7
  - Time-bin 3 `(2015.04.01–2015.09.30)`: 91.6
  - Time-bin 4 `(2015.10.01–2016.05.03)`: 146.9
- Fiducial mass:
  - Time-bin 1: 105.4 ± 5.3 kg
  - Time-bin 2: 107.2 ± 5.4
  - Time-bin 3: 99.2 ± 5.0
  - Time-bin 4: 98.4 ± 4.9

(33500 ± 1700) kg days

WIMP-search data

- Traditional blinding (example seen here) masks the signal region completely.
- **Challenge** (seen very often in this community):
  - One is also blind to rare backgrounds and pathologies.
- One need not go to this extreme in order to mitigate bias.

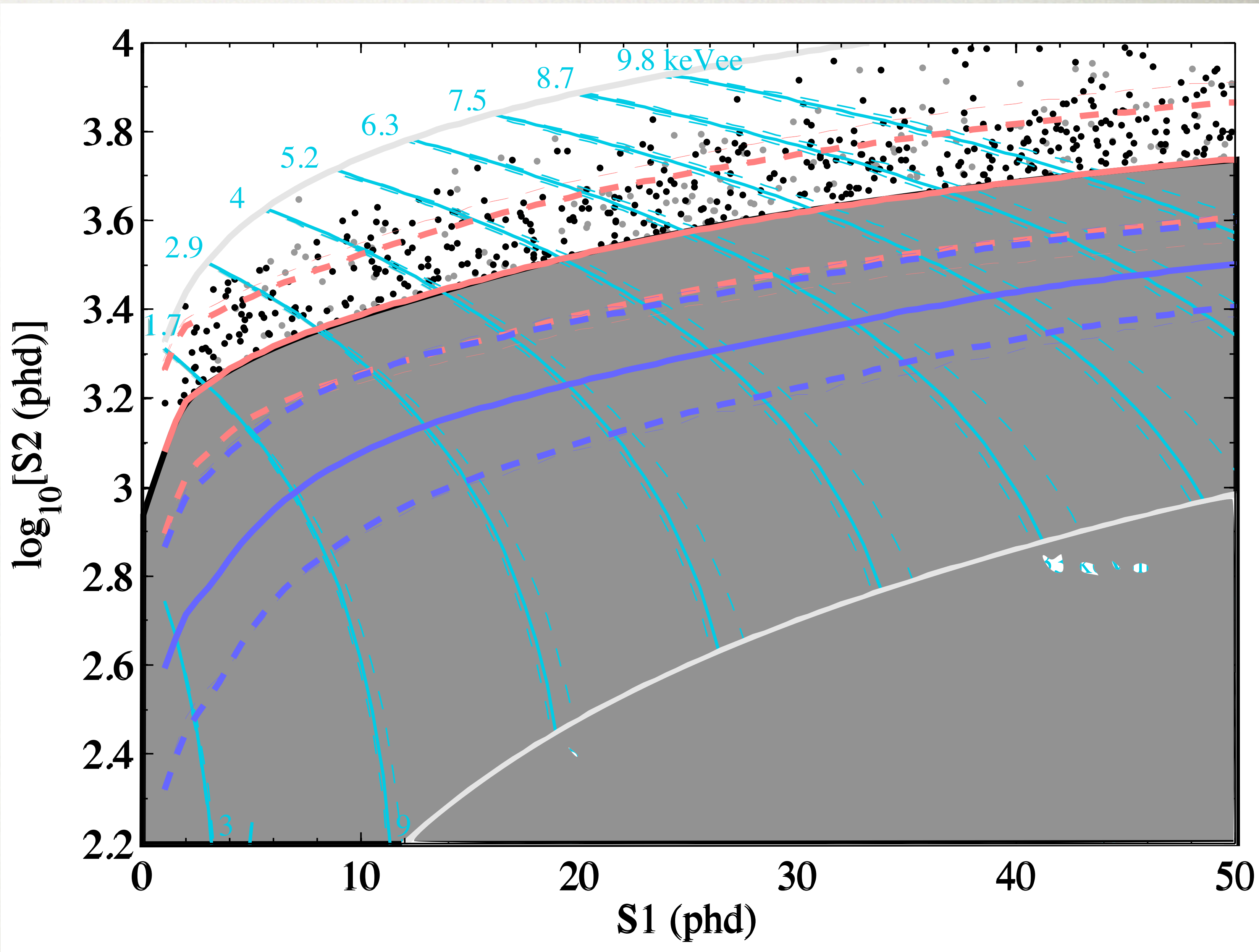

WIMP-search data

- Traditional blinding (example seen here) masks the signal region completely.
- **Challenge** (seen very often in this community):
  - One is also blind to rare backgrounds and pathologies.
- One need not go to this extreme in order to mitigate bias.

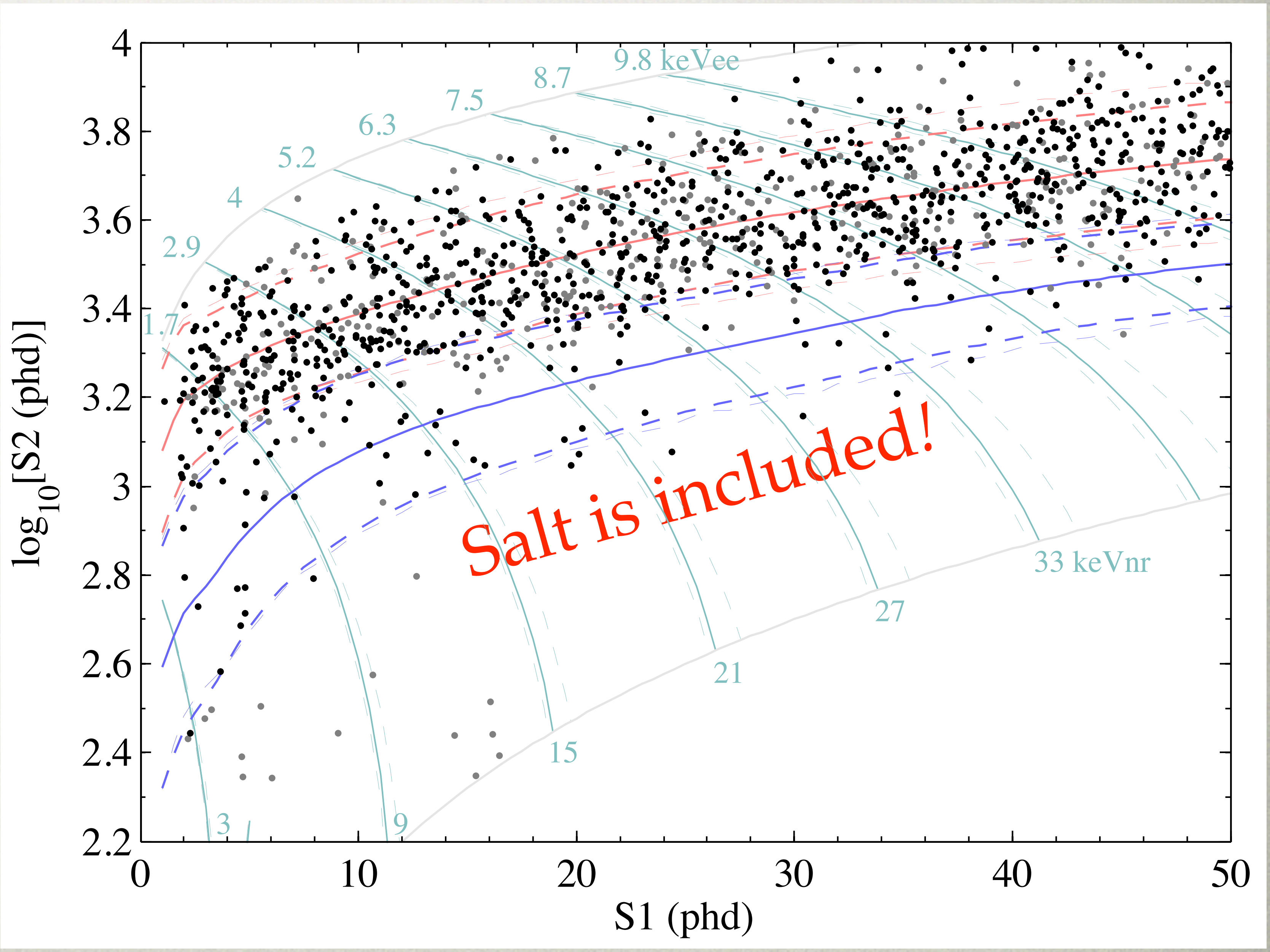

WIMP-search data

- Instead of traditional blinding, we employ a technique where fake signal events (“salt”) are injected into the data stream.
- Fake events are injected at the level of raw waveforms, and are built from calibration data (not simulation).
- Mitigates bias while allowing for scrutinization of individual events.
- Used already in neutrino experiments and searches for fractional charge.

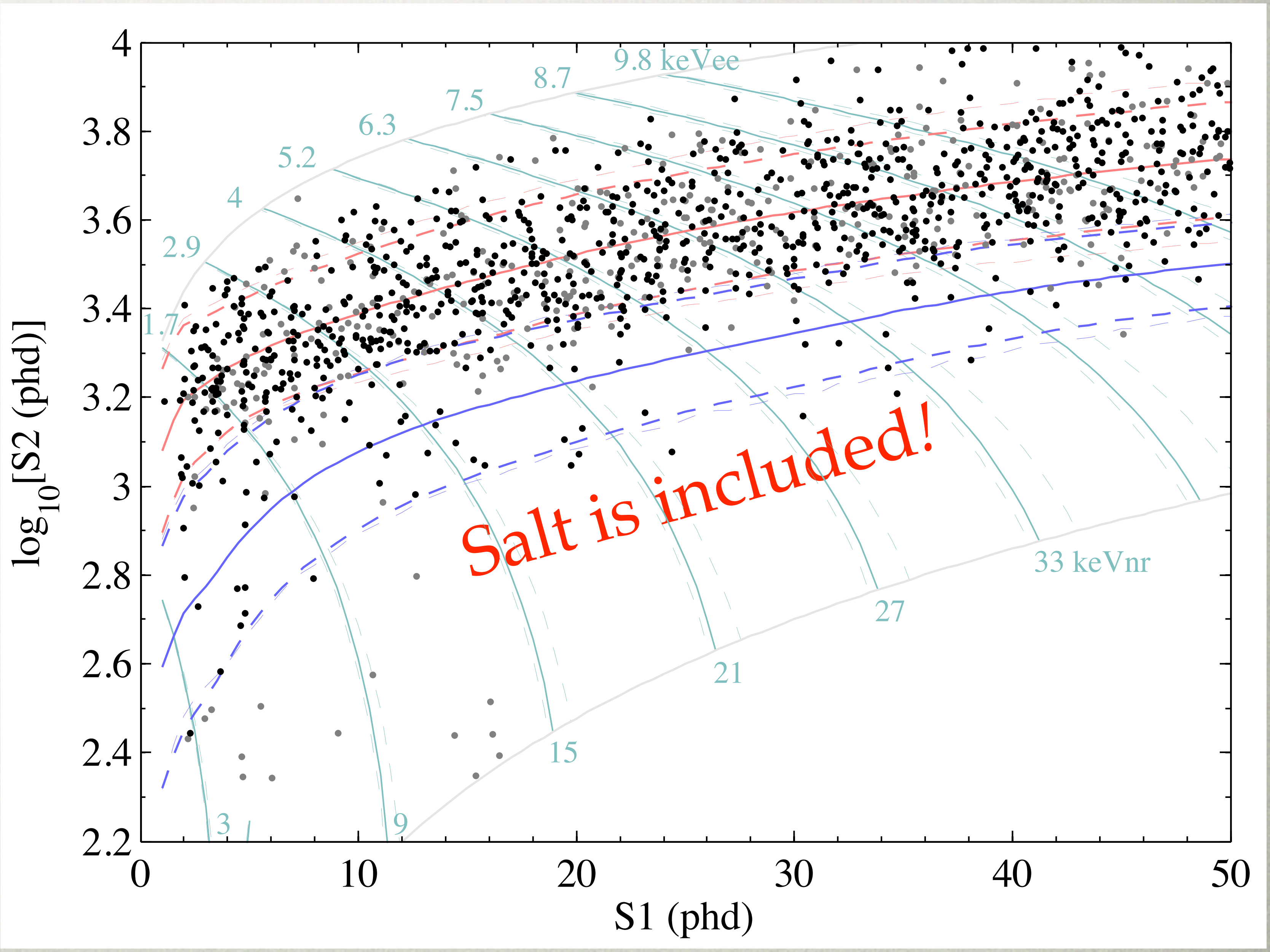

WIMP-search data

- This plot shows the data from our 16 “detectors” stacked on top of each other.
- Dots are events:
  - Gray: within 1cm of our fiducial boundary
  - Black: bulk events
- Salt is not yet identified here.

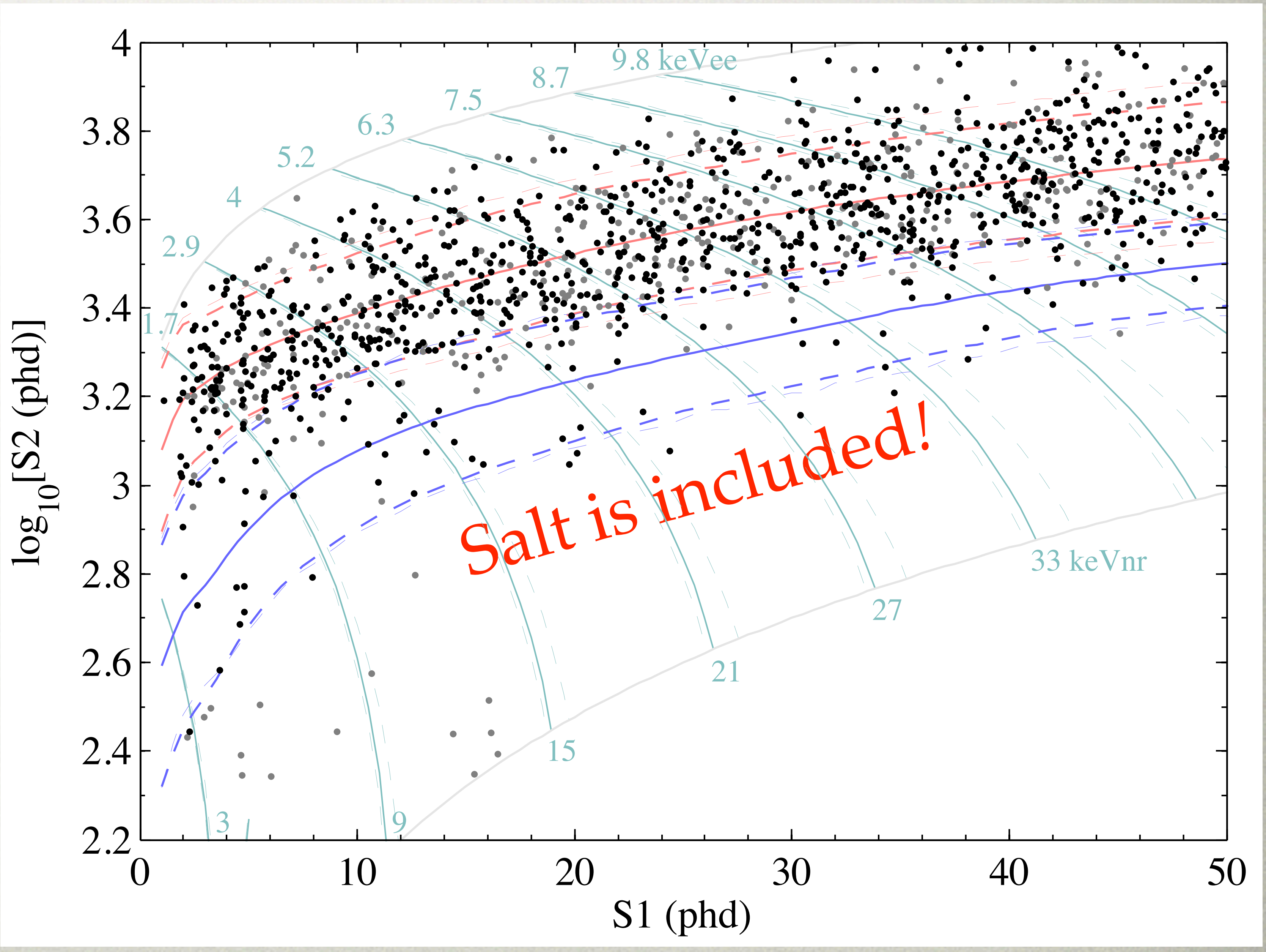

WIMP-search data

- This plot shows the data from our 16 "detectors" stacked on top of each other.
- Dots are events:
  - Gray: within 1cm of our fiducial boundary
  - Black: bulk events
- Red and blue curves are the ER and NR bands, respectively.
- With salt removed.

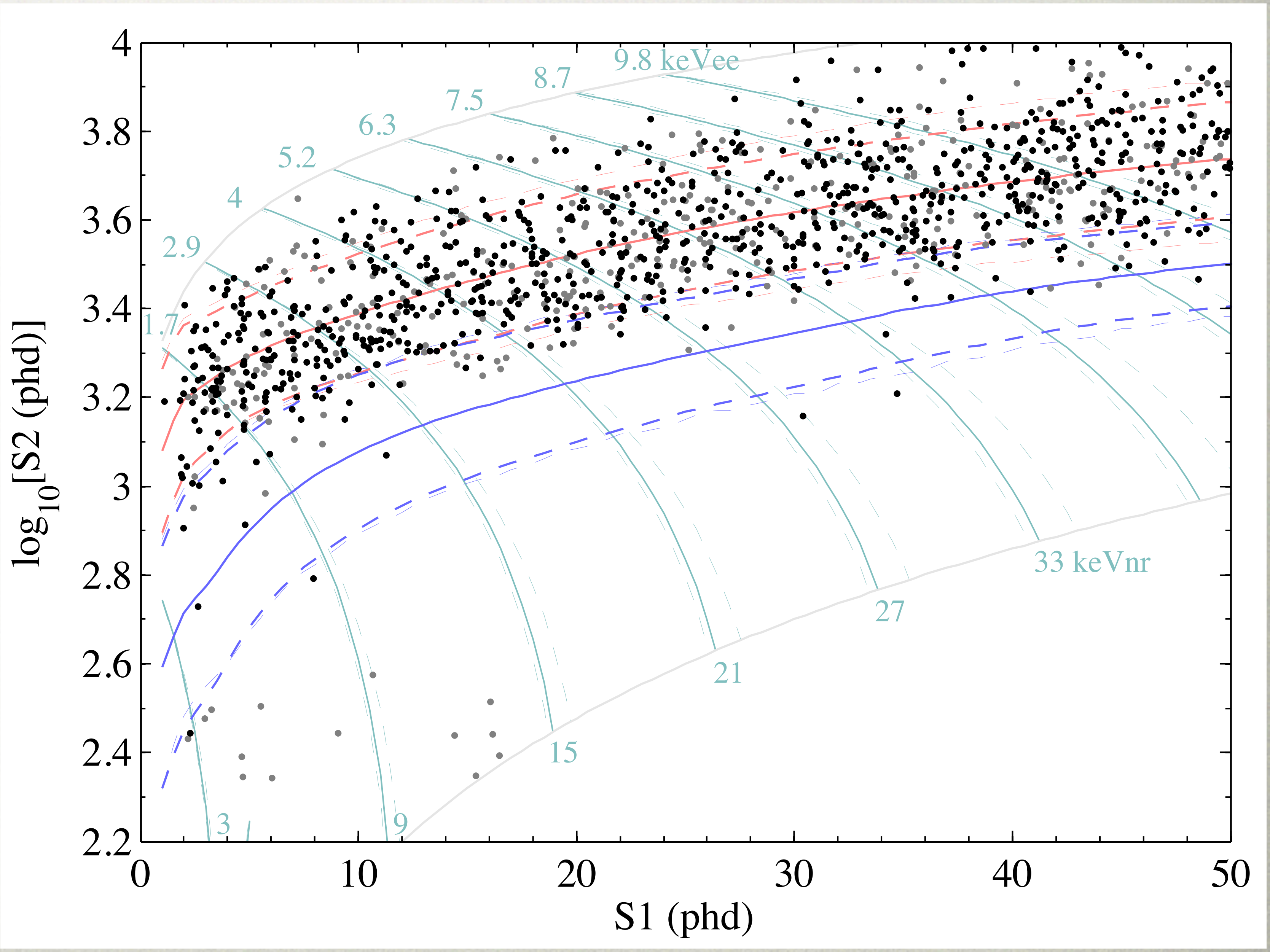

WIMP-search data

- After salting, events outside the ER band were scrutinized again.
- Two populations of rare pathological events were identified, that had contributed three particularly dangerous events.

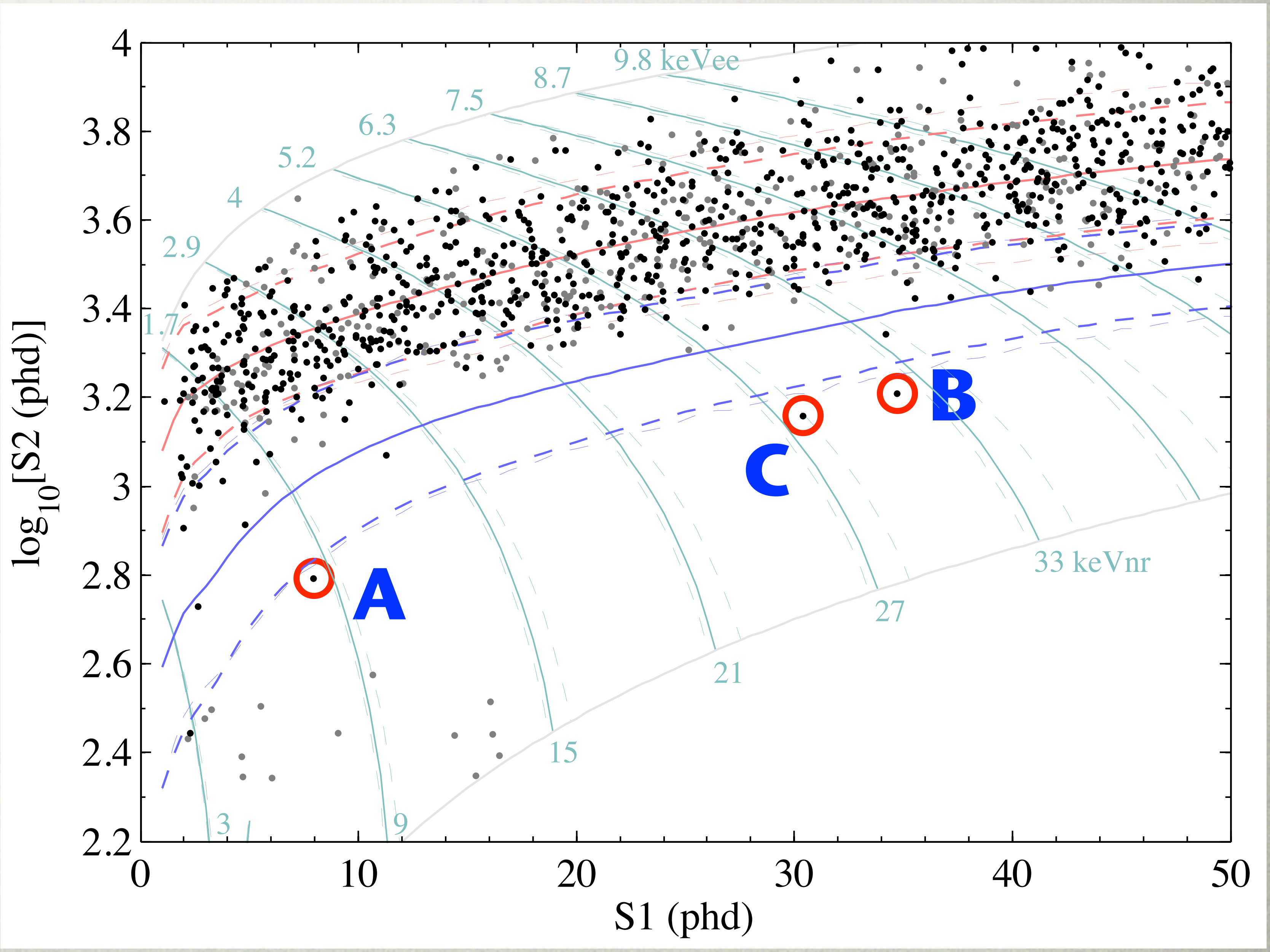

Three pathological events

- Events **A** and **B** have ~80% of the light in a single top-edge PMT. Consistent with energy deposited outside the TPC, and light leaking through a gap near the edge of the PMT array. p of $O(10^{-9})$ and $O(10^{-10})$ for A and B, respectively.
- Event **C** is highly concentrated under a few top PMTs and has a time structure consistent with gas scintillation emission. Event came after high rate in preceding 1 second.
- Since these events do not correspond to interactions in the TPC, we develop cuts [post-un-salting] to target them.

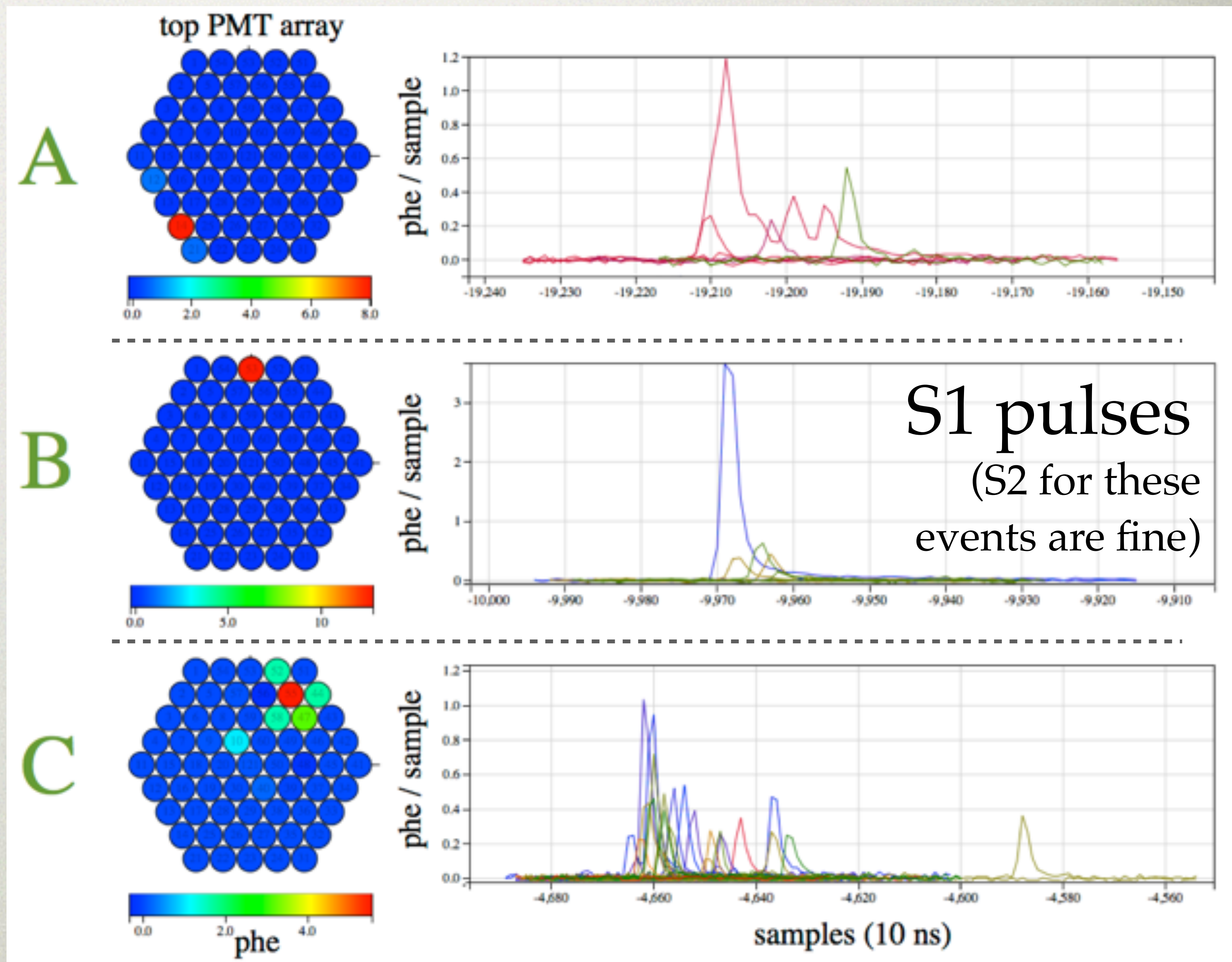

Three pathological events

- Post-un-salting cuts:
  - Loose cuts (high signal acceptance), defined on calibration data.
  - Flat signal acceptance.

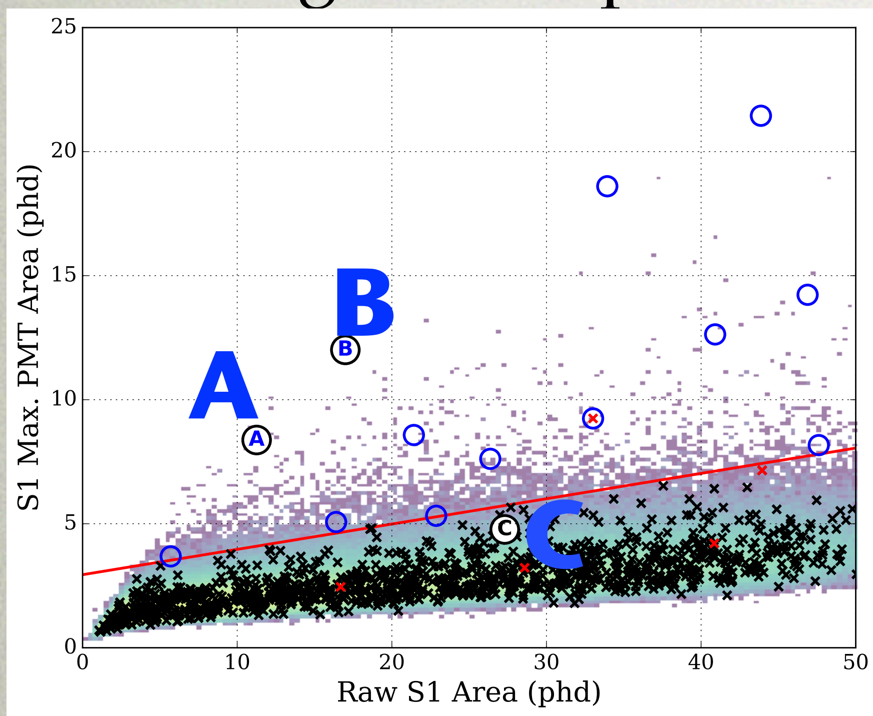

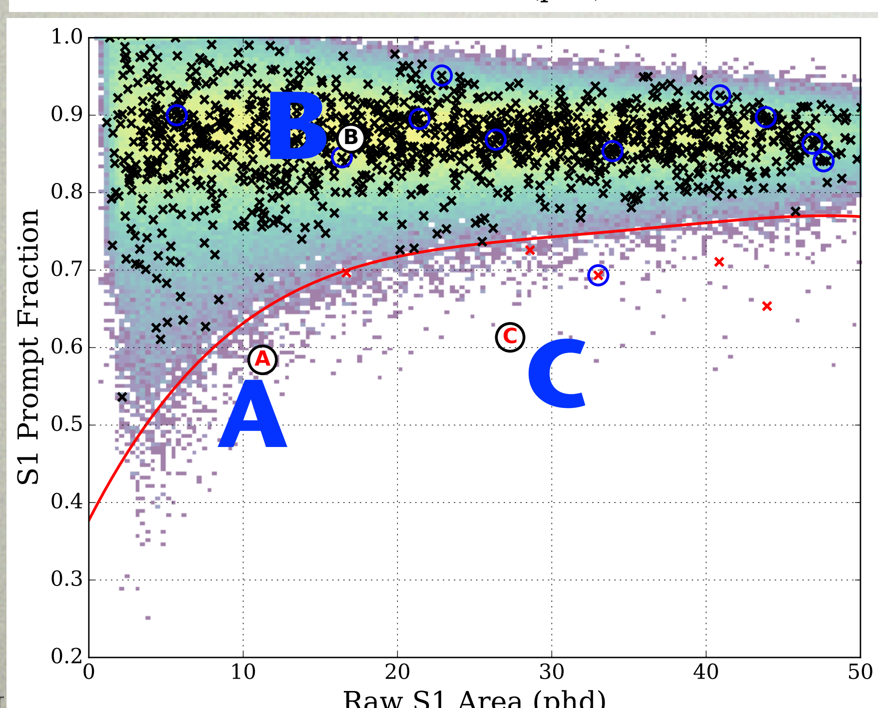

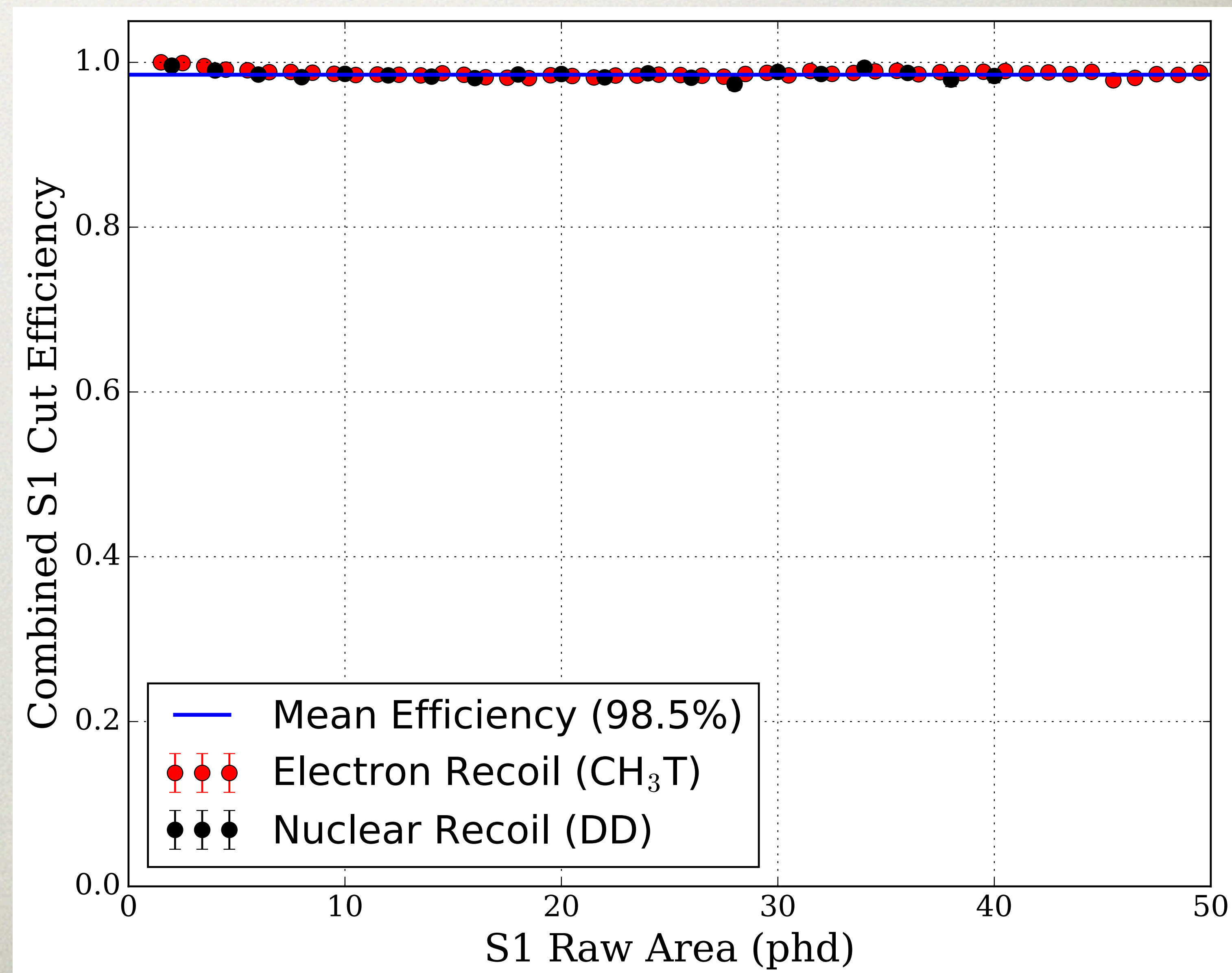

WIMP-search data

- This plot shows the data from our 16 “detectors” stacked on top of each other.
- Dots are events:
    - Gray: within 1cm of the radial fiducial boundary
    - Black: bulk events
- Red and blue curves are the ER and NR bands, respectively.
- Salt is removed.
- red events: removed by post-unsalting cuts.

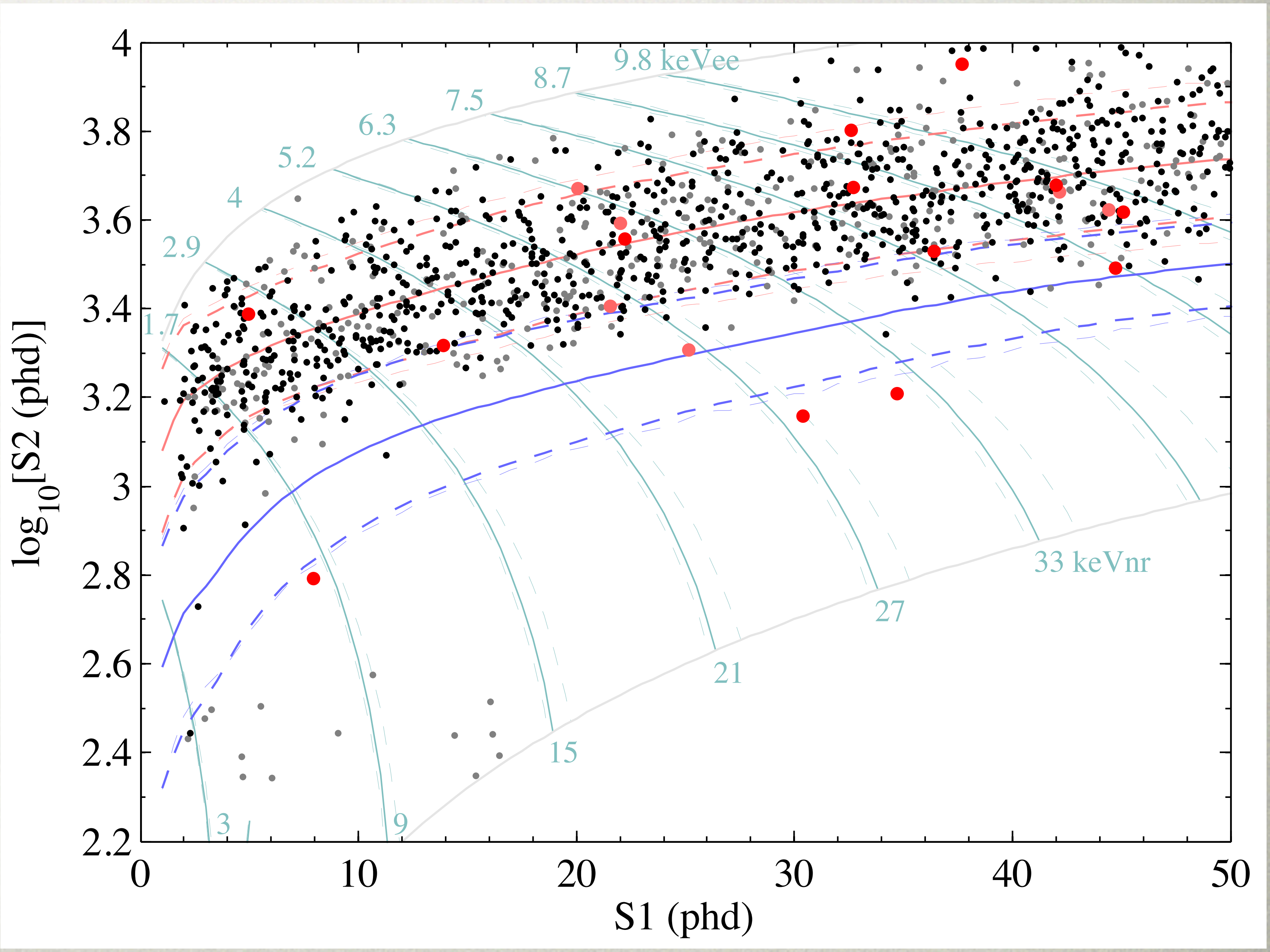

WIMP-search data

- This plot shows the data from our 16 "detectors" stacked on top of each other.
- Dots are events:
  - Gray: within 1cm of the radial fiducial boundary
  - Black: bulk events
- Red and blue curves are the ER and NR bands, respectively.
- Salt is removed.
- Post-un-salting cuts applied.
- p-value = 40% consistent with background-only hypothesis.

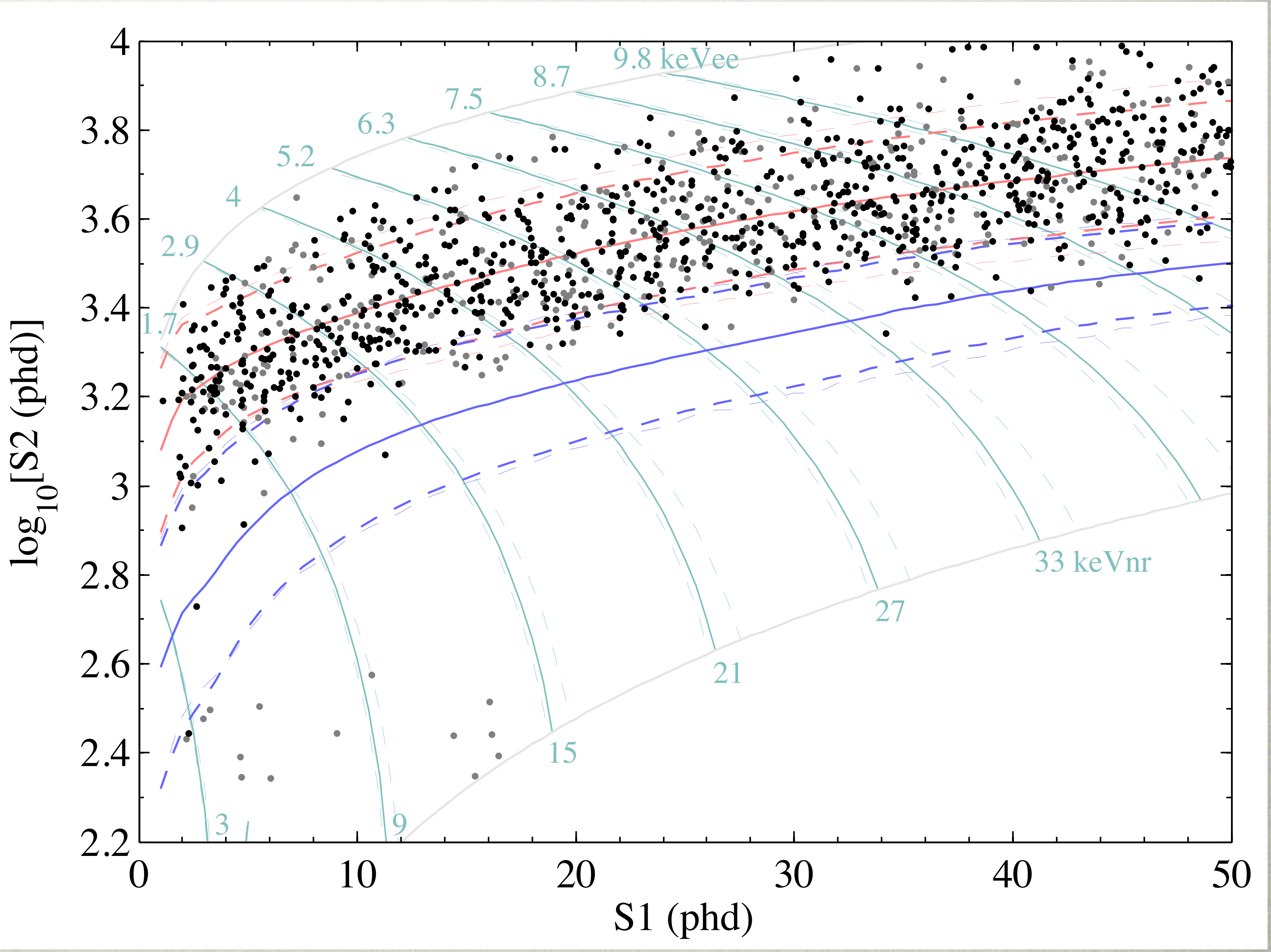

SI WIMP-nucleon exclusion

- Brazil bands show the 1- and 2-sigma range of expected sensitivities, based on random BG-only experiments.
- **Factor of 4 improvement** over the previous LUX result in the high WIMP masses
- Minimum exclusion of **2.2 x 10^{-46} cm^2** at 50 GeV

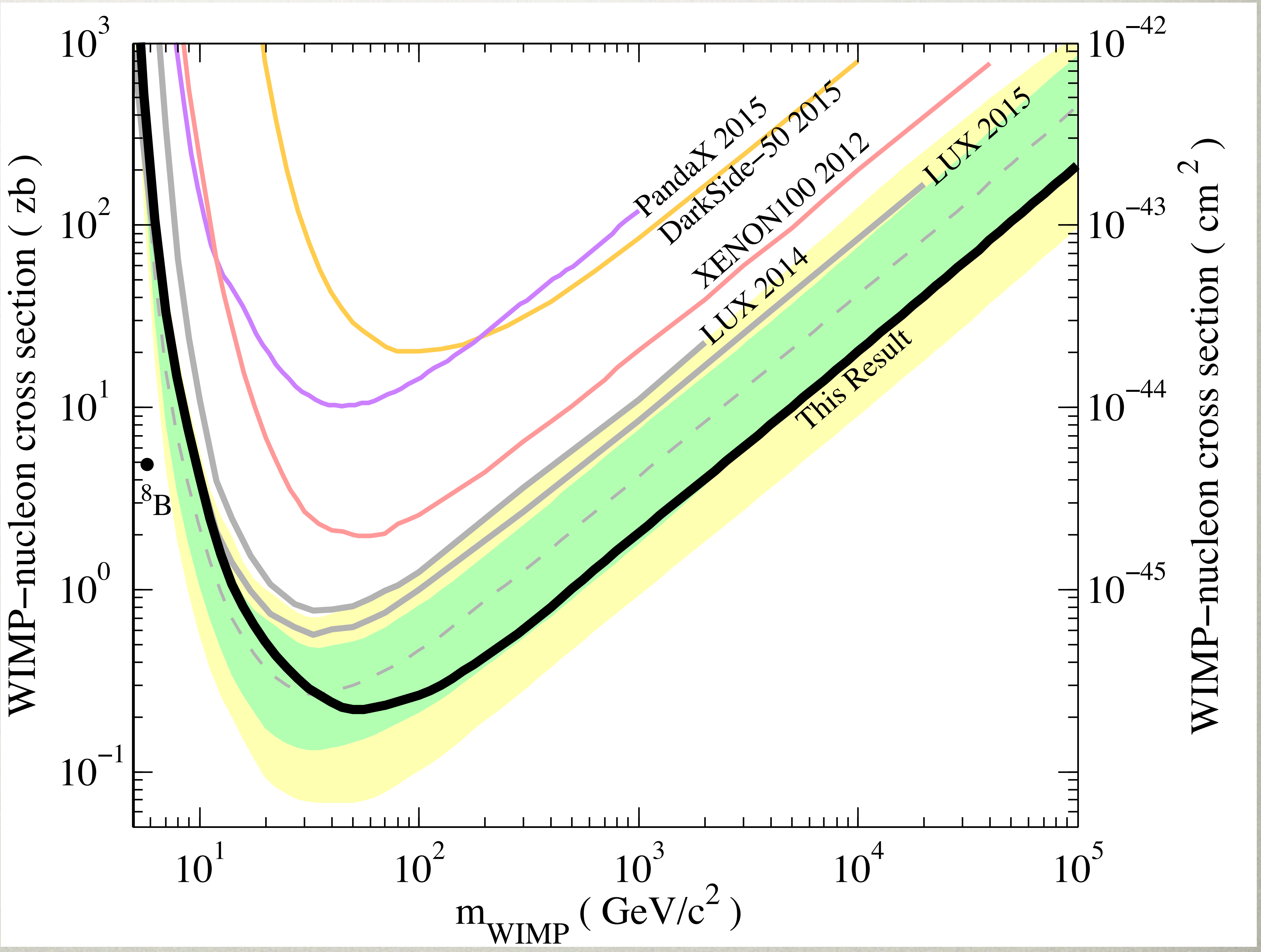

SI WIMP-nucleon exclusion

- Brazil bands show the 1- and 2-sigma range of expected sensitivities, based on random BG-only experiments.
- **Factor of 4 improvement** over the previous LUX result in the high WIMP masses
- Minimum exclusion of **2.2 x 10^{-46} cm^2** at 50 GeV

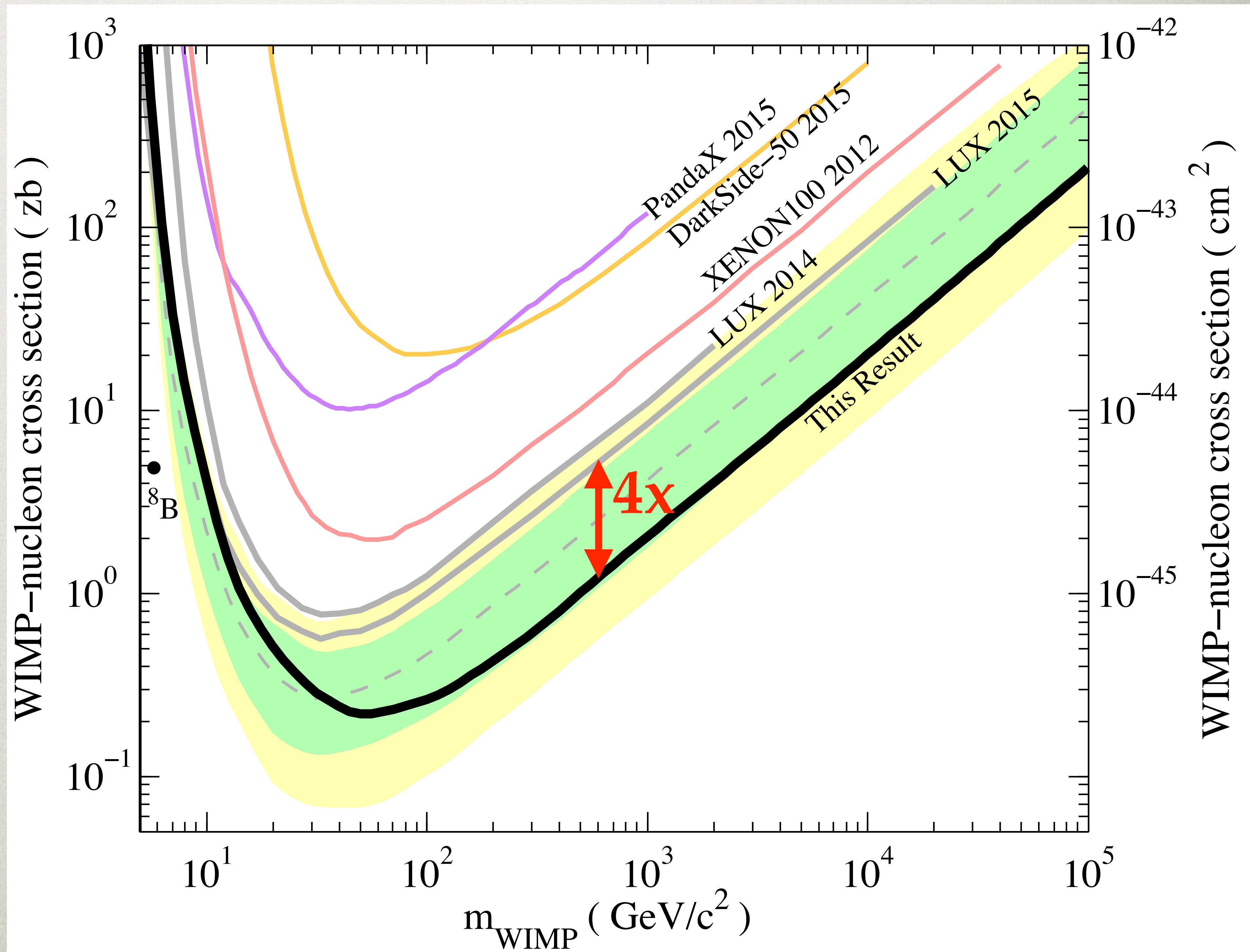

Summary and next steps

- New world-leading result from LUX's 332 live-day search, cutting into un-probed parameter space. Excluding SI WIMPs down to 0.22 zepto barns
- Publication to be submitted soon; more details on this analysis available today at `luxdarkmatter.org`
- More analyses forthcoming (SD, axion, ALPs, etc.)
- LUX is currently performing a series of end-of-run calibration campaigns.
- Onwards and downwards: LUX-ZEPLIN (LZ) experiment under construction, 7 tonne active mass (2020).